Open quantum systems, effective Hamiltonians and device characterisation

Open Quantum Systems, Effective Hamiltonians, and Device Characterisation

By

Stephen Neil Alexander Duffus

A Doctoral Thesis

Submitted in partial fulfilment for the requirements

for the award of PhD of Loughborough University

June 2018

Acknowledgements

I would like to thank Dr. Vincent Dwyer for playing such a important role throughout the course of my PhD, I wouldn't have got to this stage without such attentive guidance. I would also like to thank Dr. Mark Everitt for providing me with many opportunities to develop as a researcher and as a person. I'd like to thank Dr. Alexandre Zagoskin for always having time for me, even if I didn't make best use of it. I would like to thank Dr Todd Tilma for his amazing hospitality during my stay in Tokyo. Many thanks go to the 'rabbit hole', namely Russell, Joe, Patrick, Will, Chris, Aidan, Laura, Czech, and Kieran, for being an unlimited source of entertainment. Finally I wish to thank my wife, Flip, who has been my rock throughout these five chaotic years.

Abstract

We investigate the some of the many subtleties in taking a microscopic approach to modelling the decoherence of an Open Quantum System. We use the RF-SQUID, which will be referred to as a simply a SQUID throughout this paper, as a non-linear example and consider different levels of approximation, with varied coupling, to show the potential consequences that may arise when characterising devices such as superconducting qubits in this manner. We first consider a SQUID inductively coupled to an Ohmic bath and derive a Lindblad master equation, to first and second order in the Baker-Campbell-Hausdorff expansion of the correlation-time-dependent flux operator. We then consider a SQUID both inductively and capacitively coupled to an Ohmic bath and derive a Lindblad master equation to better understand the effect of parasitic capacitance whilst shedding more light on the additions, cancellations and renormalisations that are attributed to a microscopic approach.

Finally we explore the impact of effective Hamiltonians on a SQUID's decoherence, produced during the Lindblad derivation process, and discuss their validity, making use of the correspondence principle and presenting effects on observables that may be experimentally verifiable.

Contents

List of Abbreviations

- VLSI: Very Large Scale Integration
- CMOS : Complementary Metal Oxide Semiconductor
- OQS: Open Quantum System
- SQUID : Superconducting Quantum Interference Device
- RSJ: Resistively Shunted Junction
- QHO: Quantum Harmonic Oscillator
- BCS: Bardeen Cooper Schrieffer
- DHO: Damped Harmonic Oscillator
- QBM: Quantum Brownian Motion
- BCH: Baker Campbell Hausdorff
- HO: Harmonic Oscillator

Chapter 1

Introduction

1.1 Motivation

Modelling and simulation of complex systems has become a crucial part of engineering design due to its ability to efficiently explore parameter space and so determine the optimal performance range of parameters as well as highlighting key failure mechanisms. As a result, simulation will be central to the design of products integrated with quantum technology [1, 2, 3, 4, 5]. For these technologies, reliable quantitive simulations of the product in question is an absolute necessity in the quest to pave the way for rapid prototyping. Modelling and Simulation have proven to be successful in classical systems, such as in the design of VLSI CMOS [2]. Simulation of complex quantum systems using classical methods brings with it many questions such as how a modelling framework can be made applicable at all levels of component of the system in question. As an example, consider an open quantum system: an ensemble consisting of multiple quantum systems coupled to an environment

which exhibits a dissipative loss of quantum information through the process of decoherence [6]. Although ideal for use in sensors, the fragile nature of the quantum state makes its use in quantum computation more difficult. Decoherence is therefore the largest threat to the development of desirable qualities, such as long coherence times and tune-ability, in technologies such as the superconducting qubits modelled in this work [1]. A standard approach that may offer a pathway for modelling the interaction between a quantum system and the environment is the master equation [3, 4, 5, 7, 8, 9, 10, 11, 12, 13] which provides a framework to enable the modelling of long term dynamics of Open Quantum Systems (OQS), over time scales much larger than that of the initial coupling, and allows for better understanding of how the environment can play such a key role in the behaviour of quantum systems. The choice of system to be modelled in this work is the Superconducting Quantum Interference Device (SQUID), commonly found in superconducting qubits and renowned for its sensitivity to an externally applied magnetic field; this sensitivity makes the SQUID a key candidate in exploring the significance of external degrees of freedom, such as magnetic flux, in decoherence channels of superconducting qubits [14]. It has often been thought that the impact of capacitive cross talk in flux-qubits, a system comprised of SQUIDs, was negligible [1]. However, it has been shown that a flux qubit's resilience to cross talk may have been overstated, and coherence times of susceptible systems may be affected by these couplings [1]; this work will show how capacitive elements of coupling can affect a SQUID's decoherence channel and energy level structure. The next section will provide an introduction to the system in question and its attributes.

1.2 SQUIDs

1.2.1 Superconductivity

After successfully liquifying helium in 1908, Dutch physicist Heike Kamerlingh Onnes explored the temperature dependence of resistivity in noble metals, particularly mercury and gold, using of a cryostat of his own design. It was found in 1911 that, below a critical temperature (T_c) of 4.2K, mercury exhibited "practically zero" resistance [15, 16], allowing an electrical current to flow without dissipation, introducing the world to superconductivity.

In 1933 it was shown that a superconducting material, is not only characterised by an infinite rise in electrical conductance, but will also exhibit diamagnetic behaviour in the presence of an external magnetic field through which almost all magnetic flux is expelled from the material; this is known as the Meissner effect [17, 18]. For particular values, the magnetic field was to found penetrate the superconductor but only within a fixed length from the surface, known as the penetration depth, λ.

In 1935, Fritz and Heinz London developed a theory to describe the Meissner effect by defining the superconducting current desnity, $\vec{j_s}$, in terms of the vector potential, $\vec{A}$, driving it [19]:

$$\vec{j_s} = -\frac{n_s e^2}{m}\vec{A} \tag{1.1}$$

where n_s is the density of superconducting charge carriers, whilst m and e denote electron mass and charge respectively. London theory showed that, by applying Ampere's law $\vec{\nabla} \times \vec{B} = \mu_0 \vec{j}$, to the above equation one could yield the differential equation:

$$\vec{\nabla}^2\vec{B} = \frac{1}{\lambda^2}\vec{B} \tag{1.2}$$

where $\vec{B}$ is the magnetic field strength and λ is the same characteristic length scale seen in the Meissner effect, this became known as the London penetration depth [19] and shows that a magnetic field reduces exponentially as it penetrates a superconductor.

The phenomenology of superconductors was further developed in 1950 by Vitaly Lazarevich Ginzburg and Lev Landau [20] through the introduction of the macroscopic wavefunction $\psi(r,t) = |\psi|e^{\phi(r)}$ as the order parameter of a superconducting phase transition, such that $|\psi|^2 \propto n_s$ with $\phi(r)$ denoting quantum mechanical phase. Minimisation of the free energy with respect to the order parameter and vector potential led Landau and Ginzburg to two equations

$$\begin{aligned} 0 &= \alpha\psi + \beta|\psi|^2\psi + \frac{1}{2m}\left(-i\hbar\vec{\nabla} - 2e\vec{A}\right)\psi \\ \vec{j_s} &= \frac{2e\hbar}{m}|\psi|^2\left(\vec{\nabla}\phi - \frac{2e}{\hbar}\vec{A}\right) \end{aligned} \tag{1.3}$$

which determine the order parameter and the superconducting current respectively; within these equation α and β act as phenomenological parameters and m is the effective mass. The theory developed by Landau and Ginzburg uses two characteristic length scales: the first being the London penetration depth, whilst the second describes the spatial evolution of the order parameter over a superconducting-normal metal boundary, known as the coherence length, ξ [20]. The ratio of the two lengths would later be

used in 1957 to define superconducting type as materials with $\lambda/\xi < 1/\sqrt{2}$ were found to energetically favour full expulsion of an external magnetic field (Type I) whilst materials with $\lambda/\xi > 1/\sqrt{2}$ would energetically favour a mixture of superconducting and normal states that would lead to magnetic penetration in the form of Abrikosov vortices (Type II) [21].

At the same time the above behaviours, the electronic specific heat at temperatures approaching absolute zero, and the effect of isotopic mass on the critical temperature itself, were addressed and a theory of superconductivity was proposed by John Bardeen, Leon Cooper, and John Schrieffer known as the BCS theory [18].

BCS was a bulk model approach built upon Leon Cooper's theory that two electrons lying at the Fermi surface of the crystal lattice would always form a bound pair provided there was a net positive interaction, no matter how small in magnitude [22]. Cooper suggested that when an electron passes through the lattice it is thought to create polarised regions within said lattice through phonon interactions; these polarised regions then attracted another electron, thus correlating the two electrons to form a pair with bosonic traits. Since these bosons have lower energies than their separate fermionic counterparts, an energy gap for single-particle excitation is produced which inhibits collisions associated to resistivity. If the thermal energy is sufficiently small, lattice vibrations will not be able to overcome this energy gap and so the electron pairs will adopt the same quantum state, propagating through the material as one system without dissipation. The supercurrent produced exists up to a critical value I_c, above which the Zeeman energy of the single electrons will overcome the condensation energy and the pair formation will

be destroyed. The energy gap is strongly related to coherence length, which characterises the finite region over which a transition between superconducting and normally conducting domains can take place [18, 23]. Although BCS is only applicable to simple materials at temperatures approaching absolute zero, it offers good insight into the phenomenon as the exact form of the attraction between correlated electrons need not be known [24]. Over the years, more complex materials with much higher critical temperatures have been found, the most notable of which was the discovery of Yttrium Barium Cooper Oxide (YBCO) which was the first superconductor with a T_c higher than 77K, the boiling point of nitrogen [25]. Currently the highest accepted T_c material is sulfur hydride with a critical temperature of 203K, with research motivated by BCS theory's dependence on phonon frequency, electron-phonon coupling strength, and density of states [26].

1.2.2 Josephson Junctions

In 1967 Brian Josephson proposed a theoretical framework from which it would be possible for a supercurrent to tunnel through an insulating layer separating two superconductors [27], which was an exentsion to the single electron tunnelling observed by Ivar Giaever in 1960 [28, 29]. This effect was later confirmed to be experimentally verifiable by theorist Philip Anderson and is now referred to as the Josephson effect [14, 30].

It has been shown, by considering the interference of macroscopic wave functions of superconducting states either side of a junction [31], that the current, I, flowing through such a junction, I, has the relation:

$$I = I_c \sin \varphi \tag{1.4}$$

where $\varphi = \phi_1 - \phi_2$ denotes the phase difference between macroscopic wave functions of the condensates $\psi_{1,2} = |\psi_{1,2}|e^{i\phi_{1,2}}$ in the two superconducting electrodes, while I_c denotes the critical current, above which a supercurrent will not flow. In the presence of a voltage U across the superconductors, the phase difference evolves according to the dynamics:

$$\frac{\mathrm{d}\varphi}{\mathrm{d}t} = 2eU/\hbar = 2\pi U/\Phi_0 \tag{1.5}$$

where e is the electronic charge, $\hbar$ is Planck's reduced constant, and $\Phi_0 = 2\pi\hbar/2e$ is the flux quantum which arises from flux quantisation of a superconducting loop [14, 32]: that is to say that the "flux contained in a closed superconducting loop is quantised in units of $[\Phi_0]$" [14] and arises from the necessity for the wave function ψ to be single valued after one complete circuit.

1.2.3 The SQUID

A SQUID can be thought of an LC circuit enclosing a Josephson junction weak link. When a SQUID is subjected to an external magnetic field, a supercurrent will flow to repel all but quantised amounts of flux which flow through the inside of the ring; this permitted flux originates from a drop in screening current due to a difference in phase in the wave function across the weak link. The total energy of a SQUID may be derived from the Lagrangian of the closed system, using the Euler-Lagrange equations to obtain the Hamiltonian [33]. Alternatively, the total energy of the SQUID subject to an external magnetic flux may be found by use of its equivalence to an LCJ circuit without damping [34].

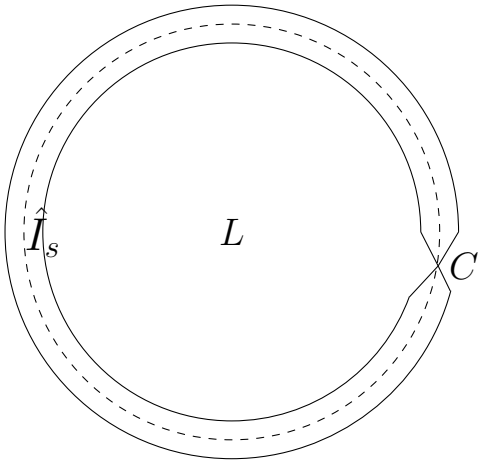

Figure 1.1: Basic Illustration of a SQUID, which is a superconducting ring with a weak link. When the ring is exposed to an external flux, a supercurrent will flow to screen said flux, tunnelling across the weak link in the process. Classically the weak link possesses a capacitance, while quantum mechanically it is responsible for the drop in phase of the wave function in each complete loop. The loop itself possesses a geometric inductance which determines the size of the observable screening current and quantised flux within the loop.

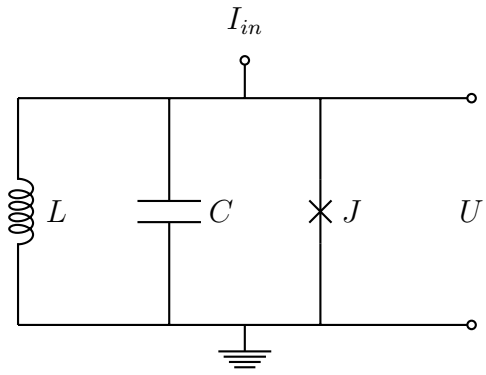

Figure 1.2: The SQUID is equivalent to a parallel circuit containing an inductor, capacitor, and Josephson junction as shown above. The voltage, U, across all three branches must be equal and the sum of the currents in each branch must equal the input current I_{in}. In the case of a damped system, a resistor would be introduced in parallel, producing the RSJ model which uses semiclassical approximations to produce a differential equation, describing the evolution of classical trajectories and is widely used to offer a classical representation of the SQUID [35].

By Kirchoff's laws, the current flowing in the circuit, neglecting noise, is given by:

$$I_{in} = C\dot{U} + I_s + I_c \sin\varphi \tag{1.6}$$

where I_s is the screening current due to the self inductance of the ring, induced by the externally applied magnetic field. The circuit's energy may be calculated from the time integral of Power $P = IU$, which yields:

$$E = \int \mathrm{d}t \left(C\dot{U}U + UI_s + UI_c \sin\varphi \right) \tag{1.7}$$

Writing the voltage as $U = L\dot{I}_s$, and the final term in terms of phase difference from Eq. (1.5), and integrating:

$$E = \frac{CU^2}{2} + \frac{LI_s^2}{2} - \frac{\Phi_0 I_c}{2\pi}\cos\varphi \tag{1.8}$$

Since the voltage across a capacitor is related to charge through $Q = CU$, the first term may be rewritten as $Q^2/2C$. The second term requires the relationship between screening current and magnetic flux which, for a SQUID exposed to external magnetic flux, is given by [36]:

$$I_s = (\Phi - \Phi_x)/L \tag{1.9}$$

where Φ and Φ_x are the SQUID flux and external flux respectively. This yields:

$$H = \frac{Q^2}{2C} + \frac{(\Phi - \Phi_x)^2}{2L} - \frac{\Phi_0 I_c}{2\pi}\cos\varphi \tag{1.10}$$

The phase, φ, and, more specifically, the difference created across the weak link is given by the gauge invariant quantised phase, $\varphi = 2\pi n - (2\pi/\Phi_0)\Phi$ [33, 37] where $(2\pi/\Phi_0)\Phi$ originates from the compensation in screening current due to movement across the weak link. Substitution of this into the cosine term and use of the relationship between critical current and Josephson energy $I_c = (\Phi_0/2\pi)\hbar\nu$, where $\hbar\nu$ is the energy of tunnelling Cooper pairs [38], yields:

$$H = \frac{Q^2}{2C} + \frac{(\Phi - \Phi_x)^2}{2L} - \hbar\nu\cos\frac{2\pi\Phi}{\Phi_0} \tag{1.11}$$

From this classical Hamiltonian it is possible to apply a quantum mechanical treatment to this macroscopic circuit through canonical quantisation of

the Lagrangian [39, 40], this casts the Hamiltonian in terms of canonical operators:

$$\hat{H} = \frac{\hat{Q}^2}{2C} + \frac{(\hat{\Phi} - \Phi_x)^2}{2L} - \hbar\nu \cos\frac{2\pi\hat{\Phi}}{\Phi_0} \tag{1.12}$$

where $\hat{Q}$ and $\hat{\Phi}$, the charge and flux operators respectively, are analogous to the position and momentum operators of the Harmonic Oscillator (HO), and share the commutation relation:

$$\left[\hat{\Phi}, \hat{Q}\right] = \mathrm{i}\hbar \tag{1.13}$$

The Hamiltonian shows harmonic behaviour in the first two terms where C is analogous with the HO system's mass [41] and shares the relationship with the system's characteristic frequency ω_0 and inductance L through $\omega_0 = 1/\sqrt{LC}$. The cosine term is then the energy lost as a result of pair tunnelling through the weak link.

It is shown in Appendix A that it is possible to simplify this Hamiltonian using the unitary translation operator $\hat{T} = \exp\left(-\mathrm{i}\hat{Q}\Phi_x/\hbar\right)$. The Hamiltonian is then said to be written in the external flux basis and may then be written as [42, 43, 44]:

$$\begin{aligned}\hat{H}' &= \hat{T}^\dagger \hat{H} \hat{T} - \mathrm{i}\hbar\hat{T}^\dagger \frac{\partial \hat{T}}{\partial t} \\ &= \frac{\hat{Q}^2}{2C} + \frac{\hat{\Phi}^2}{2L} - \hbar\nu \cos\left(\frac{2\pi}{\Phi_0}\left(\hat{\Phi} + \Phi_x\right)\right) - \hat{Q}\frac{\partial \Phi_x}{\partial t}\end{aligned} \tag{1.14}$$

For the cases studied in this work, the external flux is assumed to either be time independent or varying adiabatically, the final term is therefore either

zero or negligible. This yields the translated Hamiltonian:

$$\hat{H}' = \hat{T}^{\dagger}\hat{H}\hat{T} = \frac{\hat{Q}^2}{2C} + \frac{\hat{\Phi}^2}{2L} - \hbar\nu\cos\left(\frac{2\pi}{\Phi_0}\left(\hat{\Phi} + \Phi_x\right)\right) \tag{1.15}$$

for the remainder of this thesis we will work in this representation. The SQUID is of particular interest in this work due to it representing a non-linear extension to the quantum harmonic oscillator and its importance in sensing as magnetometers and gradiometers, and its inclusion in fundamental components in quantum computer designs from D-Wave, IBM and Google [45, 46].

1.3 Environmental Effects

The quantum properties of systems, such as the SQUID's superposition of screening currents which arise due to a double well potential created at external magentic flux of $\Phi_x = \Phi_0/2$ [47], are often short lived after preparation due to the system not being closed. It is impossible to isolate a system indefinitely from the invasive nature of the environment, the resulting destruction of the quantum state is known as decoherence [6, 48]. To model this, one will often consider a much larger quantum system, composed of the two subsystems: the system of interest and what is known as the environment, reservoir, or bath. Each subsystem is described by its own Hamiltonian and the interaction between them maintains a constant information exchange between the system and bath [49].

The defining features of the environment and how it interacts with a quantum system can be split into three closely linked attributes. The first of the three is the interaction Hamiltonian from which the other two features

are derived. In this work we will look at the inductive and capacitive coupling of a SQUID to its environment by analogy with the HO, therefore acting as a natural extension to previous models. The couplings effectively correlate the SQUIDs 'position' (flux) and/or 'momentum' (charge) to each of an infinite number of individual oscillators within the bath, which, within the Markovian framework that will be discussed later, is assumed to be in a thermalised state with a negligible relaxation time relative to the system.

Another common way of modelling a SQUID coupled to an environment is through its approximation to a two level system, such as when coupling to nitrogen vacancies in diamond [50]; this approximation limits the explored parameter space as Φ_x is fixed at close to half of a flux quantum ($\Phi_x \approx 0.5\Phi_0$) which reduces the potential impact of energy leakage to excited levels on the system, a factor that gains significance later in this thesis. The choice instead to couple through flux and charge allows for a larger exploration of parameter space and the associated effects, which is crucial if one is to attempt a more detailed characterisation. Non-linear couplings [51, 52], are also common and change the behaviour of the ensemble considered significantly.

The second attribute which defines a bath is its correlation function, a tool used to approximate the dynamic information of the system-bath ensemble, we will return to specific details in the next section but for now we note that it is possible to define the correlation function in terms of the third attribute: the spectral density, $J(\omega)$, a function used to describe the absorption and emission of energy which result from the interaction between system and bath.

Consider a system coupled to a set of harmonic oscillators, the energy

exchange between the oscillators of the bath and the system will depend on the frequency at which they oscillate as well the proximity in which they lie relative to each other. The relationship between the energy exchange and the frequency, ω, of these oscillators is generally given by [53]:

$$J(\omega) \propto \omega^{\alpha} \tag{1.16}$$

Where the value of α dictates the linearity of this relationship and thus the type of bath considered. For Ohmic dissipation, which is commonly used in models involving the HO and Quantum Brownian Motion (QBM), a linear damping effect is present and the exponent takes the value $\alpha = 1$. The high temperature extension to an Ohmic bath is the thermal bath which plays a crucial part in the assumptions made in explaining the process of Quantum Brownian Motion (QBM) which will be discussed later in this chapter.

Although the nature of the phenomenon is widely debated, decoherence is the most accepted cause of the loss of quantum information through the interaction with the environment [6, 48] and describes the non-unitary loss as a system undergoes a quantum-classical transition; for the case of the SQUID this would be shown in the reduction of the macroscopic superposition of supercurrent states into only one. The ultimate goal in developing quantum technologies with longer coherence times is to overcome this destructive phenomenon either by creating more resilient systems, or by using interaction to the environment to control the process itself [52, 54, 55].

1.4 Master Equation

There are a number of ways to model a quantum system and its interaction with its environment, such examples include quantum Langevin equations [56], projection operator techniques [57] and quantum master equations, the latter of which possesses analytic solutions and thus making it an appealing framework. Master equations may prove effective in forming part of an engineering design strategy [45]. The master equation is widely used as a tool that provides a good phenomenological approach to describing the ensemble average of an open quantum system, through modelling of a statistical mixture of several quantum states, known as the density matrix. The starting point for any master equation begins with the assumption that the system-environment ensemble is closed; its evolution can therefore be described by the Louiville von-Neumann Equation:

$$\frac{\mathrm{d}\rho}{\mathrm{d}t} = -\frac{\mathrm{i}}{\hbar}[H, \rho] \tag{1.17}$$

where ρ is the density matrix of the total system and H is the total Hamiltonian given by:

$$\hat{H} = \hat{H}_S + \hat{H}_B + \hat{H}_I \tag{1.18}$$

where H_s, H_B and H_I represent the Hamiltonians which describe the system, the environment (bath) and the interaction between them respectively. There are many requirements that the density matrix must satisfy for this approach to be valid, these include hermiticity, positivity and the normalisation condition that $\mathrm{Tr}\{\rho\} = 1$. As with [57, 58] we require the information of the system alone and therefore acquire this information from the ensemble

to create a master equation for the reduced density matrix. That is to say that it is necessary to trace out the environment so that the dynamics of the system can be investigated. The first step is therefore to move into the interaction picture [57, 58]. Within this frame, the density matrix is defined as:

$$\tilde{\rho} = e^{\frac{\mathrm{i}\hat{H}_0 t}{\hbar}} \rho e^{\frac{-\mathrm{i}\hat{H}_0 t}{\hbar}} \tag{1.19}$$

where $\hat{H}_0 = \hat{H}_S + \hat{H}_B$. Equation (1.17) then reduces to:

$$\frac{\mathrm{d}\tilde{\rho}}{\mathrm{d}t} = -\frac{\mathrm{i}}{\hbar}[\tilde{H}_I(t), \tilde{\rho}] \tag{1.20}$$

since $\tilde{H}_I(t) = e^{\frac{\mathrm{i}\hat{H}_0 t}{\hbar}} \hat{H}_I e^{\frac{-\mathrm{i}\hat{H}_0 t}{\hbar}}$ is the only object that does not commute with the $\hat{H}_0$ in this new picture. Integration of the above expression between the limits of $s \in (0, t)$, where $s = 0$ is the moment the interaction begins, yields:

$$\begin{aligned} \int_0^t \mathrm{d}s \frac{\mathrm{d}\tilde{\rho}(s)}{\mathrm{d}t} &= -\frac{\mathrm{i}}{\hbar} \int_0^t \mathrm{d}s[\tilde{H}_I(s), \tilde{\rho}(s)] \\ \tilde{\rho}(t) &= \tilde{\rho}(0) - \frac{\mathrm{i}}{\hbar} \int_0^t \mathrm{d}s[\tilde{H}_I(s), \tilde{\rho}(s)] \end{aligned} \tag{1.21}$$

Substituting for $\tilde{\rho}(t)$ in the right hand side of equation (1.20) gives:

$$\frac{\mathrm{d}\tilde{\rho}}{\mathrm{d}t} = -\frac{\mathrm{i}}{\hbar}[\tilde{H}_I(t), \tilde{\rho}(0)] - \frac{1}{\hbar^2} \int_0^t \mathrm{d}s[\tilde{H}_I(t), [\tilde{H}_I(s), \tilde{\rho}(s)]] \tag{1.22}$$

1.4.1 Born and Markov Approximations

At this stage, the density matrix of the total system is rewritten and takes the form:

$$\tilde{\rho} = \tilde{\rho}_S(t) \otimes \tilde{\rho}_B(t) + \tilde{\rho}_c(t) \tag{1.23}$$

where $\tilde{\rho}_S(t)$, $\tilde{\rho}_B(t)$ and $\tilde{\rho}_c(t)$ represent the density matrices of the system and the environment, as well as the entanglement (or correlation) between them. As in [58], it is assumed that the bath relaxation time, τ_B is far smaller than that of the system, τ. Since the spectral width is proportional to the reciprocal of the these quantities [58], it is assumed that the spectral width of the environment is far greater than that of the system with which it is interacting. By making this assumption it possible to make the Born approximation [58] and neglect the effect of $\tilde{\rho}_c(t)$; that is to say that at some given time $s = 0$ the system and bath are uncorrelated. Linking this to the system in question, the SQUID, this can be thought of as the moment that the superconducting state is formed, producing an effectively separable, uncorrelated state [45]. Since the environment is taken to be very large, the system's impact, or back action, on it is assumed to be very small, and it relaxes back to its initial state rapidly as a result; significant changes are only observed in the system over relatively large times and the environment can be assumed to time-independent and in thermal equilibrium. With this in mind, (1.22) becomes:

$$\frac{\mathrm{d}\tilde{\rho}}{\mathrm{d}t} = -\frac{\mathrm{i}}{\hbar}[\tilde{H}_I(t), \tilde{\rho}_S(0) \otimes \rho_B] - \frac{1}{\hbar^2}\int_0^t \mathrm{d}s[\tilde{H}_I(t), [\tilde{H}_I(s), \tilde{\rho}_S(s) \otimes \rho_B]] \quad (1.24)$$

To find the master equation for the system, the environment is traced out of equation (1.24), $\rho_S = \mathrm{Tr}_B\{\rho\}$, which yields:

$$\begin{aligned}\frac{\mathrm{d}\tilde{\rho}_S(t)}{\mathrm{d}t} =& -\frac{\mathrm{i}}{\hbar}\,\mathrm{Tr}_B\left([\tilde{H}_I(t),\tilde{\rho}_S(0)\otimes\rho_B]\right)\\ &-\frac{1}{\hbar^2}\int_0^t \mathrm{d}s\,\mathrm{Tr}_B\left([\tilde{H}_I(t),[\tilde{H}_I(s),\tilde{\rho}_S(s)\otimes\rho_B]]\right)\end{aligned} \tag{1.25}$$

This expression can be simplified if a further assumption is made, in order to do this one must consider the general form of the interaction Hamiltonian, $\tilde{H}_I(t)$. If the interaction takes a linear coupling of the form $\hat{H}_I = \sum_\alpha \hat{A}_\alpha \otimes \hat{X}_\alpha$ where α is an observable attributed to operators $\hat{A}$ and $\hat{X}$ acting in the space of the system and bath respectively; in the present model this is the case and so the assumption $\langle \hat{X}_\alpha \rho_B\rangle = \mathrm{Tr}_B(\hat{X}_\alpha\rho_B) = 0$ is made. Physically speaking, this assumption ensures that the mean value of the interaction Hamiltonian averaged over the density matrix of the environment is zero [58]. This assumption can also be made in the interaction picture:

$$\langle \tilde{X}_\alpha(t)\rho_B\rangle = \mathrm{Tr}_B\{\tilde{X}_\alpha(t)\rho_B\} = \mathrm{Tr}_B\left\{e^{\frac{\mathrm{i}\hat{H}_0 t}{\hbar}}\hat{X}_\alpha e^{\frac{-\mathrm{i}\hat{H}_0 t}{\hbar}}\rho_B\right\} \tag{1.26}$$

Due to the cyclic nature of the trace this can be written:

$$\begin{aligned}\mathrm{Tr}_B(\tilde{X}_\alpha(t)\rho_B) &= \mathrm{Tr}_B\left\{e^{\frac{\mathrm{i}\hat{H}_0 t}{\hbar}}\hat{X}_\alpha e^{\frac{-\mathrm{i}\hat{H}_0 t}{\hbar}}\rho_B\right\}\\ &= \mathrm{Tr}_B\left\{\hat{X}_\alpha e^{\frac{-\mathrm{i}\hat{H}_0 t}{\hbar}}\rho_B e^{\frac{\mathrm{i}\hat{H}_0 t}{\hbar}}\right\}\\ &= \mathrm{Tr}_B\left\{\hat{X}_\alpha\tilde{\rho}_B(-t)\right\}\\ &= \mathrm{Tr}_B\left\{\hat{X}_\alpha\rho_B\right\}\end{aligned} \tag{1.27}$$

Since the density matrix of the bath is time independent. This cyclic property can also be used to show the effect of linear interactions on the first term in

(1.22):

$$\begin{aligned}\mathrm{Tr}_B\left\{[\tilde{H}_I(t),\tilde{\rho}(0)]\right\} &= \sum_\alpha \mathrm{Tr}_B\left\{[\hat{A}_\alpha\otimes\hat{X}_\alpha,\tilde{\rho}_S(0)\otimes\rho_B]\right\}\\ &= \sum_\alpha [\hat{A}_\alpha,\tilde{\rho}_S(0)]\,\mathrm{Tr}_B\left\{\hat{X}_\alpha\rho_B-\rho_B\hat{X}_\alpha\right\}\\ &= \sum_\alpha [\hat{A}_\alpha,\tilde{\rho}_S(0)]\left(\mathrm{Tr}_B\left\{\hat{X}_\alpha\rho_B\right\}-\mathrm{Tr}_B\left\{\rho_B\hat{X}_\alpha\right\}\right)\\ &= 0\end{aligned} \tag{1.28}$$

With this assumption the master equation reduces to:

$$\frac{\mathrm{d}\tilde{\rho}_S(t)}{\mathrm{d}t} = -\frac{1}{\hbar^2}\int_0^t \mathrm{d}s\,\mathrm{Tr}_B\left\{[\tilde{H}_I(t),[\tilde{H}_I(s),\tilde{\rho}_S(s)\otimes\rho_B]]\right\} \tag{1.29}$$

The next problem to be addressed is that posed by the timescales that appear within this model. To ensure irreversible dynamics, a Markovian approximation is made; this assumes that the system is only dependent on its current state and not on its state at any time in the past. The system is therefore said to be memoryless [58, 57] which allows us to apply the condition $\rho_S(s)\to\rho_S(t)$. This gives us the Redfield equation [59]:

$$\frac{\mathrm{d}\tilde{\rho}_S(t)}{\mathrm{d}t} = -\frac{1}{\hbar^2}\int_0^t \mathrm{d}s\,\mathrm{Tr}_B\left\{[\tilde{H}_I(t),[\tilde{H}_I(s),\tilde{\rho}_S(t)\otimes\rho_B]]\right\} \tag{1.30}$$

This expression still depends on the initial state of the system since the inner commutator term does not depend on the system's current state. To ensure the system remains memoryless, the Markovian approximation is made by first making the change of variable $s=t-\tau$; this brings the following limits

of integration:

$$\begin{aligned} s &= t - \tau, \\ \mathrm{d}s &= -\mathrm{d}\tau, \\ \lim_{s\to t} \tau &= 0, \\ \lim_{s\to 0} &= t, \\ \Rightarrow \int_0^\infty \mathrm{d}s = -\int_\infty^0 \mathrm{d}\tau &= \int_0^\infty \mathrm{d}\tau \end{aligned} \tag{1.31}$$

The upper limit of integration can also be extended to infinity since the time evolution of the system is far larger than its decoherence time. This gives the final general form of the master equation in the interaction picture:

$$\frac{\mathrm{d}\tilde{\rho}_S(t)}{\mathrm{d}t} = -\frac{1}{\hbar^2}\int_0^\infty \mathrm{d}\tau \,\mathrm{Tr}_B \left\{ [\tilde{H}_I(t), [\tilde{H}_I(t-\tau), \tilde{\rho}_S(t)\otimes\rho_B]] \right\} \tag{1.32}$$

1.4.2 Transformation Back into the Schrödinger Picture

The last step is to transform back into the Schrödinger picture. In the Schrödinger picture, equation (1.32) takes the form:

$$\begin{aligned} &\frac{\mathrm{d}}{\mathrm{d}t}\left(e^{\frac{\mathrm{i}\hat{H}_0 t}{\hbar}}\rho_S(t)e^{-\frac{\mathrm{i}\hat{H}_0 t}{\hbar}}\right) = \\ &-\frac{1}{\hbar^2}\int_0^\infty \mathrm{d}\tau \,\mathrm{Tr}_B \left\{ \left[e^{\frac{\mathrm{i}\hat{H}_0 t}{\hbar}} H_I e^{-\frac{\mathrm{i}\hat{H}_0 t}{\hbar}}, \left[e^{\frac{\mathrm{i}\hat{H}_0 t}{\hbar}} H_I(-\tau) e^{-\frac{\mathrm{i}\hat{H}_0 t}{\hbar}}, e^{\frac{\mathrm{i}\hat{H}_0 t}{\hbar}}\rho_S(t)e^{-\frac{\mathrm{i}\hat{H}_0 t}{\hbar}}\otimes\rho_B \right] \right] \right\} \end{aligned} \tag{1.33}$$

The following calculations show how equation (1.33) can be reduced through contraction of exponent terms. Consider the commutator:

$$\left[e^{\hat{\mu}}\hat{A}e^{-\hat{\mu}}, \left[e^{\hat{\mu}}\hat{B}e^{-\hat{\mu}}, \left[e^{\hat{\mu}}\hat{C}e^{-\hat{\mu}}\right]\right]\right] \tag{1.34}$$

If one expands (1.34) and then simplifies, one can see that:

$$\begin{aligned}\left[e^{\hat{\mu}}\hat{A}e^{-\hat{\mu}}, \left[e^{\hat{\mu}}\hat{B}e^{-\hat{\mu}}, \left[e^{\hat{\mu}}\hat{C}e^{-\hat{\mu}}\right]\right]\right] &= \left[e^{\hat{\mu}}\hat{A}e^{-\hat{\mu}}, \left(e^{\hat{\mu}}\hat{B}e^{-\hat{\mu}}e^{\hat{\mu}}\hat{C}e^{-\hat{\mu}} - e^{\hat{\mu}}\hat{C}e^{-\hat{\mu}}e^{\hat{\mu}}\hat{B}e^{-\mu}\right)\right] \\ &= \left[e^{\hat{\mu}}\hat{A}e^{-\hat{\mu}}, e^{\hat{\mu}}\hat{B}\hat{C}e^{-\hat{\mu}} - e^{\hat{\mu}}\hat{C}\hat{B}e^{-\hat{\mu}}\right] \\ &= \left[e^{\hat{\mu}}\hat{A}e^{-\hat{\mu}}, e^{\hat{\mu}}[\hat{B},\hat{C}]e^{-\hat{\mu}}\right] \\ &= e^{\hat{\mu}}[\hat{A},[\hat{B},\hat{C}]]e^{-\hat{\mu}}\end{aligned} \tag{1.35}$$

where the property of unitary transforms $\hat{U}\hat{U}^{\dagger} = e^{-\hat{\mu}}e^{\hat{\mu}} = \mathbb{1}$ has been used, with $\mathbb{1}$ being the identity operator. The above derivations show that equation (1.32) can be reduced to:

$$\begin{aligned}&\frac{\mathrm{d}}{\mathrm{d}t}\left(e^{\frac{\mathrm{i}\hat{H}_S t}{\hbar}}\rho_S(t)e^{-\frac{\mathrm{i}\hat{H}_S t}{\hbar}}\right) \\ =&-\frac{1}{\hbar^2}\int_0^{\infty}\mathrm{d}\tau\,\mathrm{Tr}_B\left\{e^{\frac{\mathrm{i}\hat{H}_0 t}{\hbar}}\left[\hat{H}_I, \left[\hat{H}_I(-\tau), \rho_S(t)\otimes\rho_B\right]\right]e^{-\frac{\mathrm{i}\hat{H}_0 t}{\hbar}}\right\} \\ &=-\frac{1}{\hbar^2}\int_0^{\infty}\mathrm{d}\tau\,\mathrm{Tr}_B\left\{e^{\frac{\mathrm{i}\hat{H}_B t}{\hbar}}e^{\frac{\mathrm{i}\hat{H}_S t}{\hbar}}\left[\hat{H}_I, \left[\hat{H}_I(-\tau), \rho_S(t)\otimes\rho_B\right]\right]e^{-\frac{\mathrm{i}\hat{H}_S t}{\hbar}}e^{-\frac{\mathrm{i}\hat{H}_B t}{\hbar}}\right\} \\ &=-\frac{1}{\hbar^2}\int_0^{\infty}\mathrm{d}\tau\,\mathrm{Tr}_B\left\{e^{\frac{\mathrm{i}\hat{H}_S t}{\hbar}}\left[\hat{H}_I, \left[\hat{H}_I(-\tau), \rho_S(t)\otimes\rho_B\right]\right]e^{-\frac{\mathrm{i}\hat{H}_S t}{\hbar}}\right\}\end{aligned} \tag{1.36}$$

where the cyclic property of trace has again been used as well the fact that H_S and H_B commute. Expansion of the LHS of (3.22) then yields:

$$\begin{aligned} & e^{\frac{\mathrm{i}\hat{H}_S t}{\hbar}} \frac{\mathrm{d}\rho_S(t)}{\mathrm{d}t} e^{-\frac{\mathrm{i}\hat{H}_S t}{\hbar}} \\ = & -\frac{\mathrm{i}}{\hbar} e^{\frac{\mathrm{i}\hat{H}_S t}{\hbar}} [\hat{H}_S, \rho_S(t)] e^{-\frac{\mathrm{i}\hat{H}_S t}{\hbar}} \\ & -\frac{1}{\hbar^2} \int_0^\infty \mathrm{d}\tau \, \mathrm{Tr}_B \left\{ e^{\frac{\mathrm{i}\hat{H}_S t}{\hbar}} \left[\hat{H}_I, \left[\hat{H}_I(-\tau), \rho_S(t) \otimes \rho_B\right]\right] e^{-\frac{\mathrm{i}\hat{H}_S t}{\hbar}} \right\} \end{aligned} \tag{1.37}$$

Pre-multiplying by $e^{-\frac{\mathrm{i}\hat{H}_S t}{\hbar}}$ and post multiplying by $e^{\frac{\mathrm{i}\hat{H}_S t}{\hbar}}$ gives:

$$\frac{\mathrm{d}\rho_S(t)}{\mathrm{d}t} = -\frac{\mathrm{i}}{\hbar}[\hat{H}_S, \rho_S(t)] - \frac{1}{\hbar^2} \int_0^\infty \mathrm{d}\tau \, \mathrm{Tr}_B \left\{ \left[\hat{H}_I, \left[\hat{H}_I(-\tau), \rho_S(t) \otimes \rho_B\right]\right] \right\} \tag{1.38}$$

Equation (1.38) is the general form of a Markovian master equation [57, 58, 59]. The first term is the Von-Neumann term and represents the free evolution of the system whereas the second term is a superoperator which describes the dissipation of the system undergoing decoherence. The common issue with an equation of this form is that it does not always conserve probability and can lead to situations which are unphysical [60]. The only form of master equation which does guarantee physicality is one of Lindblad type [61, 62] and so it is often necessary, albeit somewhat *ad-hoc*, to transform the above equation accordingly. The Lindblad transformation is explained and discussed in detail throughout this thesis, the general form of a Lindblad equation is given by [61]

$$\frac{\mathrm{d}\rho}{\mathrm{d}t} = -\frac{\mathrm{i}}{\hbar}[\hat{H}, \rho] + \frac{1}{2} \sum_j \left\{ [\hat{L}_j, \rho \hat{L}_j^\dagger] + [\hat{L}_j \rho, \hat{L}_j^\dagger] \right\} \tag{1.39}$$

where once again the free evolution is described by the first term and the dissipation is now given in terms of Lindblad operators, L_j [61].

The assumption that the environment possesses a very small relaxation time of the environment renders a memoryless system as its state only depending on the present time and not its history; this is known as the Markovian framework and works on the most part for classical environments which are large enough that interactions with a quantum system have negligible back action. For more susceptible reservoirs, one would need to consider such an impact of the system on the bath; such a model would be non-Markovian in nature: Markovian models represent only a small group in a much larger set dominated by non-Markovian models which can vary greatly in their definition. As a result there are many different ways to characterise a non-Markovian system [63] and it is advised to use more than one measure when considering these kinds of models. In this line of work, the Markovian framework is preferred due to its elegance and simplicity, Non-Markovian dynamics are therefore not discussed, for a review please refer to [64].

As will be discussed in this thesis, there are many issues raised when considering the master equation to solve physical situations: one such issue exist in the requirement to add terms that ensure matrix positivity to the equations thus making it of Lindblad type; this adjustment has negligible impact when utilised in the high temperature limit like that used in Quantum Brownian Motion [48, 57, 60] due to their inverse proportionality to temperature. The justification of such terms becomes more difficult when the low temperature limits are considered, such as in this thesis, as these terms may no longer become a small perturbation.

Another issue raised in this approach is the impact of frequency shift and squeezing terms in the Hamiltonian which arise from construction of a Lindblad dissipator and can impact on system observables, potentially leading to mischaracterisation. The decision to omit or renormalise these terms for the case of the harmonic oscillator is discussed along with analysis on the impacts made by terms of this nature on more complex systems, in particular the SQUID.

We will next review the phenomenon that is Quantum Brownian Motion, which lays the foundations for a lot of the work developed in this thesis. The key analytical steps will be highlighted and assumptions, and their validity, will be discussed in detail.

1.5 Quantum Brownian Motion

A commonly used method for extracting a master equation for solid state ensembles originates from the Caldeira Leggett equation [65, 66], a first attempt to describe environmentally induced dissipation which naturally extends into the phenomenon of Quantum Brownian Motion [57]. By the end of this section one will see that the equation obtained is Markovian in nature, despite looking different to those seen in quantum optics. The methods used here are a natural starting point in the analysis presented in the thesis.

QBM describes the dynamics of a particle in a general potential $U(\hat{x})$ coupled to an Ohmic bath modelled as an infinite number of harmonic oscillators in the high temperature limit. The separate Hamiltonian of each

subsystem, as well as the interaction between them, is given by [48, 57]:

$$\begin{aligned} H_S &= \frac{\hat{p}^2}{2m} + U(\hat{x}) \\ H_B &= \sum_n \frac{\hat{p}_n^2}{2m_n} + \frac{1}{2} m_n \omega_n^2 \hat{x}_n^2 \\ H_I &= -\hat{x} \sum_n \kappa_n \hat{x}_n = -\hat{x}\hat{B} \end{aligned} \tag{1.40}$$

where $\hat{p}$, $\hat{p}_n$, $\hat{x}$ and $\hat{x}_n$ represent the momentum and position operators of the system and environment respectively. For the case of the harmonic oscillator $U(\hat{x}) = m\omega_0^2\hat{x}^2/2$ where m, m_n, ω_0 and ω_n mass and the frequency of the system and each environmental mode respectively; we will see, however, in later sections how this can be extended to more complex potential such as that possessed by the SQUID. The bath operator, $\hat{B} = \sum_n \kappa_n \hat{x}_n$, will be used when defining the bath correlation functions. The operators in (1.40) are connected through the familiar commutation relation:

$$[\hat{x}, \hat{p}] = i\hbar \tag{1.41}$$

Since linear coupling is assumed between both system and bath mode position, the coupling is said to be bilinear; this gives rise to a renormalisation of the potential, similar in nature to a Lamb shift, the double counting of which can be prevented by introducing a counter term $H_C = \sum_n \frac{\kappa_n^2}{2m_n\omega_n^2}\hat{x}^2$ into the total Hamiltonian. This added term transforms the total Hamiltonian to give

[59]:

$$\begin{aligned} H &= H_S + H_B + H_I + H_C \\ &= \frac{\hat{p}^2}{2m} + \frac{1}{2}m\omega_0^2\hat{x}^2 + \frac{1}{2}\sum_n \left[\frac{\hat{p}_n^2}{m_n} + m_n\omega_n^2\left(\hat{x}_n - \frac{\kappa_n}{m_n\omega_n^2}\hat{x}\right)^2\right] \end{aligned} \tag{1.42}$$

In solid state systems such as the SQUID, this renormalisation of the Hamiltonian is equivalent to the shift in system parameters such as inductance and capacitance as a result of coupling to the environment [36, 67, 68]. Said quantities in the system Hamiltonian are therefore not the bare values of the system alone but shifted by a value proportional to the coupling strength with the environment; this will be discussed in more detail below.

We can write equation (1.38) in terms of free evolution and dissipation terms such that $\frac{\mathrm{d}}{\mathrm{d}t}\rho_S(t) = -\frac{\mathrm{i}}{\hbar}[\hat{H}_S, \rho_S(t)] + \mathcal{K}\rho_S(t)$, where:

$$\mathcal{K}\rho_S(t) = -\frac{1}{\hbar^2}\int_0^\infty \mathrm{d}\tau\, \mathrm{Tr}_B\left\{\,[H_I, [H_I(-\tau), \rho_S(t)\otimes\rho_B]]\,\right\} \tag{1.43}$$

The commutator in this expression can be rewritten in terms of bath correlation functions. Substituting the interaction Hamiltonian for this model in Eq. (1.40) and rearranging using the nature of commutators gives:

$$\begin{aligned} \mathcal{K}\rho_S(t) = -\frac{1}{\hbar^2}\int_0^\infty \mathrm{d}\tau \frac{1}{2}\Big(&\Big\langle[\hat{B}, \hat{B}(-\tau)]\Big\rangle_B[\hat{x}, \{\hat{x}(-\tau), \rho_S\}] \\ &+ \Big\langle\{\hat{B}, \hat{B}(-\tau)\}\Big\rangle_B[\hat{x}, [\hat{x}(-\tau), \rho_S]]\Big) \end{aligned} \tag{1.44}$$

where the expectation value of an operator is given by the partial trace of

the tensor product of said operator with the bath density matrix, $\langle A \rangle_B = \mathrm{Tr}_B \{A\rho\}$. The expectation value of the product of the bath functions are at different times define the correlation functions $C_1(\tau)$, and its Hermitian conjugate, $C_2(\tau)$:

$$\begin{aligned} C_1(\tau) &= \left\langle \hat{B}\hat{B}(\tau) \right\rangle_B \\ C_2(\tau) &= \left\langle \hat{B}(\tau)\hat{B} \right\rangle_B \end{aligned} \tag{1.45}$$

By expressing the bath functions in terms of annihilation and creation operators, as shown in detail later, as well as using the thermalised state of the bath, one can express the commutation, $[C_1(\tau), C_2(\tau)] = C_1(\tau)C_2(\tau) - C_2(\tau)C_1(\tau)$, and anticommutation, $\{C_1(\tau), C_2(\tau)\} = C_1(\tau)C_2(\tau) + C_2(\tau)C_1(\tau)$, of the two correlation functions which have the form:

$$C_1(\tau) = \sum_n \frac{\hbar\kappa_n^2}{2m_n\omega_n} \left(\coth\left(\frac{\hbar\omega_n}{2k_BT}\right) \cos(\omega_n\tau) - \mathrm{i}\sin(\omega_n\tau) \right) \tag{1.46}$$

and

$$C_2(\tau) = \sum_n \frac{\hbar\kappa_n^2}{2m_n\omega_n} \left(\coth\left(\frac{\hbar\omega_n}{2k_BT}\right) \cos(\omega_n\tau) + \mathrm{i}\sin(\omega_n\tau) \right) \tag{1.47}$$

by combining Eq. (1.46) and Eq. (2.14) in linear combinations to yield two

new quantities:

$$\begin{aligned} C_1(\tau) - C_2(\tau) &= \left\langle [\hat{B}, \hat{B}(-\tau)] \right\rangle_B = -2\mathrm{i}\hbar \sum_n \frac{\kappa_n^2}{2m_n\omega_n} \sin(\omega_n \tau) = -\mathrm{i}D(-\tau) \\ C_1(\tau) + C_2(\tau) &= \left\langle \{\hat{B}, \hat{B}(-\tau)\} \right\rangle_B = 2\hbar \sum_n \frac{\kappa_n^2}{2m_n\omega_n} \coth\left(\frac{\hbar\omega_n}{2k_BT}\right) \cos(\omega_n \tau) \\ &= D_1(-\tau) \end{aligned} \tag{1.48}$$

The first quantity in (1.48), $D(-\tau)$, is known as the dissipation kernel while the second quantity, $D_1(-\tau)$, is termed the noise kernel [57]; named accordingly due to the respective information which they possess which contributes to a system's decoherence channel. At this stage we introduce the spectral density, which for a thermal bath, is given by:

$$J(\omega) = \sum_n \frac{\kappa_n^2}{2m_n\omega_n} \delta(\omega - \omega_n) \tag{1.49}$$

Using the property of the Dirac delta function:

$$f(n') = \int_{-\infty}^{\infty} dn f(n) \delta(n - n') \tag{1.50}$$

the dissipation and noise kernels can therefore be written in terms of this spectral density. The resulting expressions are:

$$\begin{aligned} D(-\tau) &= 2\hbar \int_0^{\infty} d\omega J(\omega) \sin(\omega\tau) \\ D_1(-\tau) &= 2\hbar \int_0^{\infty} d\omega J(\omega) \coth\left(\frac{\hbar\omega}{2k_BT}\right) \cos(\omega\tau) \end{aligned} \tag{1.51}$$

Expressions of this form play a pivotal role in the analysis that follows in later sections as it allows the master equation to be integrated:

$$\begin{aligned}\frac{d}{dt}\rho_S(t) = &-\frac{\mathrm{i}}{\hbar}[H_S, \rho_S(t)] \\ &+\frac{1}{\hbar^2}\int_0^\infty \mathrm{d}\tau\Big(\frac{\mathrm{i}}{2}D(-\tau)[\hat{x}, \{\hat{x}(-\tau), \rho_S(t)\}] \\ &-\frac{1}{2}D_1(-\tau)[\hat{x}, [\hat{x}(-\tau), \rho_S(t)]]\Big)\end{aligned} \tag{1.52}$$

Evaluation of the integrals presented above is made possible by use of transformation into the interaction picture once more, such that $\hat{x}(-\tau) = \exp\left(-\mathrm{i}\hat{H}_S\tau/\hbar\right)\cdot\hat{x}\cdot\exp\left(\mathrm{i}\hat{H}_S\tau/\hbar\right)$ and expanding the τ dependent functions by use of the Baker-Campbell-Hausdorff formula [69]:

$$\boxed{e^{\hat{X}}\hat{Y}e^{-\hat{X}} = \hat{Y} + [\hat{X}, \hat{Y}] + \frac{1}{2!}[\hat{X}, [\hat{X}, \hat{Y}]] + \frac{1}{3!}[\hat{X}, [\hat{X}, [\hat{X}, \hat{Y}]]] + ...} \tag{1.53}$$

This expansion is a fundamental part of the work used in this thesis as it allows the equations to be simplified and therefore remain analytically solvable. For sufficiently small τ, as often assumed in the literature [48, 57], the series may be truncated at first order

$$\hat{x}(-\tau) \approx \hat{x}(0) - \frac{\mathrm{i}\tau}{\hbar}\left[\hat{H}_S, \hat{x}(0)\right] = \hat{x} - \frac{\tau}{m}\hat{p} \tag{1.54}$$

gives rise to the Caldeira-Leggett equation [66]:

$$\frac{d}{dt}\rho_S(t) = \underbrace{-\frac{\mathrm{i}}{\hbar}[H_S, \rho_S(t)]}_{\text{Free evolution}}\underbrace{-\frac{\mathrm{i}\gamma}{\hbar}[\hat{x}, \{\hat{p}, \rho_S(t)\}]}_{\text{Dissipation}}\underbrace{-\frac{2m\gamma k_B T}{\hbar^2}[\hat{x}, [\hat{x}, \rho_S(t)]]}_{\text{Noise}} \tag{1.55}$$

where the terms in Eq. (1.55) are labelled with their physical description.

This equation can be easily transformed into a Lindblad type equation through the addition of a minimally invasive term in the high temperature limit, the process for which is explained in greater detail later in this work. The framework given above is the foundation of the work explored in this thesis. Later we will also discuss the validity of truncation of the above BCH series, as the affect of logarithmic terms are overlooked. For the case of the Harmonic oscillator the whole series can be evaluated and the equation is therefore exact [70]. It therefore raises questions on the validity of implementing these master equation techniques on any system other than the HO, something that will be investigated here.

Exploring a different system to test the order of approximation and the approximations themselves, as well altering the interaction between system and bath, the temperature of which impacts greatly on the long term dynamics, sheds a new light on the master equation approaches for systems other than the harmonic oscillator or Brownian particle. The next chapter will highlight how changing these factors may impact on the decoherence model of non-trivial system, in particular the SQUID, and show how external degrees of freedom may play a larger role in dissipation than that shown in first order master equation models.

Chapter 2

Master Equation Techniques in SQUIDS

2.1 Introduction

In this chapter we compare predictions made by different levels of approximation using master equation techniques and discuss their importance in characterising superconducting ensembles, namely the case of a SQUID ring inductively coupled to an Ohmic bath whose nature suitably describes that of a tank circuit, to which SQUIDs are commonly coupled [36, 71]. As well as their large number of applications in quantum technologies, the non-perturbative nature of the non-linear Josephson Junction term in the SQUID Hamiltonian provides a natural method of testing the suitability of using master equations for quantitative engineering in systems other than those seen in quantum optics, with which the master equation framework is most closely associated [57, 47].

It has been shown in the literature that an exact solution to QBM of an HO has been found to all orders of Born Approximation [72, 73] which shows a logarithmic dependence on bath cut-off frequency Ω; this suggests that Ω must be finite, as it is treated in this thesis, proving the importance of appropriate bath characterisation in modelling quantum systems. Often the master equation for simpler systems is truncated to first order with the assumption that second order contributions are small if not negligible; this is often accepted due to the perturbative nature of the interaction with the bath.

This chapter will highlight the key features of higher order master equations and how they differ from their lower order counterparts; showing that early truncation neglects environmentally dependent terms for the case of the SQUID ring-bath ensemble. Equations are derived for first and second order approximation, in the sense of Eq. (1.54), using widely accepted techniques and their predictions compared through their influence on observable quantities at the steady state, such as purity and screening current. The analysis, and implications of each step, are discussed along with their generally bespoke nature which will become more apparent as we progress. Although relatively simple compared to that seen in the Born series expansion, the analysis presented here provides significant differences between first and second order models and gives good insight into the implications of using a master equation approach for non-trivial quantum systems.

2.2 Theory

We will next consider the general dissipator of the master equation (1.43) and apply it to a SQUID system coupled to an Ohmic bath, taking different

orders of B-C-H expansion (see Appendix B) to produce a dissipation model with a stronger dependence on external factors than previously shown.

2.2.1 A SQUID inductively Coupled To an Ohmic Bath

The model considered in this chapter consists of a SQUID coupled to a Ohmic bath modelled as an infinite number of harmonic oscillators at absolute zero temperature, the total Hamiltonian of which takes the form $H_{TOT} = H_S + H_B + H_I$. The separate Hamiltonian of each subsystem, as well as the interaction between them, is given in the external flux basis by:

$$\begin{aligned} H_S &= \frac{\hat{Q}^2}{2C} + \frac{\hat{\Phi}^2}{2L} - \hbar\nu \cos\left(\frac{2\pi}{\Phi_0}(\hat{\Phi} + \Phi_x)\right) \\ H_B &= \sum_n \frac{\hat{Q}_n^2}{2C_n} + \frac{\hat{\Phi}_n^2}{2L_n} \\ H_I &= -\hat{\Phi}\sum_n \kappa_n \hat{\Phi}_n = -\hat{\Phi}\hat{B}_\Phi \end{aligned} \tag{2.1}$$

where $\hat{Q}$, $\hat{Q}_n$, $\hat{\Phi}$ and $\hat{\Phi}_n$ represent the charge and flux operators of the system and environment respectively. C, C_n, and L_n are the capacitance and inductance of the system and each environmental mode respectively. C is analogous to the system's mass while L is an effective inductance, which is modified on coupling with an environment, an effect that will be discussed later. It is noted that an alternate approach would be to derive the Lagrangian using circuit theory for a SQUID coupled to a tank circuit, from that the Hamiltonians of both system, bath and interaction may be written exactly [74, 68]. The use of effective parameters however, as presented in this thesis, is sufficient to provide adequate findings.

The bare capacitance C_0 and inductance L_0 values are related to the system's natural frequency through the relation $\omega^2 = \frac{1}{L_0 C_0}$, for the case of inductive coupling, the capacitance undergoes no renormalisation and so $C = C_0$. The bath operator $\hat{B}_\Phi = \sum_n \kappa_n \Phi_n$ has the same properties as the bath function in the QBM case.

Using the same steps as those found in §1.4, one can use the above Hamiltonian to obtain the dissipator, $\mathcal{K}\rho_S(t)$ for this model:

$$\begin{aligned}\mathcal{K}\rho_S(t) - \frac{1}{\hbar^2}\int_0^\infty d\tau\, \mathrm{Tr}_B\left\{[H_I,[H_I(-\tau),\rho_S(t)]]\right\} \\ = -\frac{1}{\hbar^2}\int_0^\infty d\tau \frac{1}{2}\Big(\Big\langle[\hat{B}_\Phi,\hat{B}_\Phi(-\tau)]\Big\rangle_B[\hat{\Phi},\{\hat{\Phi}(-\tau),\rho_S\}] \\ + \Big\langle\{\hat{B}_\Phi,\hat{B}_\Phi(-\tau)\}_B\Big\rangle[\hat{\Phi},[\hat{\Phi}(-\tau),\rho_S]]\Big)\end{aligned} \tag{2.2}$$

In order to understand the applicability of master equation processes for bath characterisation, the key features and approximations used to produce the integral form of the dissipator will be discussed. We once again make use of the correlation functions, which in this case analogously take the form:

$$\begin{aligned}C_1(-\tau) &= \mathrm{Tr}_B\left\{\hat{B}\hat{B}(-\tau)\rho_B\right\} \\ C_2(-\tau) &= \mathrm{Tr}_B\left\{\hat{B}(-\tau)\hat{B}\rho_B\right\}\end{aligned} \tag{2.3}$$

Although the zero temperature limit will be explored for this model, it is important to understand the nature of all terms within this analysis; initially keeping the temperature dependence throughout key parts of the derivation accounts for this. Our starting point therefore requires the consideration of

a general environment, assumed to be a statistical ensemble that remains in thermal equilibrium at finite temperature, T, throughout its interaction with the system in question, in other words:

$$\rho_B = \frac{e^{-\beta H_B}}{\mathrm{Tr}_B\{e^{-\beta H_B}\}} \tag{2.4}$$

where $\beta = \frac{1}{k_B T}$. The partial trace of any quantity over the density matrix of the bath defines the average of the quantity [48, 57]:

$$\mathrm{Tr}_B\left\{\frac{Ae^{-\beta H_B}}{\mathrm{Tr}_B\, e^{-\beta H_B}}\right\} = \Big\langle A \Big\rangle_B \tag{2.5}$$

Using the above definitions, we can proceed to the Correlation function, using equation Eq. (2.3) the correlation function can simply be written as:

$$C(\tau) = \mathrm{Tr}_B\left\{\hat{B}\hat{B}(-\tau)\rho\right\} = \Big\langle \hat{B}\hat{B}(-\tau)\Big\rangle_B \tag{2.6}$$

where the bath operator $\hat{B}$ is given by:

$$\hat{B} = \sum_n \kappa_n \hat{\Phi}_n = \sum_n \sqrt{\frac{\hbar\kappa_n^2}{2C_n\omega_n}}\Big(\hat{b}_n^\dagger + \hat{b}_n\Big) \tag{2.7}$$

and $\hat{b}_n^\dagger$ and $\hat{b}_n$ are the bosonic creation and annihilation operators:

$$b_n^\dagger = \frac{1}{\sqrt{2}}\Big(\sqrt{\frac{C_n\omega_n}{\hbar}}\hat{\Phi}_n + \mathrm{i}\sqrt{\frac{1}{C_n\omega_n\hbar}}\hat{Q}_n\Big)$$
$$\hat{b}_n = \frac{1}{\sqrt{2}}\Big(\sqrt{\frac{C_n\omega_n}{\hbar}}\hat{\Phi}_n - \mathrm{i}\sqrt{\frac{1}{C_n\omega_n\hbar}}\hat{Q}_n\Big)$$

$\hat{B}(-\tau)$ can be written in the interaction picture as:

$$\hat{B}(-\tau) = e^{-\frac{\mathrm{i}H_B\tau}{\hbar}}\hat{B}e^{\frac{\mathrm{i}H_B\tau}{\hbar}} = \sum_n \sqrt{\frac{\hbar\kappa_n^2}{2C_n\omega_n}}e^{-\frac{\mathrm{i}H_B\tau}{\hbar}}\left(\hat{b}_n^\dagger + \hat{b}_n\right)e^{\frac{\mathrm{i}H_B\tau}{\hbar}}$$

The correlation function $\left\langle \hat{B}\hat{B}(-\tau)\right\rangle_B$ can thus be rewritten:

$$\left\langle \hat{B}\hat{B}(-\tau)\right\rangle_B = \sum_n \frac{\hbar\kappa_n^2}{2C_n\omega_n}\left\langle \left(\hat{b}_n^\dagger + \hat{b}_n\right)\left(e^{-\frac{\mathrm{i}H_B\tau}{\hbar}}\hat{b}_n^\dagger e^{\frac{\mathrm{i}H_B\tau}{\hbar}} + e^{-\frac{\mathrm{i}H_B\tau}{\hbar}}\hat{b}_n e^{\frac{\mathrm{i}H_B\tau}{\hbar}}\right)\right\rangle$$

Expanding the brackets out and noting that $H_B = \hbar\omega_n(\hat{n}_n + 1/2)$, the expression now becomes:

$$\begin{aligned}\left\langle \hat{B}\hat{B}(-\tau)\right\rangle_B = \sum_n \frac{\hbar\kappa_n^2}{2C_n\omega_n}\Big\langle &\hat{b}_n^\dagger e^{-\mathrm{i}\omega_n\tau(\hat{n}_n+1/2)}\hat{b}_n^\dagger e^{\mathrm{i}\omega_n\tau(\hat{n}_n+1/2)} \\ &+ \hat{b}_n^\dagger e^{-\mathrm{i}\omega_n\tau(\hat{n}_n+1/2)}\hat{b}_n e^{\mathrm{i}\omega_n\tau(\hat{n}_n+1/2)} \\ &+ \hat{b}_n e^{-\mathrm{i}\omega_n\tau(\hat{n}_n+1/2)}\hat{b}_n^\dagger e^{\mathrm{i}\omega_n\tau(\hat{n}_n+1/2)} \\ &+ \hat{b}_n e^{-\mathrm{i}\omega_n\tau(\hat{n}_n+1/2)}\hat{b}_n e^{\mathrm{i}\omega_n\tau(\hat{n}_n+1/2)}\Big\rangle\end{aligned}$$

Since the factors of 1/2 in the exponents cancel, the correlation function reduces to:

$$\begin{aligned}\left\langle \hat{B}\hat{B}(-\tau)\right\rangle_B = \sum_n \frac{\hbar\kappa_n^2}{2C_n\omega_n}\Big\langle &\hat{b}_n^\dagger e^{-\mathrm{i}\omega_n\tau\hat{n}_n}\hat{b}_n^\dagger e^{\mathrm{i}\omega_n\tau\hat{n}_n} + \hat{b}_n^\dagger e^{-\mathrm{i}\omega_n\tau\hat{n}_n}\hat{b}_n e^{\mathrm{i}\omega_n\tau\hat{n}_n} \\ &+ \hat{b}_n e^{-\mathrm{i}\omega_n\tau\hat{n}_n}\hat{b}_n^\dagger e^{\mathrm{i}\omega_n\tau\hat{n}_n} + \hat{b}_n e^{-\mathrm{i}\omega_n\tau\hat{n}_n}\hat{b}_n e^{\mathrm{i}\omega_n\tau\hat{n}_n}\Big\rangle\end{aligned}$$

Re-expressing this using Baker-Campbell-Hausdorff formula, gives:

$$e^{-\mathrm{i}\omega_n\tau\hat{n}_n}\hat{b}_n^\dagger e^{\mathrm{i}\omega_n\tau\hat{n}_n} = \hat{b}_n^\dagger + (-\mathrm{i}\omega_n\tau)[\hat{n}_n, \hat{b}_n^\dagger] + \frac{(-\mathrm{i}\omega_n\tau)^2}{2!}[\hat{n}_n, [\hat{n}_n, \hat{b}_n^\dagger]] + \frac{(-\mathrm{i}\omega_n\tau)^3}{3!}[\hat{n}_n, [\hat{n}_n, [\hat{n}_n, \hat{b}_n^\dagger]]] + ...$$

Using the commutation relations for $\hat{n}_n$, $\hat{b}_n^\dagger$ and $\hat{b}_n$:

$$\hat{n}_n = \hat{b}_n^\dagger \hat{b}_n$$
$$[\hat{b}_n, \hat{b}_m^\dagger] = \delta_{n,m}$$
$$\Rightarrow \hat{b}_n\hat{b}_n^\dagger = \hat{\mathbb{1}} + \hat{n}_n$$

where $\delta_{n,m}$ is the kronecker delta, equal to 1 if $n = m$ and 0 for all other cases. It is possible to find the commutator between the creation and number operators:

$$[\hat{n}_n, \hat{b}_m^\dagger] = [\hat{b}_n^\dagger\hat{b}_n, \hat{b}_m^\dagger] = \hat{b}_n^\dagger[\hat{b}_n, \hat{b}_m^\dagger] + [\hat{b}_n^\dagger, \hat{b}_m^\dagger]\hat{b}_n$$
$$= \hat{b}_n^\dagger\delta_{n,m}$$

which yields:

$$e^{-\mathrm{i}\omega_n\tau\hat{n}_n}\hat{b}_n^\dagger e^{\mathrm{i}\omega_n\tau\hat{n}_n} = \hat{b}_n^\dagger\left(1 + (-\mathrm{i}\omega_n\tau) + \frac{(-\mathrm{i}\omega_n\tau)^2}{2!} + \frac{(-\mathrm{i}\omega_n\tau)^3}{3!} + ...\right)$$

The above is simply the power series for the exponential, thus the exponential term can be written as:

$$e^{-\mathrm{i}\omega_n\tau\hat{n}_n}\hat{b}_n^\dagger e^{\mathrm{i}\omega_n\tau\hat{n}_n} = \hat{b}_n^\dagger e^{-\mathrm{i}\omega_n\tau}$$

Likewise, using the same method it can be shown that:

$$e^{-\mathrm{i}\omega_n\tau\hat{n}}\hat{b}_n e^{\mathrm{i}\omega_n\tau\hat{n}} = \hat{b}_n e^{\mathrm{i}\omega_n\tau}$$

Using the previous two identities and substituting them into the expression for the correlation function gives the result:

$$\left\langle \hat{B}\hat{B}(-\tau)\right\rangle_B = \sum_n \frac{\hbar\kappa_n^2}{2C_n\omega_n}\left\langle \hat{b}_n^{\dagger 2}e^{-\mathrm{i}\omega_n\tau} + \hat{b}_n^\dagger\hat{b}_n e^{\mathrm{i}\omega_n\tau} + \hat{b}_n^2 e^{\mathrm{i}\omega_n\tau} + \hat{b}_n\hat{b}_n^\dagger e^{-\mathrm{i}\omega_n\tau}\right\rangle \quad (2.8)$$

In order to ensure single photon energy conservation, only terms that maintain the initial state of the system are considered; this is known as the rotating wave approximation [48]. In terms of this analysis, only $\hat{b}_n\hat{b}_n^\dagger$ and $\hat{b}_n^\dagger\hat{b}_n$ terms are kept and other non conserving terms are neglected. Taking this into consideration, the correlation function now becomes:

$$\left\langle \hat{B}\hat{B}(-\tau)\right\rangle_B = \sum_n \frac{\hbar\kappa_n^2}{2C_n\omega_n}\left\langle \hat{b}_n^\dagger\hat{b}_n e^{\mathrm{i}\omega_n\tau} + \hat{b}_n\hat{b}_n^\dagger e^{-\mathrm{i}\omega_n\tau}\right\rangle \quad (2.9)$$

If we recall the definition of the number operator, $\hat{n}_n = \hat{b}_n^\dagger\hat{b}_n$ as well as the commutation relation between annihilation and creation operators, substitution into equation (2.9) yields:

$$\left\langle \hat{B}\hat{B}(-\tau)\right\rangle_B = \sum_n \frac{\hbar\kappa_n^2}{2C_n\omega_n}\left\langle \hat{n}_n e^{\mathrm{i}\omega_n\tau} + (\mathbb{1} + \hat{n}_n)e^{-\mathrm{i}\omega_n\tau}\right\rangle \quad (2.10)$$

Since $\hat{n}_n$ is the number operator, the mean value of this operator gives the average occupation number of the n^{th} oscillator [48] in the environment and

is given by the Bose-Einstein distribution [48, 75]:

$$\langle n \rangle = N_n = \frac{1}{e^{\frac{\hbar\omega_n}{k_B T}} - 1} \tag{2.11}$$

Substituting this result into expression (2.10) yields:

$$\left\langle \hat{B}\hat{B}(-\tau) \right\rangle_B = \sum_n \frac{\hbar\kappa_n^2}{2C_n\omega_n} \left(N_n e^{\mathrm{i}\omega_n\tau} + (1+N_n) e^{-\mathrm{i}\omega_n\tau} \right) \tag{2.12}$$

Using Euler's formula Eq. (2.12) can be rewritten [76]:

$$\begin{aligned} \left\langle \hat{B}\hat{B}(-\tau) \right\rangle_B &= \sum_n \frac{\hbar\kappa_n^2}{2C_n\omega_n} \Big(N(\cos\omega_n\tau + \mathrm{i}\sin\omega_n\tau) \\ &\qquad + (1+N_n)(\cos\omega_n\tau - \mathrm{i}\sin\omega_n\tau) \Big) \\ &= \sum_n \frac{\hbar\kappa_n^2}{2C_n\omega_n} \Big((1+2N_n)\cos\omega_n\tau - \mathrm{i}\sin\omega_n\tau \Big) \end{aligned}$$

Use of Eq. (2.11) allows $1 + 2N_n$ to be written as:

$$\begin{aligned} 1 + 2N_n &= 1 + \frac{2}{e^{\frac{\hbar\omega_n}{k_B T}} - 1} \\ &= \frac{e^{\frac{\hbar\omega_n}{k_B T}} + 1}{e^{\frac{\hbar\omega_n}{k_B T}} - 1} \\ &= \frac{e^{\frac{\hbar\omega_n}{2k_B T}} + e^{-\frac{\hbar\omega_n}{2k_B T}}}{e^{\frac{\hbar\omega_n}{2k_B T}} - e^{-\frac{\hbar\omega_n}{2k_B T}}} \\ &= \frac{\cosh\left(\frac{\hbar\omega_n}{2k_B T}\right)}{\sinh\left(\frac{\hbar\omega_n}{2k_B T}\right)} \\ \Rightarrow 1 + 2N_n &= \coth\left(\frac{\hbar\omega_n}{2k_B T}\right) \end{aligned}$$

Finally the correlation function can therefore be expressed as:

$$\left\langle \hat{B}\hat{B}(-\tau)\right\rangle_B = \sum_n \frac{\hbar\kappa_n^2}{2C_n\omega_n}\left(\coth\left(\frac{\hbar\omega_n}{2k_BT}\right)\cos\left(\omega_n\tau\right) - \mathrm{i}\sin\left(\omega_n\tau\right)\right) \quad (2.13)$$

Using the same method, it can also be shown that:

$$\left\langle \hat{B}(-\tau)\hat{B}\right\rangle_B = \sum_n \frac{\hbar\kappa_n^2}{2C_n\omega_n}\left(\coth\left(\frac{\hbar\omega_n}{2k_BT}\right)\cos\left(\omega_n\tau\right) + \mathrm{i}\sin\left(\omega_n\tau\right)\right) \quad (2.14)$$

Correlation functions (2.13) and (2.14) can be combined to form two new quantities:

$$\begin{aligned}\left\langle \hat{B}\hat{B}(-\tau)\right\rangle_B - \left\langle \hat{B}(-\tau)\hat{B}\right\rangle_B &= \left\langle [\hat{B},\hat{B}(-\tau)]\right\rangle_B \\ \left\langle \hat{B}\hat{B}(-\tau)\right\rangle_B + \left\langle \hat{B}(-\tau)\hat{B}\right\rangle_B &= \left\langle \{\hat{B},\hat{B}(-\tau)\}\right\rangle_B\end{aligned} \quad (2.15)$$

which are written explicitly as:

$$\begin{aligned}\left\langle [\hat{B},\hat{B}(-\tau)]\right\rangle_B &= -2\mathrm{i}\hbar\sum_n \frac{\kappa_n^2}{2C_n\omega_n}\sin\left(\omega_n\tau\right) = -\mathrm{i}D(-\tau) \\ \left\langle \{\hat{B},\hat{B}(-\tau)\}\right\rangle_B &= 2\hbar\sum_n \frac{\kappa_n^2}{2C_n\omega_n}\coth\left(\frac{\hbar\omega_n}{2k_BT}\right)\cos\left(\omega_n\tau\right) = D_1(-\tau)\end{aligned} \quad (2.16)$$

The first quantity in (2.16), $D(-\tau)$, is known as the dissipation [57] kernel while the second quantity, $D_1(-\tau)$, is termed the noise kernel [57]. At this stage we introduce a function that describes the physical properties of the environment, the spectral density. In very much the same way that the power spectral density is related to the autocorrelation function in signal processing [77], the effective spectral density is related to the bath correlation function

via a Fourier transform: It is considered *effective* as its different couplings carry weightings and are smoothed when written in terms of the spectral density, $n(\omega) = (\pi/\hbar)\sum_n \delta(\omega - \omega_n)$ [78]. The effective spectral density for a thermal bath is given by:

$$J(\omega) = \sum_n \frac{\kappa_n^2}{2C_n\omega_n}\delta(\omega - \omega_n)$$

using the property of the Dirac Delta function:

$$f(n') = \int_{-\infty}^{\infty} \mathrm{d}n f(n)\delta(n - n')$$

since the frequencies of the bath modes are real and positive, only the positive region of free space is included and thus the dissipation and noise kernels can be written in terms of the spectral density. The resulting expressions are:

$$\begin{aligned} D(-\tau) &= 2\hbar \int_0^{\infty} \mathrm{d}\omega J(\omega)\sin(\omega\tau) \\ D_1(-\tau) &= 2\hbar \int_0^{\infty} \mathrm{d}\omega J(\omega)\cos(\omega\tau)\coth\left(\frac{\hbar\omega}{2k_BT}\right) \end{aligned}$$

For an Ohmic Bath, the zero temperature limit is taken for the above kernels, since $\lim_{x\to\infty}\coth(x) = 1$, this yields:

$$\begin{aligned} D(-\tau) &= 2\hbar \int_0^{\infty} \mathrm{d}\omega J(\omega)\sin(\omega\tau) \\ D_1(-\tau) &= 2\hbar \int_0^{\infty} \mathrm{d}\omega J(\omega)\cos(\omega\tau) \end{aligned} \tag{2.17}$$

The master equation, in terms of the newly defined noise and dissipation

kernels, is thus:

$$\frac{\mathrm{d}}{\mathrm{d}t}\rho_S(t) = -\frac{\mathrm{i}}{\hbar}[H_S, \rho_S(t)] + \frac{1}{\hbar^2}\int_0^\infty \mathrm{d}\tau\Big(\frac{\mathrm{i}}{2}D(-\tau)[\hat{\Phi}, \{\hat{\Phi}(-\tau), \rho_S(t)\}] - \frac{1}{2}D_1(-\tau)[\hat{\Phi}, [\hat{\Phi}(-\tau), \rho_S(t)]]\Big) \tag{2.18}$$

2.2.1.1 Spectral Density and Kernel Evaluation

As discussed in Chapter 1, an Ohmic bath possesses a linear damping rate independent of frequency. The relationship between the bath's effective spectral density and frequency in the low frequency limit is also linear due to the smoothing of $J(\omega) = \sum_n \delta(\omega - \omega_n)$ [78, 79], that is to say that if the effective spectral density is flat over over a finite range of relevant frequencies, the spectral density in the low frequency limit may be written:

$$J(\omega) = \frac{2C\gamma}{\pi}\omega$$

where γ is the damping coefficient representing the dissipative effect of the bath [57]. In a high frequency regime, a cut-off frequency is required, to ensure convergence, and so the spectral density becomes:

$$J(\omega) = \frac{2C\gamma}{\pi}\omega\frac{\Omega^2}{\Omega^2 + \omega^2} \tag{2.19}$$

where Ω is a cut-off frequency which yields the Lorentz-Drude cut-off function [48, 57]. It is worth noting that a Lorentz Drude cut-off is chosen here however the choice of cut-off can take many forms [79]. All forms are valid provided they give the appropriate behaviour in the high frequency limit.

The explicit expressions for the dissipation and noise kernels are given

by:

$$D(-\tau) = 2C\gamma\hbar\Omega^2 e^{-\Omega|\tau|}\,\mathrm{sgn}\,\tau$$

and

$$D_1(-\tau) = \frac{2C\hbar\gamma\Omega^2\omega_c}{\pi}\frac{\pi}{\Omega}e^{-\Omega|\tau|}$$

respectively. Although the expression for the dissipation kernel is exact, the choice of a Lorentz Drude cut off in the zero temperature limit brings with it the necessity to approximate the noise kernel so that convergence is ensured. As a result, the results presented in this thesis show the minimal effect on system dynamics and further analysis, which lies beyond the scope of this thesis, is expected to put greater emphasis on the effects presented here. For details on how to find the explicit form of the kernels and the approximations associated to the noise kernel, please refer to Appendix C. Substituting both kernels in to the integral form of the master equation [80] allows it to be written as:

$$\frac{d}{dt}\rho_S(t) = -\frac{\mathrm{i}}{\hbar}[H_S, \rho_S(t)] + \frac{C\gamma\Omega}{\hbar}\int_0^\infty d\tau\Big(\mathrm{i}\Omega e^{-\Omega|\tau|}[\hat{\Phi}, \{\hat{\Phi}(-\tau), \rho_S(t)\}] - \frac{\omega_0}{2}e^{-\Omega|\tau|}(-\tau)[\hat{\Phi}, [\hat{\Phi}(-\tau), \rho_S(t)]]\Big) \tag{2.20}$$

This expression allows us to integrate with respect to τ which requires expanding the correlation-time-dependent flux, $\hat{\Phi}(-\tau)$, as a power series and truncating at the appropriate level of approximation; this will be shown in the next section.

2.2.1.2 Integral Evaluation

Expression Eq. (2.20) has been obtained by use of familiar techniques associated with the Born Markov framework, whilst taking the zero temperature limit and approximating the noise kernel by $D_1(\tau) \approx \omega_c \int (J(\omega)/\omega) \cos(\omega\tau)\, \mathrm{d}\tau$. To evaluate the integral form of the master equation and produce its final form, the correlation-time-dependent flux is expanded as a power series in τ such that:

$$\hat{\Phi}(-\tau) = \sum_n \hat{A}_n[\hat{\Phi}]\tau^n \tag{2.21}$$

where the $A_n[\hat{\Phi}]$ terms are found by equating powers of τ from the Baker Campbell Hausdorff expansion of $\hat{\Phi}(\tau) = e^{-\mathrm{i}\hat{H}_s\tau/\hbar}\hat{\Phi}e^{\mathrm{i}\hat{H}_s\tau/\hbar}$.

$$\begin{aligned}\hat{\Phi}(-\tau) = \hat{\Phi} + \tau\left[-\frac{i\hat{H}_S}{\hbar}, \hat{\Phi}\right] + \frac{\tau^2}{2!}\left[-\frac{i\hat{H}_S}{\hbar}, \left[-\frac{i\hat{H}_S}{\hbar}, \hat{\Phi}\right]\right] \\ + \cdots + \frac{\tau^n}{n!}\left[-\frac{i\hat{H}_S}{\hbar}, ..., \left[-\frac{i\hat{H}_S}{\hbar}, \hat{\Phi}\right]\right]\end{aligned} \tag{2.22}$$

The master equation can therefore be written:

$$\begin{aligned}\frac{d}{dt}\rho_S(t) = -\frac{\mathrm{i}}{\hbar}[H_S, \rho_S(t)] + \frac{C\gamma\Omega}{\hbar}\sum_n \int_0^\infty \tau^n e^{-\Omega|\tau|} d\tau \Big(\mathrm{i}\Omega[\hat{\Phi}, \hat{A}_n[\hat{\Phi}], \rho_S(t)\}] \\ -\frac{\omega_0}{2}[\hat{\Phi}, [\hat{A}_n[\hat{\Phi}], \rho_S(t)]] \Big)\end{aligned} \tag{2.23}$$

Using the identity for the gamma function [81]:

$$\int_0^\infty \tau^n e^{-\Omega\tau} d\tau = \frac{\Gamma(n+1)}{\Omega^{n+1}} = \frac{n!}{\Omega^{n+1}}$$

The equation may be written:

$$\begin{aligned}\frac{d}{dt}\rho_S(t) = &-\frac{\mathrm{i}}{\hbar}[\hat{H}_S, \rho_S(t)] + \frac{\mathrm{i}\gamma C\Omega}{\hbar}\sum_n \frac{n!}{\Omega^n}\left[\hat{\Phi}, \left\{\hat{A}_n[\hat{\Phi}], \rho_S(t)\right\}\right] \\ &- \frac{C\gamma\omega_0}{2\hbar}\sum_n \frac{n!}{\Omega^n}\left[\hat{\Phi}, \left[\hat{A}_n[\hat{\Phi}], \rho_S(t)\right]\right]\end{aligned} \tag{2.24}$$

This master equation is complete, as the series has not yet been truncated, but it is not of Lindblad form; this can offer problematic intermediate dynamics, such as violating positivity of the density matrix [60]. We solve this issue by transforming the equation into Lindblad form. The next sections will explore the level of approximation of Eq. (2.24) and their corresponding manipulation to Lindblad form.

2.2.1.3 First Order Equation

It is customary to truncate the series Eq. (2.21) within Eq. (2.24) at first order in τ for a generic system. In this section we will perform the same truncation to offer a basis for comparison when considering the second order equations discussed later. The n-dependent terms in Eq. (2.24) may

be approximated to:

$$\begin{aligned}\sum_n \frac{n!}{\Omega^n} A_n &\approx A_0 + \frac{1}{\Omega} A_1 \\ &\approx \hat{\Phi} - \frac{i\hat{Q}}{2\hbar C\Omega}[\hat{Q}, \hat{\Phi}] \\ &\approx \hat{\Phi} - \frac{\hat{Q}}{\Omega C}\end{aligned} \tag{2.25}$$

where the commutation relation Eq. (1.13) has been used with the properties of linear combinations of operators. Substitution of (2.25) into Eq. (2.24) yields:

$$\begin{aligned}\frac{d}{dt}\rho = &-\frac{i}{\hbar}[\hat{H}'_S, \rho] + \frac{iC\gamma\Omega}{\hbar}[\hat{\Phi}^2, \rho] - \frac{i\gamma}{\hbar}[\hat{\Phi}, \{\hat{Q}, \rho\}] \\ &- \frac{C\omega_0\gamma}{2\hbar}\left([\hat{\Phi}, [\hat{\Phi}, \rho]] - \frac{1}{\Omega C}[\hat{\Phi}, [\hat{Q}, \rho]]\right)\end{aligned} \tag{2.26}$$

The second term in Eq. (2.26) is simply a first order renormalisation of the potential, more specifically it is a shift in SQUID's inductance by a factor of $\lambda = \frac{2\Omega\gamma}{\omega_0^2(1+2\Omega\gamma/\omega_0^2)}$ [36, 71, 82] and can therefore be absorbed into the free evolution part of the equation to give:

$$\begin{aligned}\frac{d}{dt}\rho = &-\frac{i}{\hbar}[H'_{S0}, \rho] - \frac{i\gamma}{\hbar}[\hat{\Phi}, \{\hat{Q}, \rho\}] \\ &- \frac{C\omega_0\gamma}{2\hbar}\left([\hat{\Phi}, [\hat{\Phi}, \rho]] - \frac{1}{\Omega C}[\hat{\Phi}, [\hat{Q}, \rho]]\right)\end{aligned} \tag{2.27}$$

where H_{S0} uses the true inductance of the SQUID ring, $L = \frac{L'}{1-\lambda}$. As it stands, equation (2.27) does not ensure that probability is conserved as it is

not of Lindblad form [60, 83]; that is to say it is not in the form:

$$\frac{d\rho}{dt} = -\frac{i}{\hbar}[H_S, \rho] + \frac{1}{2}\sum_j \left\{ [L_j, \rho L_j^\dagger] + [L_j \rho, L_j^\dagger] \right\} \tag{2.28}$$

where $\rho_S(t)$ has been replaced with ρ for convenience and L_j are the non-unitary Lindblad operators. If a Lindblad of the form $L = \alpha\hat{\Phi} + \beta\hat{Q}$ is assumed, with $L^\dagger = \alpha^*\hat{\Phi} + \beta^*\hat{Q}$, and $\alpha\beta^* = \mu + i\nu$, equation (2.28) can be written in the form:

$$\begin{aligned} \frac{d}{dt}\rho = &-\frac{i}{\hbar}[\hat{H}'_S, \rho] \\ &-\frac{|\alpha|^2}{2}[\hat{\Phi}, [\hat{\Phi}, \rho]] + i\nu[\hat{\Phi}, \{\hat{Q}, \rho\}] - \mu[\hat{\Phi}, [\hat{Q}, \rho]] - \frac{|\beta|^2}{2}[\hat{Q}, [\hat{Q}, \rho]] \end{aligned} \tag{2.29}$$

Equating coefficients in equations (2.27) and (2.29) yields:

$$\begin{aligned} |\alpha|^2 &= \frac{C\omega_0\gamma}{\hbar} \\ \nu &= -\frac{\gamma}{\hbar} \\ \mu &= -\frac{\gamma\omega_0}{2\hbar\Omega} \end{aligned} \tag{2.30}$$

Using the identity, $|\beta|^2 = \frac{\mu^2+\nu^2}{|\alpha|^2}$, allows (2.27) to be put into Lindblad form by introducing an additional term, yielding:

$$\begin{aligned} \frac{d}{dt}\rho = &-\frac{i}{\hbar}[\hat{H}'_S, \rho] - \frac{i\gamma}{\hbar}[\hat{\Phi}, \{\hat{Q}, \rho\}] \\ &-\frac{C\omega_0\gamma}{2\hbar}\left([\hat{\Phi}, [\hat{\Phi}, \rho]] - \frac{1}{\Omega C}[\hat{\Phi}, [\hat{Q}, \rho]] \right) \\ &\underbrace{-\frac{\gamma}{2C\hbar\omega_0}\left(1 + \frac{\omega_0^2}{4\Omega^2}\right)[\hat{Q}, [\hat{Q}, \rho]]}_{\text{Additional term}} \end{aligned} \tag{2.31}$$

Referring back to the Lindblad of the form $\hat{L} = \alpha\hat{\Phi}+\beta\hat{Q}$, where $\beta^* = \alpha\beta^*/|\alpha|$, the above equation corresponds to a Lindblad of:

$$\hat{L} = \sqrt{\frac{C\omega_0\gamma}{\hbar}}\hat{\Phi} + \sqrt{\frac{\gamma}{C\omega_0\hbar}}\left(\mathrm{i} - \frac{\omega_0}{2\Omega}\right)\hat{Q} \tag{2.32}$$

To better understand the key parameters on which the master equation depends, it is preferred to move into a dimensionless representation; this will become even more important for higher order cases when more terms are introduced. A dimensionless representation also allows an easy method to check the validity of the equation using dimensional analysis. Within this representation the flux and charge operators become dimensionless and are replaced by the quantities $\hat{X} = \sqrt{\frac{C\omega_0}{\hbar}}\hat{\Phi}$, $\hat{P} = \sqrt{\frac{1}{C\hbar\omega_0}}\hat{Q}$ respectively.

Now that the master equation is one of Lindblad form, it satisfies the expressions:

$$\begin{aligned}
\frac{\mathrm{d}\rho}{\mathrm{d}t} &= -\frac{\mathrm{i}}{\hbar}[\hat{H},\rho] + \frac{1}{2}\left([\hat{L},\rho\hat{L}^\dagger] + [\hat{L}\rho,\hat{L}^\dagger]\right) \\
\hat{H} &= \hat{H}_{S_1} + \frac{\hbar\gamma}{2}\left(\hat{X}\hat{P} + \hat{P}\hat{X}\right) \\
\hat{L} &= \gamma^{\frac{1}{2}}\left[\hat{X} + \left(\mathrm{i} - \frac{\xi}{2}\right)\hat{P}\right]
\end{aligned} \tag{2.33}$$

where we have defined $\xi = \omega_0/\Omega$.

It is worth noting that the addition of $[\hat{Q},[\hat{Q},\rho]]$ to Eq. (2.27) brings with it some interesting points of discussion. In the high cut-off limit where $\xi \to 0$, the Lindblad presented in Eq. (2.33) reduces to a Lindblad, $\hat{L} = \sqrt{2\gamma}\hat{a}$ which differs from the general high temperature Lindblad produced in QBM, $\hat{L}_{QBM} = \alpha'\hat{a} + \beta'\hat{a}^\dagger$. The increase in weighting of the creation operator as

temperature increases is a consequence of the higher energy states explored in QBM, where the system is subject to thermal noise. The $\Omega \to \infty$ limit therefore suggests that the assumption of using a reduced Lindblad implies significant changes to the master equation and therefore the dynamics of the system. By putting Eq. (2.27) into Lindblad form, the second term is split into dissipative and squeezing terms. The dissipative term contributes towards the Lindblad while the squeezing term is absorbed in an effective Hamiltonian. It will be shown in a later chapter that this term is necessary to maintain quantum-classical correspondence [84, 35, 85, 86] because the Lindblad solely describes damping without accounting for the associated frequency shifts. The details of these terms, their effect, and the validity including them, will be discussed later.

2.2.1.4 Second Order Equation

As previously highlighted in §2.1, it is often assumed that first order truncation is sufficient for models of this type but higher order contributions may hold more weight than previously thought, it is therefore important to explore the expansion of Eq. (2.21) to second order in τ to unveil any potential qualitative, if not quantitative, differences between first and second order models. Similar to the case of first order truncation in §2.2.1.3, expanding the sum $\sum_n n!\Omega^{-n}\hat{A}_n$ to second order yields:

$$\begin{aligned}\sum_n \frac{n!}{\Omega^n}A_n &\approx A_0 + \frac{1}{\Omega}A_1 + \frac{2}{\Omega^2}A_2 \\ &\approx \hat{\Phi} - \frac{\hat{Q}}{\Omega C} - \frac{\omega^2}{\Omega^2}\left(\hat{\Phi} + \frac{2\pi\hbar\nu L}{\Phi_0}\sin\left(\frac{2\pi}{\Phi_0}(\hat{\Phi}+\Phi_x)\right)\right)\end{aligned} \tag{2.34}$$

where the external flux dependence, originating from the non-linear SQUID potential, can be seen to enter the dissipator for the first time [45], a significant finding because this anharmonic nature is not seen in any first order model. Substituting (2.34) into Eq. (2.24) now gives:

$$\begin{aligned}\frac{\mathrm{d}\rho_S}{\mathrm{d}t} =& -\frac{\mathrm{i}}{\hbar}[\hat{H}_S,\rho_S(t)] + \frac{\mathrm{i}\gamma\Omega C}{\hbar}\Bigg(\overbrace{\left(1-\frac{\omega_0^2}{\Omega^2}\right)[\hat{\Phi}^2,\rho_S(t)]]}^{\text{renormalises } L} - \overbrace{\frac{1}{\Omega C}[\hat{\Phi},\{\hat{Q},\rho_S(t)\}]}^{1^{\text{st}}\text{ order dissipation}} \\ &- \overbrace{\frac{2\pi\hbar\nu L}{\Phi_0}\frac{\omega_0^2}{\Omega^2}\left[\hat{\Phi},\left\{\sin\left(\frac{2\pi}{\Phi_0}(\hat{\Phi}+\Phi_x)\right),\rho_S(t)\right\}\right]}^{2^{\text{nd}}\text{ order dissipation}}\Bigg) \\ &- \frac{\gamma\omega_0 C}{2\hbar}\Bigg(\underbrace{\left(1-\frac{\omega_0^2}{\Omega^2}\right)[\hat{\Phi},[\hat{\Phi},\rho_S(t)]]}_{1^{\text{st}}\text{ and }2^{\text{nd}}\text{ order noise}} - \underbrace{\frac{1}{\Omega C}[\hat{\Phi},[\hat{Q},\rho_S(t)]]}_{1^{\text{st}}\text{ order in cutoff}} \\ &- \underbrace{\frac{2\pi\hbar\nu L}{\Phi_0}\frac{\omega_0^2}{\Omega^2}\left[\hat{\Phi},\left[\sin\left(\frac{2\pi}{\Phi_0}(\hat{\Phi}+\Phi_x)\right),\rho_S(t)\right]\right]}_{2^{\text{nd}}\text{ order cutoff}}\Bigg)\end{aligned} \tag{2.35}$$

where once again $\hat{H}_S$ consists of the true inductance of the SQUID ring after second order renormalisation is accounted for [45], i.e. $L \to L/(1-\lambda)$ where $\lambda = \left(2\gamma\Omega\left(1-\frac{\omega_0^2}{\Omega^2}\right)\right)/\omega_0^2\left(1+\frac{2\gamma\Omega}{\omega_0^2}\left(1-\frac{\omega_0^2}{\Omega^2}\right)\right)$. The first term in Eq. (2.35) once again demonstrates free evolution of the system, while the second acts as a second order renormalisation of the system inductance which cancels with the aforementioned shift, so that bare values may be used in the system Hamiltonian. The third and fourth terms describe first and second order dissipative effects which may be broken down into damping and frequency shift terms whose

nature will be discussed in detail in Chapter 4; note that external flux dependence in the dissipator is seen for the first time in this fourth term. The fifth term describes noise which has a small second order contribution while the sixth and seventh terms show first and second order cut-off terms which are usually neglected when the high cut-off limit is assumed. The second order contribution in the fifth term, as well as the sixth and seventh terms therefore transform the Lindblad away from the familiar bosonic operators seen in the first order case. As with the first order case, Eq. (2.35) is not of Lindblad form and therefore does not necessarily ensure positivity of the density matrix, nor can it guarantee physical dynamics. To remedy this, the equation is put into a Lindblad equation by use of two Lindblads of the form $\hat{L}_1 = \alpha_1\hat{\Phi} + \epsilon_1\hat{Q}$ and $\hat{L}_2 = \alpha_2\hat{\Phi} + \epsilon_2 \sin\left(\frac{2\pi}{\Phi_0}(\hat{\Phi} + \Phi_x)\right)$. This assumption arrives from comparison between first order terms and their resulting Lindblad, with the terms found in the second order equation. The first takes the familiar form of a linear combination of creation and annihilation operators, while the second is a function of external flux, Φ_x, and acts as a correction to environmental influences.

In order to produce the two Lindblads, which can be found in the same manner as the first order by equating coeffcients of commutator terms with α_1, α_2, ϵ_1, and ϵ_2, the fifth term in Eq. (2.35) requires splitting so that it can contribute to both. There is some freedom with which this is done; the weighting of the split between Lindblads $\hat{L}_1$ and $\hat{L}_2$ is denoted by the splitting parameter ζ and is allocated in such a way that $-(1-\zeta)\frac{\gamma\omega_0 C}{2\hbar}\left(1 - \frac{\omega_0^2}{\Omega^2}\right)\cdot [\hat{\Phi}, [\hat{\Phi}, \rho_S(t)]]$ contributes to $\hat{L}_1$ and $-\zeta\frac{\gamma\omega_0 C}{2\hbar}\left(1 - \frac{\omega_0^2}{\Omega^2}\right)[\hat{\Phi}, [\hat{\Phi}, \rho_S(t)]]$ contributes to $\hat{L}_2$ [45]. To ensure convergence of this perturbative model, it is sensible to

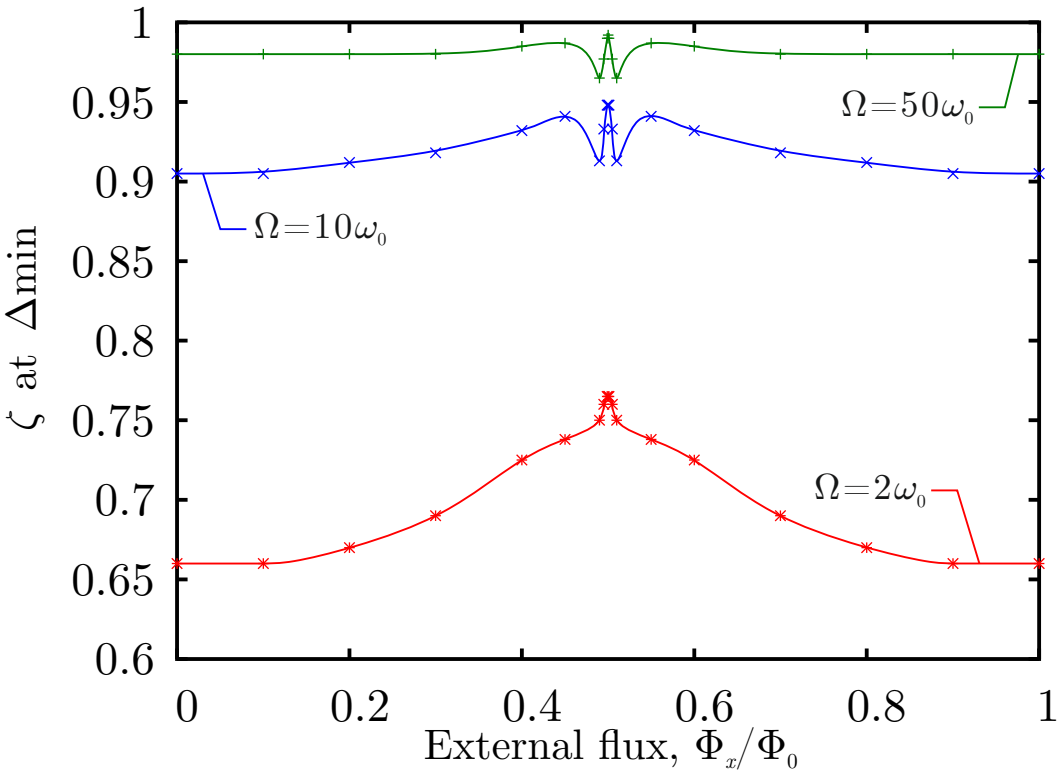

Figure 2.1: A plot of the second order weighting parameter ζ, which minimises the difference between first and second order steady state purities (Δ_{min}), as a function of external flux Φ_x for varying values of bath cut-off frequency Ω. [45]

minimise the contribution made by higher order terms so that they do not dominate. The splitting parameter is therefore selected so that the difference between first and second order steady state purities is kept to a minimum. This minimal difference, denoted by Δ_{min}, is used to calculate the value of ζ that satisfies this condition for a range of external flux and bath cut-off values; this is shown in Fig. 2.1 which suggests a non-linear dependence, of the splitting ζ, on external flux. Although unusual compared to simpler

systems, such as the HO which would provide a constant split due to the smaller number of control parameters, this result is not surprising as SQUID rings are capable of non-linearly affecting on the tank circuits, modelled as harmonic oscillators, to which they are coupled. It is therefore only to be expected that the modelling process should also yield a non-linear dependence on Φ_x. As a result, the splitting parameter is written as function of both external flux and bath cut-off frequency $\zeta(\Omega, \Phi_x)$. From Fig. 2.1, it is reasonable to approximate the cut-off dependence of $\zeta(\Omega, \Phi_x)$ with the series $\zeta(\Omega) = \sum_{n=1}(-1)^{n-1}\xi^{n-1}$, which corresponds to ζ values of approximately 0.980, 0.909, 0.664 at $\Phi_x = 0$ for bath cut-off values of $\Omega = 50\omega_0$, $10\omega_0$, and $2\omega_0$ respectively. This approximation extends to $\zeta \approx 1 - \omega_0/\Omega = 1 - \xi$ as cut-off frequency is increased and for high cut-offs suffices for use in a minimally invasive master equation (especially away from $\Phi_x = 0.5$). With this choice, the Lindblad operator $\hat{L}_1$ again approaches the annihilation operator in the high cut-off limit, where $\xi \to 0$. For the remainder of this chapter a bath cut-off frequency of $\Omega = 10\omega_0$ is used for second order analysis, which is suitably far away from $\Omega = 2\omega_0$ to justify the latter approximation ($\zeta = 1 - \omega_0/\Omega$) carrying forward. It is interesting to note that the function as a whole appears to have an oscillatory dependence on Φ_x but, as this begins to decrease with increasing Ω, it will not be discussed in detail here. We will see in the next chapter an alternate method for calculating Lindblads, this will also display the non-trivial nature of these Lindblads' dependence on SQUID control parameters.

In the same way that the first order equation contained an $\left[\hat{X}\hat{P} + \hat{P}\hat{X}, \rho\right]$ term describing a frequency shift, the second order equation is no different.

Extra squeezing and frequency shifts are enclosed within the fourth term in Eq. (2.35), the effects of which will be topic for discussion in Chapter 4. If the additional terms, required to bring the equation into Lindblad form, are included in Eq. (2.35), for $\zeta = 1 - \xi$, one obtains [45]:

$$\begin{aligned}
\frac{\mathrm{d}\rho}{\mathrm{d}t} &= -\frac{\mathrm{i}}{\hbar}[\hat{H}, \rho] + \frac{1}{2}\sum_j \left([\hat{L}_j, \rho \hat{L}_j^\dagger] + [\hat{L}_j \rho, \hat{L}_j^\dagger] \right) \\
\hat{H} &= \hat{H}_{S_2} + \frac{\hbar\gamma}{2}\left(\hat{X}\hat{P} + \hat{P}\hat{X} \right) + \sqrt{\beta\xi\frac{\nu}{\Omega}}\gamma\hat{X}\sin\left(\sqrt{\frac{\beta\omega_0}{\nu}}\hat{X} + 2\pi\frac{\Phi_x}{\Phi_0} \right) \\
\hat{L}_1 &= \gamma^{\frac{1}{2}}\left[\sqrt{(1-\xi)(1-\xi^2)}\hat{X} + \left(\mathrm{i} - \frac{\xi}{2} \right)\sqrt{\frac{1}{(1-\xi)(1-\xi^2)}}\hat{P} \right] \\
\hat{L}_2 &= \gamma^{\frac{1}{2}}\Bigg[\sqrt{\xi(1-\xi^2)}\hat{X} \\
&\qquad + \sqrt{\frac{\xi}{(1-\xi^2)}}\left(\mathrm{i} - \frac{\xi}{2} \right)\sqrt{\beta\frac{\nu}{\omega_0}}\sin\left(\sqrt{\frac{\beta\omega_0}{\nu}}\hat{X} + 2\pi\frac{\Phi_x}{\Phi_0} \right) \Bigg]
\end{aligned} \tag{2.36}$$

where $\beta = 2\pi L I_c/\Phi_0$, related to the critical current $I_c = 2\pi\hbar\nu/\Phi_0$, is the hysteretic coefficient and is frequently used in semi-classical analysis to separate hysteretic ($\beta > 1$) from non-hysteretic behaviour ($\beta \leq 1$) [87]. In the next section the effects of both first and second order equations on the decoherence of the SQUID will be presented through their impact on steady state purity, and other observables such as screening current [45].

2.3 Results

As has been discussed previously, the Lindblad chosen to describe the dissipation in Eq. (2.33) is dependent on the bath cut-off frequency, through the parameter $\xi = \omega_0/\Omega$. The effect of changing ξ on the environmental

Table 2.1: Chosen system parameters and their values [45].

Symbol	Quantity	Value
L	System Inductance	3×10^{-10}H
C	System Capacitance	5×10^{-15}F
ω_0	System Characteristic Frequency	8.16×10^{11}Hz
γ	Damping Rate	$0.005\omega_0$
$\hbar\nu$	Josephson Energy	9.99×10^{-22}J

decoherence described by Eq. (2.33) is shown in Fig. 2.2 and is displayed in this work by analysing the purity $\mathrm{Tr}\{\rho^2\}$ of the steady state solution as a function of bath cut-off frequency and external flux.

It is worth noting again that in the high cut-off limit $\Omega \to \infty$ the chosen Lindblad reduces to the Lindblad $\hat{L} = \sqrt{2\gamma}\hat{a}$, a pre-existing choice of Lindblad used to describe dissipation in SQUIDs [52, 88, 89, 90, 91], but, as was emphasised in §2.2.1.4, choosing this Lindblad requires modification of the master equation, existing in the form of effective Hamiltonians and 'minimally invasive' additions, and therefore the interaction itself between the system and environment.

The general shape of Fig. 2.2 is a well with gradual increases in purity as external flux approaches $\Phi_x = 0.5$ from either side, at which point the purity drops sharply to approximately $\mathrm{Tr}\{\rho^2\} = 0.5$; this is due to the fact that the SQUID's potential becomes a double well where the ground energy eigenstate is a superposition of macroscopically distinct states, other wise known as a Schrödinger Cat [52], localised in the bottom of each well. The state therefore decoheres into a statistical mixture and equally localises in each well. Notice that the purity falls to just below a half; this interesting result is due to mixing of excited states and will be discussed in more detail

in the next chapter.

Table 2.1 shows the system parameters chosen for all calculations in this section, these values are consistent with literature [52, 92], with Josephson coupling energy related to critical current through $\hbar\nu = I_c\Phi_0/2\pi$, where $\Phi_0 = h/2e$ is the flux quantum and I_c is the critical current of the weak link (which in this case is approximately a value of $I_c \approx 3\mu$A).

The parameters γ and Ω characterise the environment with which the SQUID, with control parameters $\hbar\nu$ and Φ_x, interacts. The rate of loss in the system is governed by γ which can be attributed to the quality factor, Q_c of the environment comprised of a cavity of harmonic oscillators and is quantified by $Q_c = 2\pi\omega_c/\gamma$ for a given cavity frequency ω_c. Quality factors of cavities can range from $Q_c \sim 10^2$ and may even exceed values of $Q_c \sim 10^6$ [45, 93, 94].

The cutoff frequency, Ω, defines the peak frequency of the bath's spectral density and has been shown to be related to a purely resistive impedance in Josephson circuits [95, 96]. Although the purity curves produced at cut-off frequencies of $\Omega = 10\omega_0$ (and higher) resemble the curve produced by an annihilating Lindblad, further analysis will show that this approximation is not as suitable as first thought.

Fig. 2.3 shows the steady state purity as a function of external flux for both first and second order models for a bath cut-off of $\Omega = 10\omega_0$, as well as the first order curve at $\Omega = 2\omega_0$; this has been used to emphasise the difference between first and second order Lindblad equations. Whereas the first order models differed by a relatively small amount for varying Ω, the difference between models is found to be greater when changing the order of

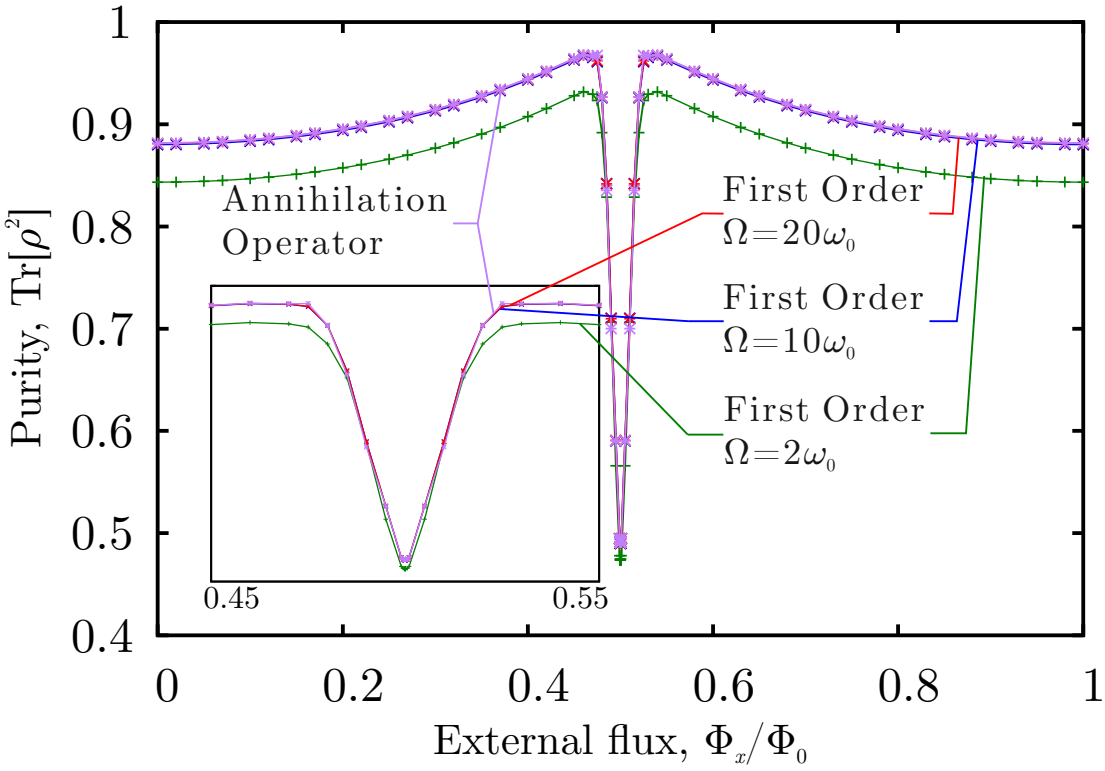

Figure 2.2: Steady state purity $\mathrm{Tr}\{\rho^2\}$, obtained through the first order master equation, plotted as a function of external flux Φ_x for varying value of bath cut-off frequency Ω. Circuit parameters are $C = 5 \times 10^{-15}$F, $L = 3 \times 10^{-10}$H and $I_c \approx 3\mu$A. [45]

approximation than when changing bath cut-off frequency; this suggests that it is not sufficient to use an annihilator Lindblad to describe the decoherence for SQUID systems. The second order model in Fig. 2.3 shows a smaller steady state purity across all values of Φ_x. This qualitatively different curve implies a greater amount of mixing with the environment than that shown by the first order model; again showing evidence that higher order contributions, with potential implications such as energy exchange, may need to be consid-

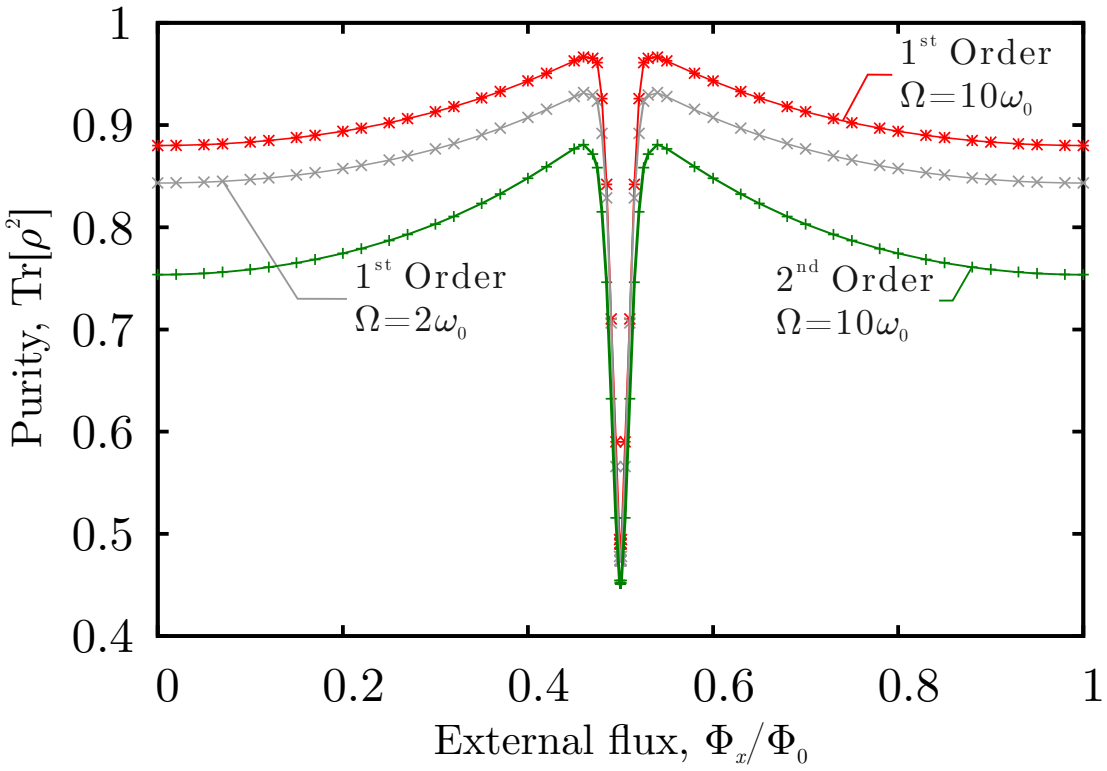

Figure 2.3: Steady state purity $\mathrm{Tr}\{\rho^2(t)\}$ obtained via first and second order Lindblad master equations Eq. (2.33) and Eq. (2.36) respectively as functions of external flux at bath cut-off frequency $\Omega = 10\omega_0$. A third curve showing the first order steady state purity at $\Omega = 2\omega_0$ is also included to emphasise the significance of higher order contributions [45].

ered when modelling the decoherence in SQUIDs. One could suggest that the second order model represents a renormalisation in Ω such that $\Omega < \omega_0$, as it appears the general trend for decreasing Ω, in the first order model, leads to a drop in purity. As this work only explores cut off frequencies found above ω_0 however, such a statement cannot be confirmed.

Although the difference between models is significant when considering the steady state purity, the difference is not so obvious when considering

steady state observables such as the screening current, as shown in Fig. 2.4 as a function of external flux. The curves for both first and second order differ only slightly which shows that device characterisation may require further analysis involving quantities such as decoherence times T_1 and T_2 rather than solely based on observables such as flux. Such subtleties shown in this model suggest it may require a range of precise methods to correctly characterise non-harmonic systems which has implications for quantum technologies, especially when considering their scalability and modelling and simulation framework for engineering design. It would then be possible to test the effectiveness of the master equation approach to modelling the decoherence of Josephson junction based devices.

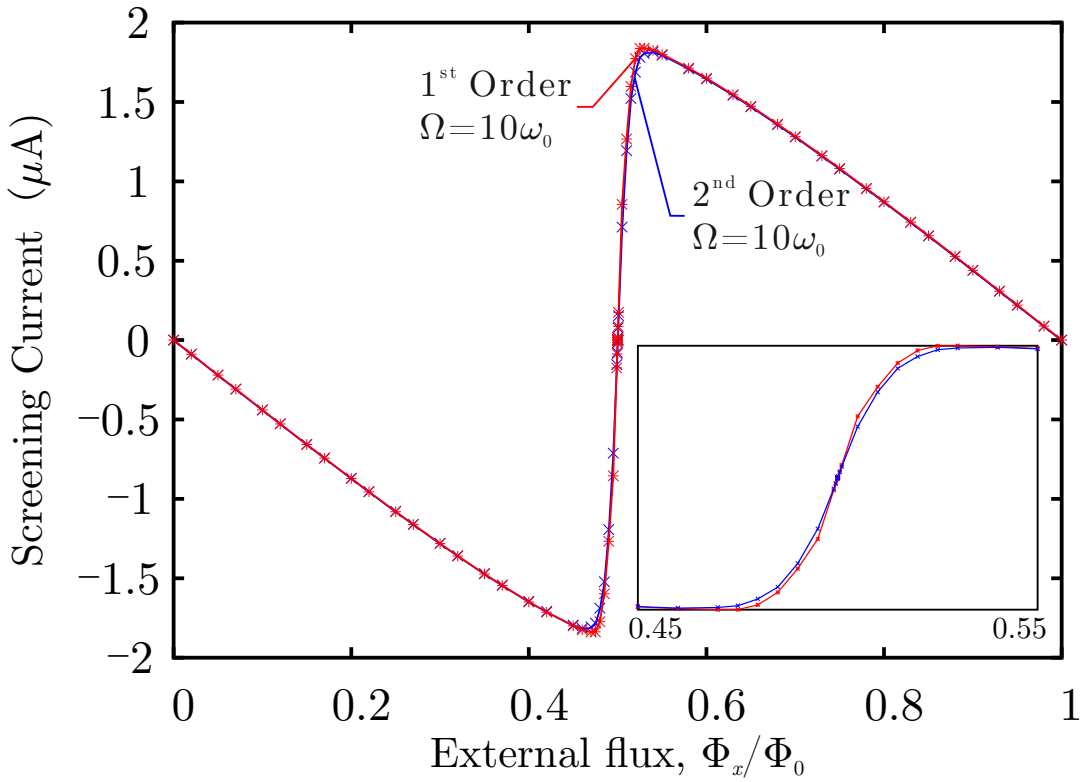

Figure 2.4: Expectation value of screening current, $\left\langle \hat{\Phi}/L \right\rangle$ plotted as a function of external flux for first order (red) and second order (blue) models at a bath cutoff frequency of $\Omega = 10\omega_0$ [45].

2.4 Summary

This chapter has extended a master equation approach to a SQUID coupled to an Ohmic bath, using what are considered standard techniques to produce a Lindblad equation to represent system decoherence. A second order equation, found through the expansion of the correlation-time-dependent flux $\hat{\Phi}(\tau)$, has produced significant effects compared to the first order model produced in the same way. This has been a necessary exploration as for cer-

tain limits, such as strong coupling or zero temperature, first order equations may be insufficient. For longer correlation timescales, higher order contributions become more significant, suggesting that first order models in this limit paints an incomplete picture, especially as these terms, for the case of the SQUID, carry a dependence on external degrees of freedom. For the zero temperature limit, producing a Lindblad model is no longer a 'minimally invasive' process as the system becomes altered when additional terms are included, an effect that would be negligible in the high temperature limit due to their inverse proportionality to temperature. The calculations presented here have been made for finite cut-off Ω as any issues faced in this limit are likely to be further emphasised in the $\Omega \to \infty$ limit. The second order corrections have been found to have a greater effect on the amount of mixing between the system and bath than that shown in first order, suggesting that these higher order contributions cannot be neglected.

It has been shown in this chapter that the dissipation of the SQUID, described by the Lindblad operators, possess a dependence on external degrees of freedom in the form of bath cut-off frequency, and more importantly, the externally applied magnetic flux. Although this approach is different to that often in quantum control, where it is assumed that all control parameters, such as Φ_x, are found within the Hamiltonian only [97], the possibility of a producing a dissipator dependent on external degrees of freedom has already been presented [98]. These findings further suggest that decoherence may be controlled through the engineering of an appropriate environment, such as a two photon bath, as designed in [99] and modelled in [52]. Although such an example would still possess single photon events, and therefore dissipation,

it is the beginning of what may be tunable environments that combat decoherence. Finding an external flux dependent Lindblad for the SQUID is a surprising result in the sense that it suggests tunability of system decoherence via environmental control parameters, but at the same time an understandable finding as the Lindblad depends on the system's Hamiltonian which possesses the same parameter [38, 92, 100].

Although it has already been suggested that Lindbladian dissipation may be dependent on external degrees of freedom [98], the findings here suggest that this is not apparent at all orders of approximation. For example, we have shown that a first order truncation of the SQUID model yields a Lindblad very similar in form to those found for QBM and for the DHO. It is only when higher orders are considered that external degrees of freedom, such as external flux, are seen to impact on the dynamics of the ensemble average. It was shown that the order of approximation had more impact on the decoherence of the SQUID than varying the bath parameters (see for example varying Ω for the first order case) and so care must be taken when considering the effect of higher order terms, such as those dependent on external flux, on modelling Josephson Junction based devices. This consideration becomes more significant when implementing observable based characterisation, as models would yield the same characteristics yet have different decoherence channels, it is therefore crucial to characterise a device through several means to prevent this oversight.

In this work a finite cut-off frequency has been used, and it has been suggested that the high cut-off limit $\Omega \to \infty$ does not exist; this claim is supported by works where a series solution to a QBM model possesses a

logarithmic term which diverges in this unphysical limit. A low temperature series solution has been proposed for this case to further raise discussion on the validity of first order truncation [101].

It will be shown in the next chapter that an alternate method for completing the Lindblad process, which uses consideration of the coefficient matrix of the master equation and diagonalisation of such, gives a clear definition of "minimally invasive" adjustment so that a positive semi-definite density matrix can be maintained throughout. Terms of similar form to these higher order contributions found in this purely inductive model are also capable of appearing at lower orders when considering parasitic capacitance as well as inductive coupling. Both of the aforementioned issues will be discussed in detail where a SQUID will be modelled to be both inductively and capacitively coupled to its environment.

Chapter 3

Parasitic Capacitance and Lindblad Construction

3.1 Introduction

In the previous chapter it was shown that the master equation approach to modelling the decoherence of a SQUID coupled to an external bath brings with it many points of interest such as the dependence of the corresponding Lindblad operators on external control parameters, with this added dependence on magnetic flux introduced in a second order BCH expansion of $\hat{\Phi}(-\tau)$. Despite a significant difference in the external flux dependence of the steady state purity of the SQUID, the screening current shows minimal difference, suggesting that characterisation based solely on observables is insufficient and a more rigorous analysis may be required to characterise superconducting devices. It was shown in particular that higher order contributions obtained through the power expansion of correlation time dependent

flux have greater weighting than might be expected based on analysis of other systems such as the SHO, bringing with it the presence of the external control variables found directly in the Lindblad operator. The source of these terms comes from the commutator of the system Hamiltonian with the charge operator and appears at second order for the purely inductive model. In this chapter we show that introducing an element of capacitive coupling along with inductive coupling will brings these terms in at an earlier stage; this is the topic of the current chapter. Despite being well covered for the case of the charge qubit [102], parasitic capacitance in floating flux qubits has largely been overlooked due to an assumed weak connection to ground [1]. A recent study, however, has suggested that reactance to ground in the microwave range can be sizeable, leading to shorter coherence times than expected and suggesting that capacitive cross talk may play a significant role in a system's decoherence [1, 103, 104].

By modelling the decoherence of a SQUID both capacitively and inductively coupled to an Ohmic bath, the environment naturally becomes more important as the effects seen in the previous chapter are emphasised; this, it turns out, is due to terms similar in form to higher order contributions, found in the purely inductive model, coming in at lower order and thus having greater impact. One such effect includes the steady state purity of the system falling to less than 0.5 at the the external flux value $\Phi_x = 0.5\Phi_0$, which suggests that the state decoheres into more than just two localised states from its initial Schrödinger cat state, created by the double well at this value of external flux. Further analysis will be performed in this chapter to find the wave functions of these states to provide a qualitative explanation

to how the system is decohering.

It has been discussed in detail that creation of the a Lindblad master equation involved the addition of "minimally invasive" terms, which were valid in the high temperature limit used in QBM but which are more difficult to justify at the zero-temperature limit due to their sizeable impact on the system's behaviour and the *ad-hoc* nature of its addition. This chapter will introduce another approach to creating these additional terms and "completing" these master equations. Such analysis will address the coefficent matrix of the master equation which for a SQUID becomes a 3×3, as opposed to the 2×2 generally used for the harmonic oscillators and in QBM [57, 105]. The Lindblads and their weighting are then found to be the eigenvectors and eigenvalues of the matrix, respectively.

3.2 Theory

3.2.1 The model

We now consider the consequences of capacitive elements to the coupling between SQUIDs and an environment which will once again be taken to be an ensemble of cavity-resonator circuits. The Hamiltonian for this model becomes:

$$\begin{aligned} H_S &= \frac{\hat{Q}^2}{2C} + \frac{\hat{\Phi}^2}{2L} - \hbar\nu \cos\left(\frac{2\pi}{\Phi_0}(\hat{\Phi} + \Phi_x)\right) \\ H_B &= \sum_n \frac{\hat{Q}_n^2}{2C_n} + \frac{\hat{\Phi}_n^2}{2L_n} \\ \hat{H}_I &= -\left(\hat{\Phi}\sum_n \kappa_n \hat{\Phi}_n + \hat{Q}\sum_n \eta_n \hat{Q}_n\right) \end{aligned} \tag{3.1}$$

where $\hat{\Phi}$, $\hat{\Phi}_n$, $\hat{Q}$, and $\hat{Q}_n$ denote the flux and charge for the system and the bath respectively. The interaction Hamiltonian may be written $\hat{H}_I = -\left(\hat{\Phi}\hat{B}_\Phi + \hat{Q}\hat{B}_Q\right)$ where the bath operators $\hat{B}_\Phi$ and $\hat{B}_Q$ are given by:

$$\begin{aligned}\hat{B}_\Phi &= \sum_n \sqrt{\frac{\kappa_n^2\hbar}{2C_n\omega_n}}\left(\hat{b}_n + \hat{b}_n^\dagger\right)\\ \hat{B}_Q &= -\mathrm{i}\sum_n \sqrt{\frac{\eta_n^2\hbar C_n\omega_n}{2}}\left(\hat{b}_n - \hat{b}_n^\dagger\right)\end{aligned} \tag{3.2}$$

The first function is exactly the same form as the bath operator in §2.2.1 while the second is introduced due to the charge coupling and is also written in terms of the bosonic creation and annihilation operators. Substituting in the dissipator of the general master equation Eq. (1.43):

$$\mathcal{K} = \frac{1}{\hbar^2}\int_0^\infty \mathrm{d}\tau\,\mathrm{Tr}_B\left\{\left[\hat{H}_I, \left[\hat{H}_I(-\tau), \rho_S\right]\right]\right\} \tag{3.3}$$

yields:

$$\begin{aligned}\mathcal{K} = \frac{1}{\hbar^2}\int_0^\infty \mathrm{d}\tau\Bigg(&\mathrm{Tr}_B\left\{\left[\hat{\Phi}\hat{B}_\Phi, \left[\hat{\Phi}(-\tau)\hat{B}_\Phi(-\tau), \rho_S\right]\right]\right\}\\ &+ \mathrm{Tr}_B\left\{\left[\hat{Q}\hat{B}_Q, \left[\hat{Q}(-\tau)\hat{B}_Q(-\tau), \rho_S\right]\right]\right\}\\ &+ \mathrm{Tr}_B\left\{\left[\hat{\Phi}\hat{B}_\Phi, \left[\hat{Q}(-\tau)\hat{B}_Q(-\tau), \rho_S\right]\right]\right\}\\ &+ \mathrm{Tr}_B\left\{\left[\hat{Q}\hat{B}_Q, \left[\hat{\Phi}(-\tau)\hat{B}_\Phi(-\tau), \rho_S\right]\right]\right\}\Bigg)\end{aligned} \tag{3.4}$$

Following the protocol introduced in §2.2.1 , this may be written as:

$$\begin{aligned}\mathcal{K} = \frac{1}{2\hbar^2}\int_0^\infty \mathrm{d}\tau \Bigg(&\left\langle \left[\hat{B}_\Phi, \hat{B}_\Phi(-\tau)\right]\right\rangle_B \left[\hat{\Phi}, \left\{\hat{\Phi}(-\tau), \rho_S\right\}\right] \\ &+\left\langle \left\{\hat{B}_\Phi, \hat{B}_\Phi(-\tau)\right\}\right\rangle_B \left[\hat{\Phi}, \left[\hat{\Phi}(-\tau), \rho_S\right]\right] \\ &+\left\langle \left[\hat{B}_Q, \hat{B}_Q(-\tau)\right]\right\rangle_B \left[\hat{Q}, \left\{\hat{Q}(-\tau), \rho_S\right\}\right] \\ &+\left\langle \left\{\hat{B}_Q, \hat{B}_Q(-\tau)\right\}\right\rangle_B \left[\hat{Q}, \left[\hat{Q}(-\tau), \rho_S\right]\right] \\ &+\left\langle \left[\hat{B}_\Phi, \hat{B}_Q(-\tau)\right]\right\rangle_B \left[\hat{\Phi}, \left\{\hat{Q}(-\tau), \rho_S\right\}\right] \\ &+\left\langle \left\{\hat{B}_\Phi, \hat{B}_Q(-\tau)\right\}\right\rangle_B \left[\hat{\Phi}, \left[\hat{Q}(-\tau), \rho_S\right]\right] \\ &+\left\langle \left[\hat{B}_Q, \hat{B}_\Phi(-\tau)\right]\right\rangle_B \left[\hat{Q}, \left\{\hat{\Phi}(-\tau), \rho_S\right\}\right] \\ &+\left\langle \left\{\hat{B}_Q, \hat{B}_\Phi(-\tau)\right\}\right\rangle_B \left[\hat{Q}, \left[\hat{\Phi}(-\tau), \rho_S\right]\right] \Bigg)\end{aligned} \tag{3.5}$$

The first two terms, highlighted in red, are simply the purely inductive contribution to the equation and can be treated in exactly the same fashion as the previous chapter. The next two terms, highlighted in blue, offer a purely capacitive contribution while the final sets are cross terms.

3.2.2 Purely Inductive Terms

3.2.2.1 Bath Correlation Functions and Spectral Density

It has already been shown that the purely inductive contribution to the dissipator may be written:

$$\mathcal{K}_{\Phi\Phi} = \frac{1}{\hbar^2}\int_0^\infty \mathrm{d}\tau \left(\frac{\mathrm{i}}{2} D_\Phi(-\tau)[\hat{\Phi}, \{\hat{\Phi}(-\tau), \rho_S\}] - \frac{1}{2} D_{\Phi 1}(-\tau)[\hat{\Phi}, [\hat{\Phi}(-\tau), \rho_S]] \right) \tag{3.6}$$

where the inductive- dissipation and noise kernels are given explicitly by:

$$\begin{aligned} D(-\tau) &= 2C\gamma_\Phi \hbar \Omega^2 e^{-\Omega|\tau|} \operatorname{sgn}\tau \\ D_1(-\tau) &= C\hbar\gamma_\Phi \Omega\omega_0 e^{-\Omega|\tau|} \end{aligned} \tag{3.7}$$

Whilst the spectral density is given by:

$$J_\Phi(\omega) = \frac{2C\gamma_\Phi}{\pi}\omega\frac{\Omega^2}{\Omega^2+\omega^2} \tag{3.8}$$

for details on this function refer to §2.2.1.1

3.2.2.2 Integration of Inductive Terms by use of B-C-H

A common means of approximating the relaxation-time dependent flux term $\hat{\Phi}(-\tau)$ is through a power series expansion in τ, such that:

$$\hat{\Phi}(-\tau) = \sum_n A_n[\hat{\Phi}]\tau^n \tag{3.9}$$

where the functional $A_n[\hat{\Phi}]$ is found by equating powers of τ from the Baker-Campbell-Hausdorff expansion of $\hat{\Phi}(-\tau) = e^{-\mathrm{i}(\hat{H}_S+\hat{H}_B)\tau/\hbar}\hat{\Phi}e^{\mathrm{i}(\hat{H}_S+\hat{H}_B)\tau/\hbar}$ in the interaction picture i.e.:

$$\begin{aligned} \hat{\Phi}(-\tau) = \hat{\Phi} + \tau\left[-\frac{\mathrm{i}}{\hbar}\hat{H}_S,\hat{\Phi}\right] + \frac{\tau^2}{2!}\left[-\frac{\mathrm{i}}{\hbar}\hat{H}_S,\left[-\frac{\mathrm{i}}{\hbar}\hat{H}_S,\hat{\Phi}\right]\right] \\ + \cdots + \frac{\tau^n}{n!}\left[-\frac{\mathrm{i}}{\hbar}\hat{H}_S,...,\left[-\frac{\mathrm{i}}{\hbar}\hat{H}_S,\hat{\Phi}\right]\right] \end{aligned} \tag{3.10}$$

Since there are elements of $\hat{H}_S$ which do not commute with $\hat{\Phi}$. Substituting expression Eq. (3.19) into Eq. (3.18) as well as using the identity

$\Omega^{n+1}\int_0^\infty \mathrm{d}\tau\tau^n e^{-\Omega\tau} = n!$, yields the expression:

$$\mathcal{K}_{\Phi\Phi} = \frac{\mathrm{i}C\gamma_\Phi\Omega}{\hbar}\left[\hat{\Phi},\left\{\sum_n \frac{n!}{\Omega^n}A_n[\hat{\Phi}],\rho_S\right\}\right] - \frac{C\gamma_\Phi\omega_0}{2\hbar}\left[\hat{\Phi},\left[\sum_n \frac{n!}{\Omega^n}A_n[\hat{\Phi}],\rho_S\right]\right] \tag{3.11}$$

where C, Ω, ω_0 carry their definitions from §2.2.1. The identities for the dissipation and noise terms are given by:

$$\begin{aligned}\frac{i}{2\hbar^2}\int_0^\infty \mathrm{d}\tau D_\Phi(-\tau)\hat{\Phi}(-\tau) &= \sum_n \frac{\mathrm{i}C\gamma_\Phi\Omega}{\hbar}\frac{n!}{\Omega^n}A_n[\hat{\Phi}] \\ -\frac{1}{2\hbar^2}\int_0^\infty \mathrm{d}\tau D_{\Phi 1}(-\tau)\hat{\Phi}(-\tau) &= -\frac{C\hbar\gamma_\Phi\omega_0}{2\hbar}\sum_n \frac{n!}{\Omega^n}A_n[\hat{\Phi}]\end{aligned} \tag{3.12}$$

Truncating this series to first order as in the inductive case, Eq. (3.11) can be reduced accordingly:

$$\sum_n \frac{n!}{\Omega^n}A_n \approx A_0 + \frac{1}{\Omega}A_1 = \hat{\Phi} - \frac{\hat{Q}}{\Omega C} \tag{3.13}$$

This creates the purely inductive contribution to the first order dissipator, which is identical to the inductive model in §2.2.1.3, but with a newly defined inductive damping rate γ_Φ. In the zero temperature limit this gives:

$$\begin{aligned}\mathcal{K}_{\Phi\Phi} =& \frac{\mathrm{i}C\gamma_\Phi\Omega}{\hbar}\left[\hat{\Phi}^2,\rho_S\right] - \frac{\mathrm{i}\gamma_\Phi}{\hbar}\left[\hat{\Phi},\left\{\hat{Q},\rho_S\right\}\right] \\ &- \frac{C\gamma_\Phi\omega_0}{2\hbar}\left[\hat{\Phi},\left[\hat{\Phi},\rho_S\right]\right] + \frac{\gamma_\Phi\omega_0}{2\hbar\Omega}\left[\hat{\Phi},\left[\hat{Q},\rho_S\right]\right]\end{aligned} \tag{3.14}$$

which is of exactly the same form as that found in §2.2.1 and will reproduce the purely inductive equation if capacitive coupling goes to zero i.e. $\eta_n \to 0$.

3.2.3 Purely Capacitive Terms

3.2.3.1 Bath Correlation Functions and Spectral Density

Let us consider the bath correlation functions $\left\langle \hat{B}_Q \hat{B}_Q(-\tau) \right\rangle_B$ and $\left\langle \hat{B}_Q(-\tau) \hat{B}_Q \right\rangle_B$ which may be written in terms of bosonic annihilation and creation operators $\hat{b}$ and $\hat{b}^\dagger$ respectively:

$$\left\langle \hat{B}_Q \hat{B}_Q(-\tau) \right\rangle_B = -\sum_n \frac{\eta_n^2 C_n \omega_n \hbar}{2} \times \left\langle \left(\hat{b}_n - \hat{b}_n^\dagger \right) \left(e^{-\frac{\mathrm{i}\hat{H}_B \tau}{\hbar}} \hat{b}_n e^{\frac{\mathrm{i}\hat{H}_B \tau}{\hbar}} - e^{-\frac{\mathrm{i}\hat{H}_B \tau}{\hbar}} \hat{b}_n^\dagger e^{\frac{\mathrm{i}\hat{H}_B \tau}{\hbar}} \right) \right\rangle_B \tag{3.15}$$

Following the same steps as for purely inductive terms, full details of which can be found in Appendix D.1, one arrives at the capacitive kernels in the zero temperature limit, given by:

$$\begin{aligned} D_Q(\tau) &= 2L\gamma_Q \hbar \Omega^2 e^{-\Omega\tau} \operatorname{sgn} \tau \\ D_{Q1}(\tau) &= L\hbar\gamma_Q \Omega \omega_0 e^{-\Omega\tau} \end{aligned} \tag{3.16}$$

where $\omega_0 = \sqrt{1/L_0 C_0}$ is the characteristic frequency of the system and γ_Q and Ω denote the capacitive damping rate and bath cut off frequency respectively. Here we use the same cut-off Ω for J_Q, given by:

$$J_Q(\omega) = \frac{2L\omega\gamma_Q}{\pi} \frac{\Omega^2}{\Omega^2 + \omega^2} \tag{3.17}$$

and J_Φ but different coupling strengths γ_Q, γ_Φ equivalent to $\frac{\kappa_n^2}{C_n\omega_n} = g^2\frac{\eta_n^2}{L_n\omega_n}$. Thus the purely capacitive element of the dissipator, $\mathcal{K}_{QQ}$ can be written:

$$\begin{aligned}\mathcal{K}_{QQ} = \frac{1}{\hbar^2}\int_0^\infty \mathrm{d}\tau\Bigg(&\frac{\mathrm{i}}{2}D_Q(\tau)\left[\hat{Q},\left\{\hat{Q}(-\tau),\rho_S\right\}\right] \\ &-\frac{1}{2}D_{Q1}(\tau)\left[\hat{Q},\left[\hat{Q}(-\tau),\rho_S\right]\right]\Bigg)\end{aligned} \tag{3.18}$$

As in the purely inductive model, these terms require integration and expansion of the correlation-time-dependent Charge operator $\hat{Q}(-\tau)$; this is performed by use of the Baker-Campbell-Hausdorff formula which will be discussed in the next section.

3.2.3.2 Integration of Capacitive Terms by use of B-C-H

Proceeding as before we approximate the relaxation-time dependent charge term $\hat{Q}(-\tau)$ is through a power series expansion in τ, such that:

$$\hat{Q}(-\tau) = \sum_n A_n[\hat{Q}]\tau^n \tag{3.19}$$

where the functional $A_n[\hat{Q}]$ is found by equating powers of τ from the Baker-Campbell-Hausdorff expansion of $\hat{Q}(-\tau) = e^{-\mathrm{i}\hat{H}_S\tau/\hbar}\hat{Q}e^{\mathrm{i}\hat{H}_S\tau/\hbar}$ in the interaction picture i.e.:

$$\begin{aligned}\hat{Q}(-\tau) = \hat{Q} + \tau\left[-\frac{\mathrm{i}}{\hbar}\hat{H}_S,\hat{Q}\right] + \frac{\tau^2}{2!}\left[-\frac{\mathrm{i}}{\hbar}\hat{H}_S,\left[-\frac{\mathrm{i}}{\hbar}\hat{H}_S,\hat{Q}\right]\right] \\ + \cdots + \frac{\tau^n}{n!}\left[-\frac{\mathrm{i}}{\hbar}\hat{H}_S,...,\left[-\frac{\mathrm{i}}{\hbar}\hat{H}_S,\hat{Q}\right]\right]\end{aligned} \tag{3.20}$$

Since there are elements of $\hat{H}_S$ which do not commute with $\hat{Q}$. Sub-

stituting expression Eq. (3.19) into Eq. (3.18) as well as using the identity $\Omega^{n+1}\int_0^\infty \mathrm{d}\tau\tau^n e^{-\Omega\tau} = n!$, yields the expression:

$$\mathcal{K}_{QQ} = \frac{\mathrm{i}L\gamma_Q\Omega}{\hbar}\left[\hat{Q},\left\{\sum_n \frac{n!}{\Omega^n}A_n[\hat{Q}],\rho_S\right\}\right] - \frac{L\gamma_Q\omega_0}{2\hbar}\left[\hat{Q},\left[\sum_n \frac{n!}{\Omega^n}A_n[\hat{Q}],\rho_S\right]\right] \tag{3.21}$$

where the identities for the dissipation and noise terms:

$$\begin{aligned}\frac{i}{2\hbar^2}\int_0^\infty \mathrm{d}\tau D_Q(-\tau)\hat{Q}(-\tau) &= \sum_n \frac{iL\gamma_Q\Omega}{\hbar}\frac{n!}{\Omega^n}A_n[\hat{Q}] \\ -\frac{1}{2\hbar^2}\int_0^\infty \mathrm{d}\tau D_{Q1}(-\tau)\hat{Q}(-\tau) &= -\frac{L\hbar\gamma_Q\omega_0}{2\hbar}\sum_n \frac{n!}{\Omega^n}A_n[\hat{Q}]\end{aligned} \tag{3.22}$$

Truncating this series to first order as in the inductive case, Eq. (3.11) can be reduced accordingly:

$$\sum_n \frac{n!}{\Omega^n}A_n \approx A_0 + \frac{1}{\Omega}A_1 = \hat{Q} + \frac{1}{\Omega}\left(\frac{\hat{\Phi}}{L} + \frac{2\pi\hbar\nu}{\Phi_0}\sin\left(\frac{2\pi}{\Phi_0}(\hat{\Phi}+\Phi_x)\right)\right) \tag{3.23}$$

This creates the purely capacitive contribution to the first order dissipator and in the zero temperature limit gives:

$$\begin{aligned}\mathcal{K}_{QQ} =& \frac{\mathrm{i}L\gamma_Q\Omega}{\hbar}\left[\hat{Q}^2,\rho_S\right] \\ &+ \frac{\mathrm{i}\gamma_Q}{\hbar}\left[\hat{Q},\left\{\hat{\Phi},\rho_S\right\}\right] + \frac{\mathrm{i}\gamma_Q}{\hbar}\left[\hat{Q},\left\{I_cL\sin\left(\frac{2\pi}{\Phi_0}(\hat{\Phi}+\Phi_x)\right),\rho_S\right\}\right] \\ &- \frac{\gamma_Q}{2C\hbar\omega_0}\left[\hat{Q},\left[\hat{Q},\rho_S\right]\right] - \frac{\gamma_Q\omega_0}{2\hbar\Omega}\left[\hat{Q},\left[\hat{\Phi},\rho_S\right]\right] \\ &- \frac{\gamma_Q\omega_0}{2\hbar\Omega}\left[\hat{Q},\left[I_cL\sin\left(\frac{2\pi}{\Phi_0}(\hat{\Phi}+\Phi_x)\right),\rho_S\right]\right]\end{aligned} \tag{3.24}$$

where again $I_c = 2\pi\hbar\nu/\Phi_0$ is the critical current for the SQUID. The first term appears in a form that will cause a renormalisation in the SQUID capacitance through coupling with the bath. What is interesting here is that this term also depends on the bath charge function which suggests that the bath flux will impact on the the system's capacitance and vice versa. The next two terms contribute to the frequency shifts and squeezing which originate from the dissipation. A familiar result here is the $\left[\hat{Q},\left[\hat{Q},\rho_S\right]\right]$ term which is a necessary addition to ensure physicality of purely inductive models [45, 57, 60]. Note here that although the term arises naturally, in order to contribute enough towards the Lindblad used in the purely inductive model, γ_Q will need to be large enough and so the coupling ratio $g^2 = \gamma_Q/\gamma_\Phi$ has a lower bound.

3.2.4 Flux-Charge Terms

3.2.4.1 Correlations $\left\langle \hat{B}_\Phi\hat{B}_Q(-\tau)\right\rangle_B$ and Spectral Density

The bath correlation functions $\left\langle \hat{B}_\Phi\hat{B}_Q(-\tau)\right\rangle_B$ and $\left\langle \hat{B}_Q(-\tau)\hat{B}_\Phi\right\rangle_B$ may be written in terms of bosonic annihilation and creation operators $\hat{b}$ and $\hat{b}^\dagger$

respectively:

$$\left\langle \hat{B}_\Phi \hat{B}_Q(-\tau) \right\rangle_B = \sum_n \frac{\eta_n \kappa_n \hbar}{2\mathrm{i}} \Bigg\langle \left(\hat{b}_n + \hat{b}_n^\dagger\right) \Bigg((e^{-\frac{\mathrm{i}\hat{H}_B \tau}{\hbar}} \hat{b}_n e^{\frac{\mathrm{i}\hat{H}_B \tau}{\hbar}} - e^{-\frac{\mathrm{i}\hat{H}_B \tau}{\hbar}} \hat{b}_n^\dagger e^{\frac{\mathrm{i}\hat{H}_B \tau}{\hbar}} \Bigg\rangle_B \tag{3.25}$$

which differs to the purely inductive and capacitive functions found in Eq. (2.9) and Eq. (D.1) through the presence of both coupling constants as well as the change of sign. Going through the steps outlined in Appendix D.2, one yields the cross coupling kernels, $D_{\Phi Q}(\tau)$, $D_{\Phi Q1}(\tau)$:

$$\begin{aligned} D_{\Phi Q}(-\tau) &= \hbar \Omega \gamma_{\Phi Q} e^{-\Omega \tau} \\ D_{\Phi Q1}(-\tau) &= \frac{2\hbar \gamma_{\Phi Q} \Omega^2}{\omega_0} e^{-\Omega \tau} \end{aligned} \tag{3.26}$$

where $\gamma_{\Phi Q}$ denotes the cross coupling damping rate. The Flux-Charge dissipator can therefore be written as:

$$\mathcal{K}_{\Phi Q} = \frac{1}{\hbar^2} \int_0^\infty \mathrm{d}\tau \Bigg(\frac{\mathrm{i}}{2} D_{\Phi Q}(\tau) \left[\hat{\Phi}, \left\{\hat{Q}(-\tau), \rho_S\right\}\right] - \frac{1}{2} D_{\Phi Q1}(\tau) \left[\hat{\Phi}, \left[\hat{Q}(-\tau), \rho_S\right]\right] \Bigg) \tag{3.27}$$

Substituting the explicit values for the noise and dissipation kernels, yields:

$$\mathcal{K}_{\Phi Q} = \frac{\mathrm{i}\gamma_{\Phi Q}}{2\hbar} \left[\hat{\Phi}, \left\{\sum_n \frac{n!}{\Omega^n} A_n[\hat{Q}], \rho_S\right\}\right] - \frac{\gamma_{\Phi Q}\Omega}{\hbar\omega_0} \left[\hat{\Phi}, \left[\sum_n \frac{n!}{\Omega^n} A_n[\hat{Q}], \rho_S\right]\right] \tag{3.28}$$

Expanding $\hat{Q}(-\tau)$ to first order and substituting yields the final form of the Flux-Charge dissipator:

$$\begin{aligned}\mathcal{K}_{\Phi Q} =& \frac{\mathrm{i}\gamma_{\Phi Q}}{2\hbar}\left[\hat{\Phi},\left\{\hat{Q},\rho_S\right\}\right] + \frac{\mathrm{i}\gamma_{\Phi Q}}{2\hbar L\Omega}\left[\hat{\Phi}^2,\rho_S\right] \\ &+ \frac{\mathrm{i}\gamma_{\Phi Q}}{2\hbar L\Omega}\left[\hat{\Phi},\left\{I_c L\sin\left(\frac{2\pi}{\Phi_0}(\hat{\Phi}+\Phi_x)\right),\rho_S\right\}\right] \\ &- \frac{\gamma_{\Phi Q}\Omega}{\hbar\omega_0}\left[\hat{\Phi},\left[\hat{Q},\rho_S\right]\right] - \frac{C\omega_0\gamma_{\Phi Q}}{\hbar}\left[\hat{\Phi},\left[\hat{\Phi},\rho_S\right]\right] \\ &- \frac{C\omega_0\gamma_{\Phi Q}}{\hbar}\left[\hat{\Phi},\left[I_c L\sin\left(\frac{2\pi}{\Phi_0}(\hat{\Phi}+\Phi_x)\right),\rho_S\right]\right]\end{aligned} \tag{3.29}$$

3.2.5 Charge-Flux Terms

3.2.5.1 Correlations $\left\langle \hat{B}_Q\hat{B}_\Phi(-\tau)\right\rangle_B$ and Spectral Density

We complete the set by now considering the correlation functions $\left\langle \hat{B}_Q\hat{B}_\Phi(-\tau)\right\rangle_B$ and $\left\langle \hat{B}_\Phi(-\tau)\hat{B}_Q\right\rangle_B$ the commutator and anticommutator of which (see Appendix D.3) may be written:

$$\begin{aligned}\left\langle\left[\hat{B}_Q,\hat{B}_\Phi(-\tau)\right]\right\rangle_B &= -2\mathrm{i}\hbar\sum_n \frac{\eta_n\kappa_n}{2}\cos(\omega_n\tau) = -\mathrm{i}D_{\Phi Q}(\tau) \\ \left\langle\left\{\hat{B}_Q,\hat{B}_\Phi(-\tau)\right\}\right\rangle_B &= -2\hbar\sum_n \frac{\eta_n\kappa_n}{2}\coth\left(\frac{\hbar\omega_n}{2k_BT}\right)\sin(\omega_n\tau) = -D_{\Phi Q1}(\tau)\end{aligned} \tag{3.30}$$

where $D_{\Phi Q}(\tau)$ and $D_{\Phi Q1}(\tau)$ are the same cross functions introduced in the previous subsection with explicit values of:

$$\begin{aligned}D_{\Phi Q}(-\tau) &= \hbar\Omega\gamma_{\Phi Q}e^{-\Omega\tau} \\ D_{\Phi Q1}(-\tau) &= \frac{2\hbar\gamma_{\Phi Q}\Omega^2}{\omega_0}e^{-\Omega\tau}\end{aligned} \tag{3.31}$$

The Flux-Charge dissipator then becomes:

$$\mathcal{K}_{Q\Phi} = -\frac{1}{\hbar^2}\int_0^\infty \mathrm{d}\tau \Bigg(\frac{\mathrm{i}}{2} D_{\Phi Q}(\tau) \left[\hat{Q}, \left\{\hat{\Phi}(-\tau), \rho_S\right\}\right] - \frac{1}{2} D_{\Phi Q 1}(\tau) \left[\hat{Q}, \left[\hat{\Phi}(-\tau), \rho_S\right]\right] \Bigg) \tag{3.32}$$

Substituting the explicit values for the noise and dissipation kernels, yields:

$$\mathcal{K}_{Q\Phi} = -\frac{\mathrm{i}\gamma_{\Phi Q}}{2\hbar}\left[\hat{Q}, \left\{\sum_n \frac{n!}{\Omega^n} A_n[\hat{\Phi}], \rho_S\right\}\right] + \frac{\gamma_{\Phi Q}\Omega}{\hbar\omega_0}\left[\hat{Q}, \left[\sum_n \frac{n!}{\Omega^n} A_n[\hat{\Phi}], \rho_S\right]\right] \tag{3.33}$$

Expanding $\hat{\Phi}(-\tau)$ to first order and substituting yields the final form of the Charge-Flux dissipator:

$$\begin{aligned}\mathcal{K}_{Q\Phi} = &-\frac{\mathrm{i}\gamma_{\Phi Q}}{2\hbar}\left[\hat{Q}, \left\{\hat{\Phi}, \rho_S\right\}\right] + \frac{\mathrm{i}\gamma_{\Phi Q}}{2\hbar C\Omega}\left[\hat{Q}^2, \rho_S\right] \\ &+ \frac{\gamma_{\Phi Q}\Omega}{\hbar\omega_0}\left[\hat{Q}, \left[\hat{\Phi}, \rho_S\right]\right] - \frac{\gamma_{\Phi Q}}{\hbar C\omega_0}\left[\hat{Q}, \left[\hat{Q}, \rho_S\right]\right]\end{aligned} \tag{3.34}$$

3.2.6 Total Dissipator

Combining $\mathcal{K}_{\Phi\Phi}$, $\mathcal{K}_{\Phi Q}$, $\mathcal{K}_{Q\Phi}$ and $\mathcal{K}_{QQ}$ gives the total expression for the dissipator:

$$
\begin{aligned}
\mathcal{K} =& \mathcal{K}_{\Phi\Phi} + \mathcal{K}_{\Phi Q} + \mathcal{K}_{Q\Phi} + \mathcal{K}_{QQ} \\
=& \frac{\mathrm{i}C\gamma_\Phi\Omega}{\hbar}\left[\hat{\Phi}^2, \rho_S\right] - \frac{\mathrm{i}\gamma_\Phi}{\hbar}\left[\hat{\Phi}, \left\{\hat{Q}, \rho_S\right\}\right] - \frac{C\gamma_\Phi\omega_0}{2\hbar}\left[\hat{\Phi}, \left[\hat{\Phi}, \rho_S\right]\right] \\
&+ \frac{\gamma_\Phi\omega_0}{2\hbar\Omega}\left[\hat{\Phi}, \left[\hat{Q}, \rho_S\right]\right] + \frac{\mathrm{i}\gamma_{\Phi Q}}{2\hbar}\left[\hat{\Phi}, \left\{\hat{Q}, \rho_S\right\}\right] + \frac{\mathrm{i}\gamma_{\Phi Q}}{2\hbar L\Omega}\left[\hat{\Phi}^2, \rho_S\right] \\
&+ \frac{\mathrm{i}\gamma_{\Phi Q}}{2\hbar L\Omega}\left[\hat{\Phi}, \left\{I_c L \sin\left(\frac{2\pi}{\Phi_0}(\hat{\Phi} + \Phi_x)\right), \rho_S\right\}\right] - \frac{\gamma_{\Phi Q}\Omega}{\hbar\omega_0}\left[\hat{\Phi}, \left[\hat{Q}, \rho_S\right]\right] \\
&- \frac{C\omega_0\gamma_{\Phi Q}}{\hbar}\left[\hat{\Phi}, \left[\hat{\Phi}, \rho_S\right]\right] - \frac{C\omega_0\gamma_{\Phi Q}}{\hbar}\left[\hat{\Phi}, \left[I_c L \sin\left(\frac{2\pi}{\Phi_0}(\hat{\Phi} + \Phi_x)\right), \rho_S\right]\right] \\
&- \frac{\mathrm{i}\gamma_{\Phi Q}}{2\hbar}\left[\hat{Q}, \left\{\hat{\Phi}, \rho_S\right\}\right] + \frac{\mathrm{i}\gamma_{\Phi Q}}{2\hbar C\Omega}\left[\hat{Q}^2, \rho_S\right] + \frac{\gamma_{\Phi Q}\Omega}{\hbar\omega_0}\left[\hat{Q}, \left[\hat{\Phi}, \rho_S\right]\right] \\
&- \frac{\gamma_{\Phi Q}}{\hbar C\omega_0}\left[\hat{Q}, \left[\hat{Q}, \rho_S\right]\right] + \frac{\mathrm{i}L\gamma_Q\Omega}{\hbar}\left[\hat{Q}^2, \rho_S\right] + \frac{\mathrm{i}\gamma_Q}{\hbar}\left[\hat{Q}, \left\{\hat{\Phi}, \rho_S\right\}\right] \\
&+ \frac{\mathrm{i}\gamma_Q}{\hbar}\left[\hat{Q}, \left\{I_c L \sin\left(\frac{2\pi}{\Phi_0}(\hat{\Phi} + \Phi_x)\right), \rho_S\right\}\right] - \frac{\gamma_Q}{2C\hbar\omega_0}\left[\hat{Q}, \left[\hat{Q}, \rho_S\right]\right] \\
&- \frac{\gamma_Q\omega_0}{2\hbar\Omega}\left[\hat{Q}, \left[\hat{\Phi}, \rho_S\right]\right] - \frac{\gamma_Q\omega_0}{2\hbar\Omega}\left[\hat{Q}, \left[I_c L \sin\left(\frac{2\pi}{\Phi_0}(\hat{\Phi} + \Phi_x)\right), \rho_S\right]\right]
\end{aligned}
\tag{3.35}
$$

which may be simplified using properties of commutators, whilst collecting like terms. Doing so yields:

$$
\begin{aligned}
\mathcal{K} =& \frac{\mathrm{i}}{\hbar}\left[\hat{H}_c', \rho_S\right] - \frac{\mathrm{i}}{\hbar}\left(\gamma_\Phi + \gamma_Q - \gamma_{\Phi Q}\right)\left[\hat{\Phi}, \left\{\hat{Q}, \rho_S\right\}\right] \\
& - \frac{\mathrm{i}}{\hbar}\left(\gamma_Q - \frac{\gamma_{\Phi Q}}{2}\right)\left[\left\{\hat{\Phi}, \hat{Q}\right\}, \rho_S\right] - \frac{C\omega_0}{\hbar}\left(\gamma_{\Phi Q} + \frac{\gamma_\Phi}{2}\right)\left[\hat{\Phi}, \left[\hat{\Phi}, \rho_S\right]\right] \\
& + \frac{\omega_0}{2\hbar\Omega}(\gamma_\Phi - \gamma_Q)\left[\hat{\Phi}, \left[\hat{Q}, \rho_S\right]\right] - \frac{1}{C\hbar\omega_0}\left(\gamma_{\Phi Q} + \frac{\gamma_Q}{2}\right)\left[\hat{Q}, \left[\hat{Q}, \rho_S\right]\right] \\
& + \frac{\mathrm{i}\gamma_{\Phi Q}}{2\hbar L\Omega}\left[\hat{\Phi}, \left\{I_c L \sin\left(\frac{2\pi}{\Phi_0}(\hat{\Phi} + \Phi_x)\right), \rho_S\right\}\right] \\
& - \frac{C\omega_0\gamma_{\Phi Q}}{\hbar}\left[\hat{\Phi}, \left[I_c L \sin\left(\frac{2\pi}{\Phi_0}(\hat{\Phi} + \Phi_x)\right), \rho_S\right]\right] \\
& + \frac{\mathrm{i}\gamma_Q}{\hbar}\left[\hat{Q}, \left\{I_c L \sin\left(\frac{2\pi}{\Phi_0}(\hat{\Phi} + \Phi_x)\right), \rho_S\right\}\right] \\
& - \frac{\gamma_Q\omega_0}{2\hbar\Omega}\left[\hat{Q}, \left[I_c L \sin\left(\frac{2\pi}{\Phi_0}(\hat{\Phi} + \Phi_x)\right), \rho_S\right]\right]
\end{aligned}
\tag{3.36}
$$

where the coloured terms highlight the contributions from Eq. (3.35) and their simplifcation in Eq. (3.36). The counter term, similar in nautre to those found in §2.2.1.3 and §2.2.1.4, given by $\hat{H}_c' = \left(C\Omega\gamma_\Phi + \frac{\gamma_{\Phi Q}}{2L\Omega}\right)\hat{\Phi}^2 + \left(L\Omega\gamma_Q + \frac{\gamma_{\Phi Q}}{2C\Omega}\right)\hat{Q}^2$ is the renormalisation of SQUID inductance and capacitance due to coupling with the environment, meaning that the initial effective values, L and C, revert back to their bare values i.e. the system parameters prior to coupling, L_0 and C_0, used in the master equation [45, 36, 71, 82]. In the dimensionless representation this becomes:

$$\begin{aligned}\mathcal{K} =& \mathrm{i}\left[\mathcal{H}_c', \rho_S\right] - \mathrm{i}\frac{(\gamma_\Phi + \gamma_Q - \gamma_{\Phi Q})}{\omega_0}\left[\hat{X}, \left\{\hat{P}, \rho_S\right\}\right] - \mathrm{i}\frac{\left(\gamma_Q - \frac{\gamma_{\Phi Q}}{2}\right)}{\omega_0}\left[\left\{\hat{X}, \hat{P}\right\}, \rho_S\right] \\ & - \frac{\left(\gamma_{\Phi Q} + \frac{\gamma_\Phi}{2}\right)}{\omega_0}\left[\hat{X}, \left[\hat{X}, \rho_S\right]\right] + \frac{(\gamma_\Phi - \gamma_Q)}{2\Omega}\left[\hat{X}, \left[\hat{P}, \rho_S\right]\right] \\ & - \frac{\left(\gamma_{\Phi Q} + \frac{\gamma_Q}{2}\right)}{\omega_0}\left[\hat{P}, \left[\hat{P}, \rho_S\right]\right] \\ & + \frac{\mathrm{i}\gamma_{\Phi Q}}{2\Omega}\sqrt{\frac{\beta\nu}{\omega_0}}\left[\hat{X}, \left\{\sin\left(\sqrt{\frac{\beta\omega_0}{\nu}}\hat{X} + 2\pi\frac{\Phi_x}{\Phi_0}\right), \rho_S\right\}\right] \\ & - \frac{\gamma_{\Phi Q}}{\omega_0}\sqrt{\frac{\beta\nu}{\omega_0}}\left[\hat{X}, \left[\sin\left(\sqrt{\frac{\beta\omega_0}{\nu}}\hat{X} + 2\pi\frac{\Phi_x}{\Phi_0}\right), \rho_S\right]\right] \\ & + \frac{\mathrm{i}\gamma_Q}{\omega_0}\sqrt{\frac{\beta\nu}{\omega_0}}\left[\hat{P}, \left\{\sin\left(\sqrt{\frac{\beta\omega_0}{\nu}}\hat{X} + 2\pi\frac{\Phi_x}{\Phi_0}\right), \rho_S\right\}\right] \\ & - \frac{\gamma_Q}{2\Omega}\sqrt{\frac{\beta\nu}{\omega_0}}\left[\hat{P}, \left[\sin\left(\sqrt{\frac{\beta\omega_0}{\nu}}\hat{X} + 2\pi\frac{\Phi_x}{\Phi_0}\right), \rho_S\right]\right]\end{aligned} \tag{3.37}$$

As the same cut-off is used for capacitive and inductive coupling (the only difference is in the constant γ) it is possible to simplify notation and write everything in terms of one damping rate, one can always write the contribution of capacitive coupling as a factor of inductive coupling, by setting the mutual damping rate to equal some ratio g times the inductive damping rate, $\gamma_{\Phi Q} = \sqrt{\gamma_\Phi \gamma_Q} = g\gamma_\Phi$ and so $\gamma_Q = g^2\gamma_\Phi = g^2\gamma$. The above expression may be reduced further to:

$$\begin{aligned}\mathcal{K} =& \mathrm{i}\left[\mathcal{H}_c', \rho_S\right] - \frac{\mathrm{i}\gamma}{\omega_0}\left(1+g^2-g\right)\left[\hat{X},\left\{\hat{P},\rho_S\right\}\right] - \frac{\mathrm{i}\gamma}{\omega_0}g\left(g-\frac{1}{2}\right)\left[\left\{\hat{X},\hat{P}\right\},\rho_S\right] \\ &- \frac{\gamma}{\omega_0}\left(g+\frac{1}{2}\right)\left[\hat{X},\left[\hat{X},\rho_S\right]\right] + \frac{\gamma}{2\Omega}\left(1-g^2\right)\left[\hat{X},\left[\hat{P},\rho_S\right]\right] \\ &- \frac{\gamma}{\omega_0}g\left(1+\frac{g}{2}\right)\left[\hat{P},\left[\hat{P},\rho_S\right]\right] \\ &+ \frac{\mathrm{i}\gamma g}{\omega_0}\sqrt{\frac{\beta\nu}{\omega_0}}\left[\frac{\omega_0}{2\Omega}\hat{X}+g\hat{P},\left\{\sin\left(\sqrt{\frac{\beta\omega_0}{\nu}}\hat{X}+2\pi\frac{\Phi_x}{\Phi_0}\right),\rho_S\right\}\right] \\ &- \frac{\gamma g}{\omega_0}\sqrt{\frac{\beta\nu}{\omega_0}}\left[\hat{X}+\frac{g\omega_0}{2\Omega}\hat{P},\left[\sin\left(\sqrt{\frac{\beta\omega_0}{\nu}}\hat{X}+2\pi\frac{\Phi_x}{\Phi_0}\right),\rho_S\right]\right]\end{aligned} \tag{3.38}$$

The counter term can now be written as $\mathcal{H}_c' = \frac{\gamma g}{2\Omega}\left(\hat{X}^2+\hat{P}^2\right) + \frac{\gamma\Omega}{\omega_0^2}\left(\hat{X}^2+g^2\hat{P}^2\right) = \left(\frac{\gamma g}{\Omega}+\frac{\gamma\Omega}{\omega_0^2}\left(1+g^2\right)\right)\left(\hat{n}+1/2\right) + \frac{\gamma\Omega}{2\omega_0^2}\left(\hat{a}^2+\hat{a}^{\dagger 2}\right)\left(1-g^2\right)$ where $\hat{n}$,$\hat{a}$, and $\hat{a}^\dagger$ are the number, annihilation and creation operators of the harmonic part of the SQUID potential respectively. Written this way, it can be seen that the first term describes a shift in the energy levels of the system, while the second describes a frequency shift and squeezing similar in nature to those brought about from $\hat{X}\hat{P}+\hat{P}\hat{X}$ terms, the effects of which will be explored in the next chapter.

3.3 Results

3.3.1 Lindblad form of the Master Equation

In order to ensure conservation of probability and represent physical intermediate dynamics, it is necessary to transform the above equation into Lindblad form; this will include the introduction of a $\left[\sin\hat{X},\left[\sin\hat{X},\rho_S\right]\right]$

term which can only be found through this transformation. We therefore recall the standard from of the generator:

$$\mathcal{L}\rho_S = -\mathrm{i}\,[H,\rho_S] + \sum_{i,j=1}^{N^2-1} a_{ij}\left(F_i\rho_S F_j^\dagger - \frac{1}{2}\left\{F_j^\dagger F_i, \rho_S\right\}\right) \tag{3.39}$$

where $F_{i,j}$ are Hermitian operators and a_{ij} represents the coefficient matrix and which can be put into Lindblad form if (a_{ij}) is positive semi-definite. In terms of our model which possesses terms such as $\hat{X}$, $\hat{P}$ and $J = \sin\hat{X}$, this matrix is a 3×3 matrix given by:

$$(a_{ij}) = \begin{pmatrix} a_{XX} & a_{XP} & a_{XJ} \\ a_{PX} & a_{PP} & a_{PJ} \\ a_{JX} & a_{JP} & a_{JJ} \end{pmatrix} \tag{3.40}$$

where the elements a_{ij} are simply the coefficients of their respective commutator terms in Eq. (3.38), corresponding to $a_{ij}/2\,[F_i,[F_j,\rho_S]]$. The matrix may be written:

$$(a_{ij}) = \frac{\gamma}{\omega_0}\begin{pmatrix} 2g{+}1 & -\mathrm{i}(1{+}g^2{-}g){-}\frac{\omega_0}{2\Omega}(1{-}g^2) & g\sqrt{\frac{\beta\nu}{\omega_0}}\left(1{+}\frac{\mathrm{i}\omega_0}{2\Omega}\right) \\ \mathrm{i}(1{+}g^2{-}g){-}\frac{\omega_0}{2\Omega}(1{-}g^2) & 2g{+}g^2 & g^2\sqrt{\frac{\beta\nu}{\omega_0}}\left(\frac{\omega_0}{2\Omega}{+}\mathrm{i}\right) \\ g\sqrt{\frac{\beta\nu}{\omega_0}}\left(1{-}\frac{\mathrm{i}\omega_0}{2\Omega}\right) & g^2\sqrt{\frac{\beta\nu}{\omega_0}}\left(\frac{\omega_0}{2\Omega}{-}\mathrm{i}\right) & 0 \end{pmatrix} \tag{3.41}$$

Terms 2,5,7 and 8 in Eq. (3.38) are all split and produce the adjoint terms in the above matrix using the cyclic property of commutators. What is produced, as well as these matrix elements, are three frequency shifts, the nature of which is discussed in chapter 4:

$$\begin{aligned}
\hat{\mathcal{H}}_{\mathcal{XP}} &= \frac{\gamma}{\omega_0}\left(\frac{3g^2}{2} - g + \frac{1}{2}\right)(\hat{X}\hat{P} + \hat{P}\hat{X}),\\
\hat{\mathcal{H}}_{XJ} &= \frac{\gamma g}{2\Omega}\sqrt{\frac{\beta\nu}{\omega_0}}\hat{X}\sin\left(\sqrt{\frac{\beta\omega_0}{\nu}}\hat{X} + 2\pi\frac{\Phi_x}{\Phi_0}\right),\\
\hat{\mathcal{H}}_{PJ} &= \frac{\gamma g^2}{2\omega_0}\sqrt{\frac{\beta\nu}{\omega_0}}\left(\hat{P}\sin\left(\sqrt{\frac{\beta\omega_0}{\nu}}\hat{X} + 2\pi\frac{\Phi_x}{\Phi_0}\right) + \sin\left(\sqrt{\frac{\beta\omega_0}{\nu}}\hat{X} + 2\pi\frac{\Phi_x}{\Phi_0}\right)\hat{P}\right)\\
&\quad + \frac{\gamma g^2\beta}{4\Omega}\cos\left(\sqrt{\frac{\beta\omega_0}{\nu}}\hat{X} + 2\pi\frac{\Phi_x}{\Phi_0}\right)
\end{aligned} \tag{3.42}$$

It is worth noting however that the final term in the equation above is a renormalisation of the system's potential and is therefore treated in exactly the same way as all other renormalisations in $\hat{\Phi}$ and $\hat{Q}$ this will be neglected when these Hamiltonians are explored.

Finding the appropriate Lindblad operators described by matrix Eq. (3.41) simply requires finding the eigenvalues and eigenvectors of (a_{ij}). To understand this process, we will use the harmonic oscillator as an example.

3.3.1.1 ASIDE: Finding the necessary Lindblad for the Harmonic Oscillator

Recall that the dissipator for the harmonic oscillator in the low temperature, high cut off limit is given by:

$$\mathcal{K}_{\mathcal{HO}} = \frac{\gamma}{\omega_0}\left(\left[\hat{X},\left[\hat{X},\rho_S\right]\right] - \mathrm{i}\left[\hat{X},\left\{\hat{P},\rho_S\right\}\right]\right) \tag{3.43}$$

the coefficient matrix corresponding to this equation is given by:

$$a_{HO} = \frac{\gamma}{\omega_0} \begin{pmatrix} 1 & -\mathrm{i} \\ \mathrm{i} & 0 \end{pmatrix} \tag{3.44}$$

As $\det(a) = -1$, this matrix is not currently positive semi-definite, a requirement for an equation to be of Lindblad type. Transforming this equation in Lindblad type involves inserting a 'minimally invasive' term to ensure that the above matrix is indeed positive semi definite; that is to say that all eigenvalues are equal to, or greater than zero and consequently the determinant of the above matrix is greater than or equal to zero. The above matrix that satisfies these conditions given by:

$$a_{HO} = \frac{\gamma}{\omega_0} \begin{pmatrix} 1 & -\mathrm{i} \\ \mathrm{i} & 1 \end{pmatrix} \tag{3.45}$$

whose determinant is equal to 0. The eigenvalues of this matrix are trivial to calculate, one of which is zero and the other is $\lambda = 2$. Reinserting the eigenvalue yields the corresponding eigenvector, since there is only one non-zero eigenvalue, there is only one eigenvector of interest:

$$\frac{\gamma}{\omega_0} \begin{pmatrix} -1 & -\mathrm{i} \\ \mathrm{i} & -1 \end{pmatrix} \begin{pmatrix} a \\ b \end{pmatrix} = 0 \tag{3.46}$$

The corresponding eigenvector is therefore:

$$\vec{e}_1 = \frac{1}{\sqrt{2}} \begin{pmatrix} 1 \\ \mathrm{i} \end{pmatrix} \tag{3.47}$$

as a_{HO} is in the position-momentum basis, this eigenvector can be thought of

as the diagonalised operators $F_{i,j}$ in Eq. (3.39) with the vector components referring to $\hat{X}$ and $\hat{P}$. The corresponding Lindblad is therefore simply the square root of eigenvalue multiplied by this new eigenvalue, that is to say:

$$L_1 = \sqrt{\frac{2\gamma}{\omega_0}}\frac{1}{\sqrt{2}}\left(\hat{X} + \mathrm{i}\hat{P}\right) = \sqrt{\frac{2\gamma}{\omega_0}}\hat{a} \tag{3.48}$$

which shows that the natural Lindblad for the harmonic oscillator is proportional to the annihilation operator.

3.3.1.2 Lindblad for the charge-coupled SQUID

We will now apply the technique of completing the coefficient matrix to the case of the SQUID. The master equation for such a system coupled to an Ohmic bath in this way must satisfy the Lindblad master equation:

$$\begin{aligned}\frac{d\rho}{dt} =& -\mathrm{i}[\hat{\mathcal{H}}', \rho] \\ &+ \frac{1}{2}\sum_j \left\{[\hat{L}_j(g), \rho\hat{L}_j^\dagger(g)] + [\hat{L}_j(g)\rho, \hat{L}_j^\dagger(g)]\right\}\end{aligned} \tag{3.49}$$

where the $\hat{L}_j(g)$ are Lindblad operators representing non-unitary loss and exist as a linear combination of the operators $\hat{X}$, $\hat{P}$, and $\sin\left(\sqrt{\frac{\beta\omega_0}{\nu}}\hat{X} + 2\pi\frac{\Phi_x}{\Phi_0}\right)$ for a SQUID. As for the QHO, finding these operators requires diagonalisation of the coefficient matrix:

$$a_{ij} = \frac{\gamma}{\omega_0}\begin{pmatrix} 2g+1 & -\mathrm{i}(1+g^2-g)-\xi(1-g^2) & g\sqrt{\frac{\beta\nu}{\omega_0}}(1+\mathrm{i}\xi) \\ \mathrm{i}(1+g^2-g)-\xi(1-g^2) & 2g+g^2 & g^2\sqrt{\frac{\beta\nu}{\omega_0}}(\xi+\mathrm{i}) \\ g\sqrt{\frac{\beta\nu}{\omega_0}}(1-\mathrm{i}\xi) & g^2\sqrt{\frac{\beta\nu}{\omega_0}}(\xi-\mathrm{i}) & 0 \end{pmatrix} \tag{3.50}$$

where $\xi = \omega_0/2\Omega$ is half the ratio of the system characteristic frequency and and bath cut off frequency, as seen in §2.2.1. We present the complete

matrix with eight out of nine elements present, as opposed to the five found in the second order inductive model [45]. The splitting of matrices seen in [45], into two 2×2 coefficient matrices is not necessary here due to the non-trivial nature of the matrix. As is often found in an equation that is not of Lindblad type, the coefficient matrix is not positive semidefinite, and so probability is not conserved. To produce a physical representation of the system, the matrix requires completing. One additional term is introduced to the above matrix to satisfy the positive semi-definite condition that requires eigenvalues to be non-negative along with their product (determinant), with reference to Eq. (3.40) this allows us to write:

$$\begin{aligned} \det(a_{ij}) &= a_{JJ}(a_{XX}a_{PP} - a_{XP}a_{PX}) - a_{PJ}(a_{XX}a_{JP} - a_{XP}a_{JX}) \\ &\quad + a_{XJ}(a_{PX}a_{JP} - a_{PP}a_{JX}) = 0 \\ \Rightarrow a_{JJ} &= \frac{a_{PJ}(a_{XX}a_{JP} - a_{XP}a_{JX}) - a_{XJ}(a_{PX}a_{JP} - a_{PP}a_{JX})}{a_{XX}a_{PP} - a_{XP}a_{PX}} \end{aligned} \tag{3.51}$$

Satisfying this condition and applying to Eq. (3.52), yields:

$$a_{ij} = \frac{\gamma}{\omega_0} \begin{pmatrix} 2g+1 & -\mathrm{i}(1+g^2-g)-\xi(1-g^2) & g\sqrt{\frac{\beta\nu}{\omega_0}}(1+\mathrm{i}\xi) \\ \mathrm{i}(1+g^2-g)-\xi(1-g^2) & 2g+g^2 & g^2\sqrt{\frac{\beta\nu}{\omega_0}}(\xi+\mathrm{i}) \\ g\sqrt{\frac{\beta\nu}{\omega_0}}(1-\mathrm{i}\xi) & g^2\sqrt{\frac{\beta\nu}{\omega_0}}(\xi-\mathrm{i}) & \frac{\beta\nu}{\omega_0}\frac{4g^4+8\xi^2g^3}{(-g^4+2g^2-1)(1+\xi^2)+4g(g^2+1)} \end{pmatrix} \tag{3.52}$$

The Lindblads and their amplitudes are both found by diagonalisation of the above matrix with the eigenvectors giving normalised Lindblads and eigenvalues giving their respective amplitudes. Since the determinant of the matrix is zero, the number of Lindblads reduces from three to two since one

of the eigenvalues of (a_{ij}) carries a weighting of zero; this is simply a result of the diagonalisation process and is often used in master equation approaches [57]. The behaviour of the Lindblad weightings are given in Fig. 3.1. It is first worth noting that due to the completion process of the coefficient matrix, there exists a singularity due to the denominator having a root equal to zero. For a cut off frequency of $\Omega = 2\omega_0$, this exists at $g = 0.2271$; any values below this gives one negative eigenvalue, thus violating the positive-semidefinite condition. There also exists a root at $g = 4.402$ but since the analysis here aims to look at smaller capacitive couplings, the region of coupling strength explored is $0.25 \leq g \leq 0.55$, where the eigenvalues appear to stabilise, whilst one remains zero throughout.

The eigeinvalues presented in Fig. 3.1 describe the weighting of each Lindblad, the non trivial g-dependence of which is presented in Fig. 3.2 and Fig. 3.3. These figures show the real and imaginary contribution from each operator, $\hat{X}$, $\hat{P}$, and $s(\hat{X}, \Phi_x) = \sin\left(\sqrt{\beta\omega_0/\nu}\hat{X} + 2\pi\Phi_x/\Phi_0\right)$, to each Lindblad L_1 and L_2 as functions of coupling ratio g; thus allowing the Lindblads in Eq. (3.49) to be quantified and the external flux dependence of the steady state purity, a measure of the dependence a quantum system's decoherence has on external degrees of freedom, to be found. The dominant effect on these Lindblad operators as g increases is not surprising. In any dissipative model involving SQUIDs one would expect to see elements of the annihilation operator [52, 88, 89, 90, 91], a common phenomenological tool used to model dissipation in harmonic oscillators, since this system is a nonlinear extension to the harmonic oscillator model; the effect of this Lindblad becomes more significant as capacitive coupling is increased. It has already been shown that

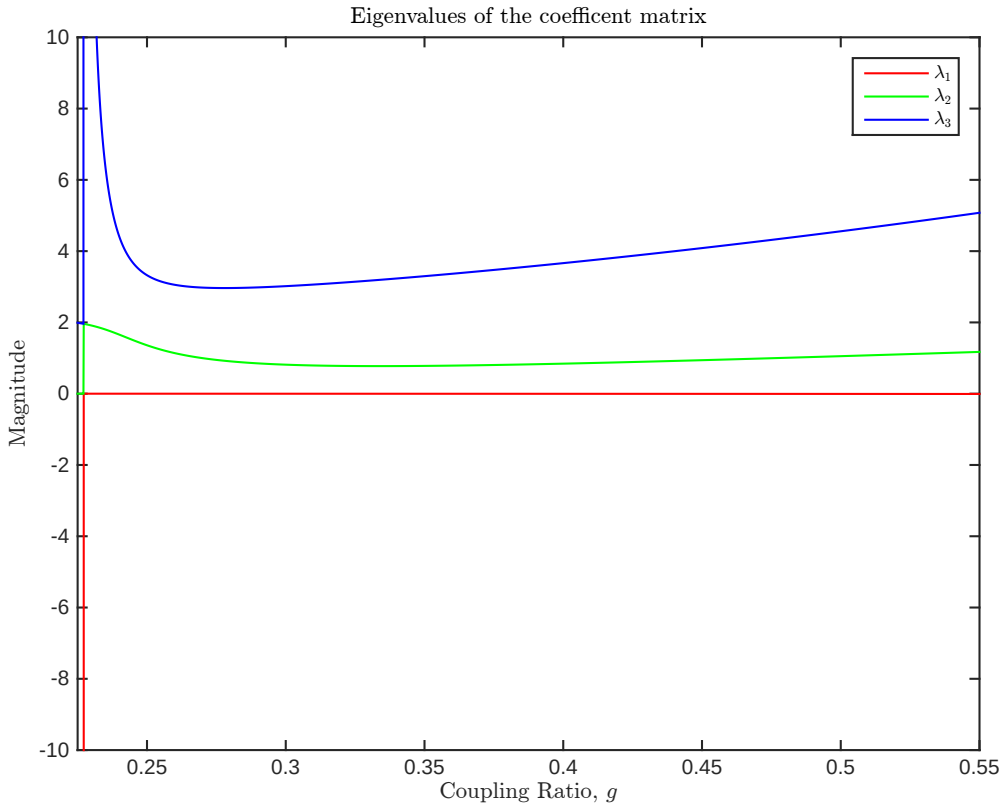

Figure 3.1: The three eigenvalues of the diagonliased coefficent matrix as a function of coupling ratio g. The discontinuity shown at small values of g, shown here as a swapping of eigenvalues, is created by the singluar nature of the additional a_{JJ} term at this value.

the decoherence of a SQUID possesses an external flux dependence [45], existing in the form of the sine operator within the Lindblad; this again can be seen here in Fig. 3.2 and Fig. 3.3. Note that the complexity of the operators reduces greatly when the high cut off limit, $\Omega \gg \omega_0$, is approached, with contributions from the position and sine operators becoming purely real and the

momentum contribution becoming purely imaginary, yielding a combination of creation and annihilation Lindblads with some external flux dependence; this arises from the reduction of Ω dependent terms in the coefficient matrix Eq. (3.52) in this limit.

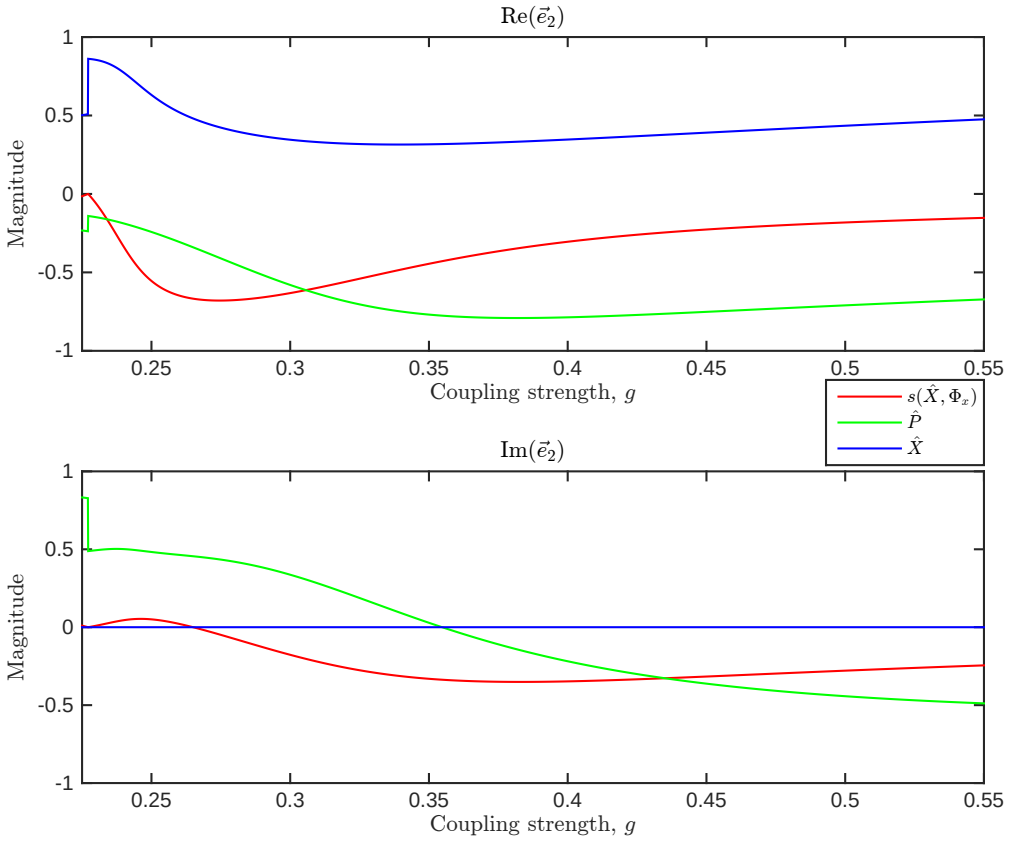

Figure 3.2: The real and imaginary components to the constituent operators of the first Lindblad, eigenvector $\vec{e}_2$ of (a_{ij}), with eigenvalue λ_2 as a function of coupling ratio g.

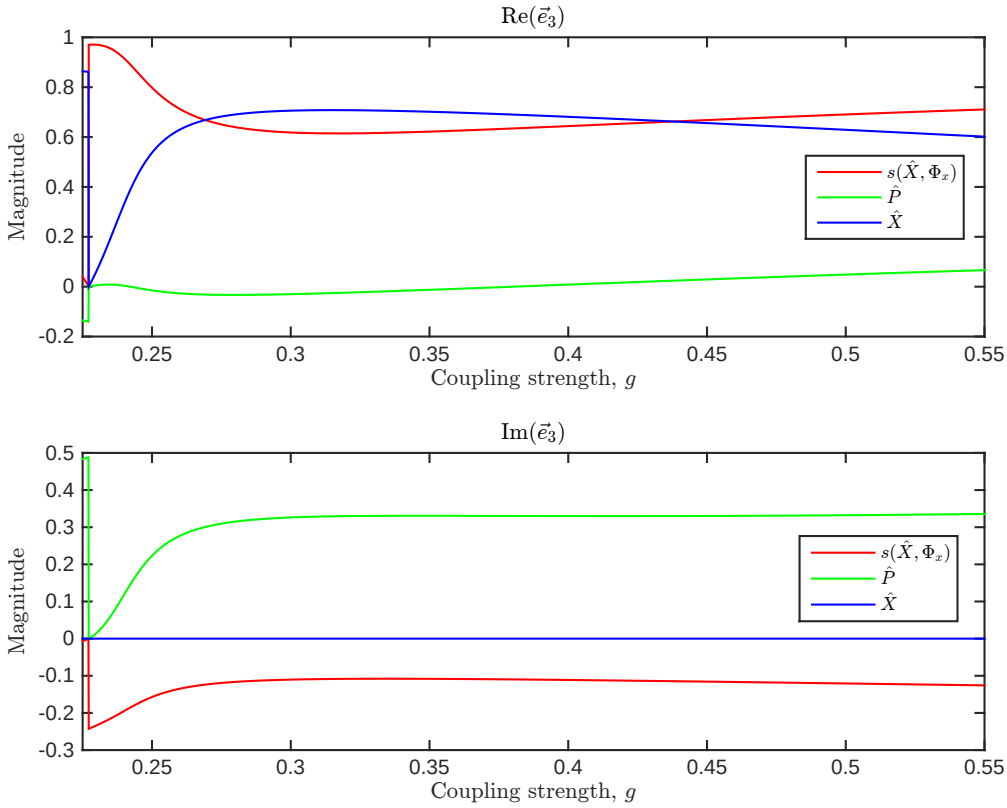

Figure 3.3: The real and imaginary components to the constituent operators of the second Lindblad with eigenvalue λ_3 as a function of coupling ratio g.

3.3.2 Decoherence due to inductive and capacitive coupling

In this work we chose to quantify the effect of capacitive coupling on decoherence of the SQUID by use of the purity of the steady state $\mathrm{Tr}\{\rho^2\}$ and its dependence on externally applied magnetic flux, in a similar way to that shown in §2.2.1.3 and §2.2.1.4. Fig. 3.4 shows the steady state-external

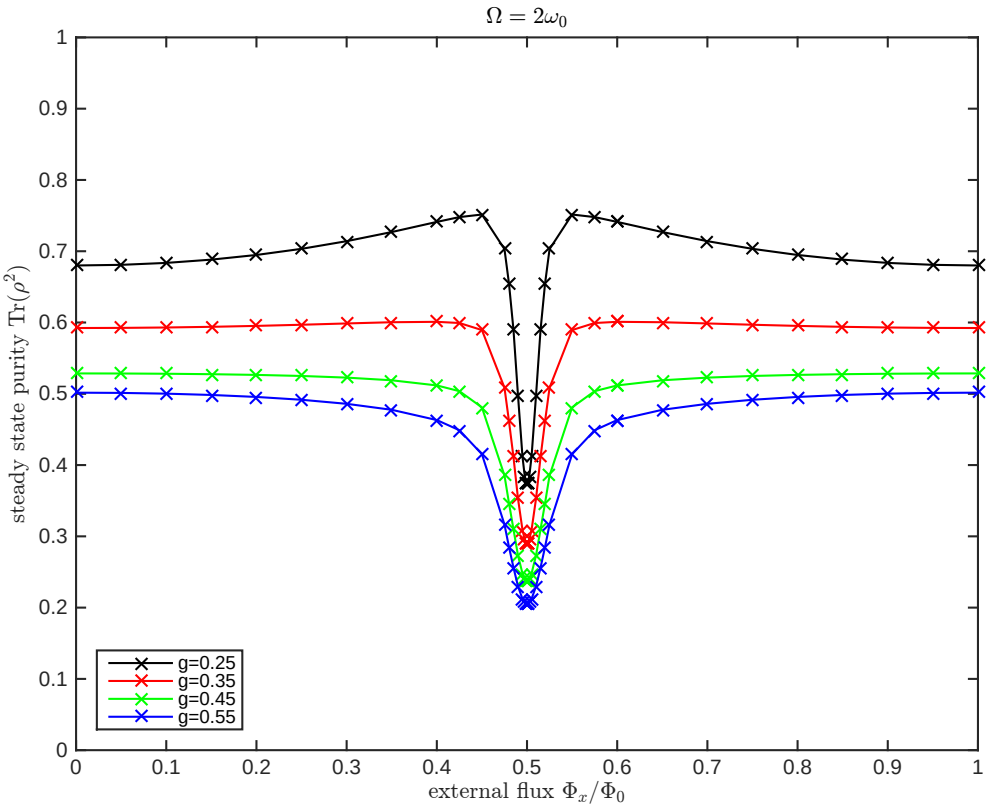

Figure 3.4: The steady state purity of a SQUID coupled inductively and capacitively to an Ohmic bath as a function of external flux for various capacitive coupling strengths at a bath cut off frequency of $\Omega = 2\omega_0$.

flux relationship for a number of coupling ratios, and therefore Lindblads, at a largely resistive bath cut-off frequency of $\Omega = 2\omega_0$. The Lindblads responsible for these dissipative effects were found using Fig. 3.1-3.3 which show their weighting and constituent operator contributions at various values g. The curves in Fig. 3.4 were produced from the steady state density matrix calculated using Eq. (3.49). For example, the black curve in Fig. 3.4 displays

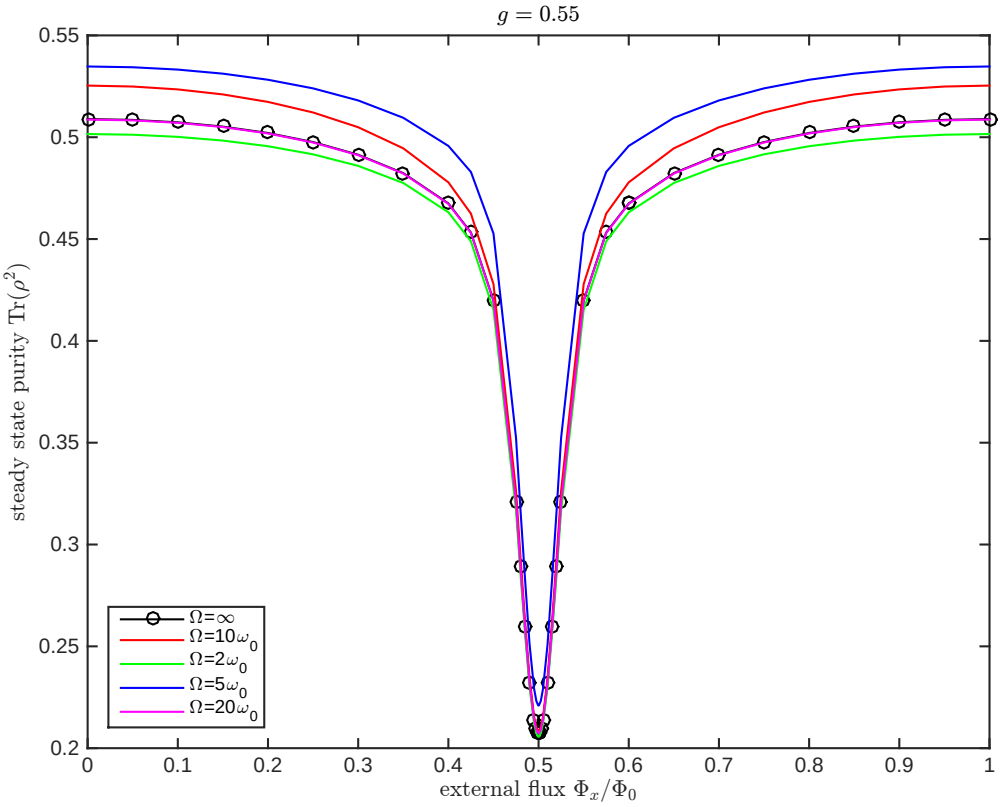

Figure 3.5: The steady state purity of a SQUID coupled inductively and capacitively to an Ohmic bath as a function of external flux for various bath cut off frequencies at a coupling ratio of $g = 0.55$.

the effect of the Lindblad operator:

$$L_1(g=0.25) = \sqrt{1.36\gamma}\left(0.63\hat{X} + (0.48\mathrm{i} - 0.24)\hat{P} + (0.05\mathrm{i} - 0.55)s(\hat{X}, \Phi_x)\right)$$
$$L_2(g=0.25) = \sqrt{3.32\gamma}\left(0.54\hat{X} + (0.22\mathrm{i} - 0.01)\hat{P} + (0.80 - 0.16\mathrm{i})s(\hat{X}, \Phi_x)\right) \tag{3.53}$$

on the steady state purity of the system. The figure shows a general drop in purity as the capacitive coupling is increased. This drop in purity suggests an increase in mixing with the environment, and a sharing of information between more than just two distinct states; this will be discussed later in this section. As the capacitive coupling is increased, the steady state purity curves change in shape, showing a strong resemblance to that produced by the annihilation operator in the purely inductive model [45] at $g = 0.25$, and progressing into a curve with a significantly different shape sloping into a wider well for a $g = 0.55$. The well, shown by the drop in purity at the half integer, arises when the SQUID decoheres from a Schrödinger cat state into a statistical mixture of left and right well occupations. The width of the well, in the steady state-external flux dependence, suggests a tolerance over which a pseudo-cat state may be made; this widens as g increases, suggesting a larger range of external flux over which a cat state might be possible as the a quasi-double well potential with similar (but not equal) minima exists over a larger range.

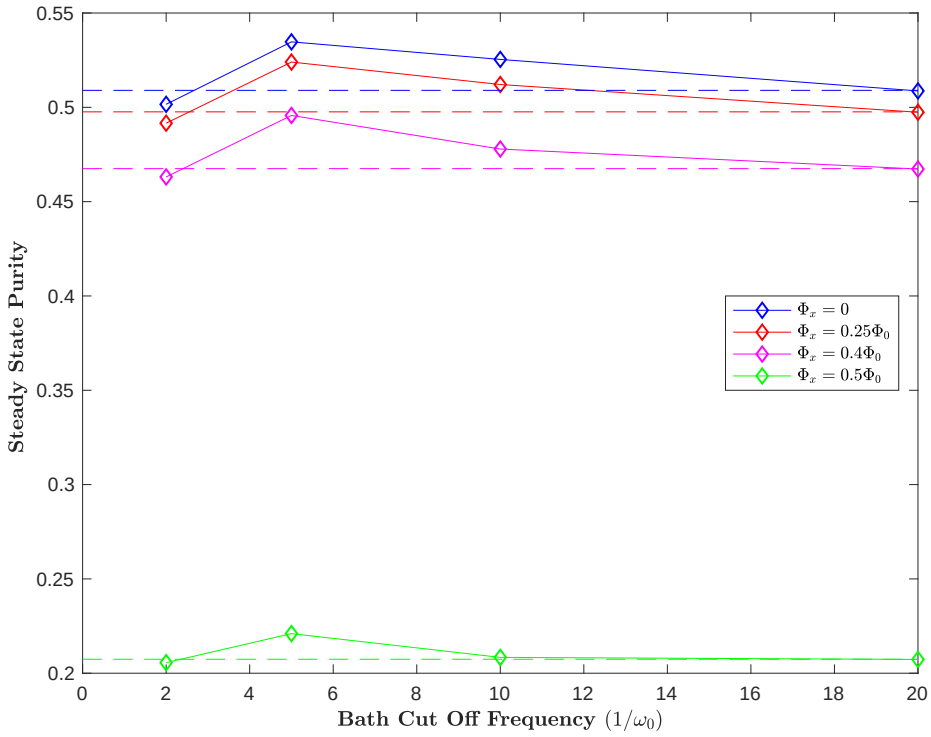

Figure 3.6: The steady state purity of the system plotted for various bath cut off frequencies (solid line) at various of external flux; this is to highlight this non-linear relationship, which settles towards a fixed value as Ω is increased. It can also be seen that the range of purity decreases as external flux is increased. The dotted lines indicate the steady state purity in the $\Omega \to \infty$ limit.

The impact of increasing g is far more significant than increasing Ω as shown in Fig. 3.5. The figure shows the steady state purity of the SQUID as a function of external flux, at a fixed coupling ratio of $g = 0.55$ and a range of bath cut off frequencies. The dependence of steady state purity on bath cut off appears to peak, at all values of external flux at around

$\Omega = 5\omega_0$ before settling towards a limit at $\Omega = \infty$, with the value at a given external flux increasing from $\Omega = 2\omega_0$ to $5\omega_0$, falling again to $20\omega_0$ before finally settling towards a fixed value as the the high cut off limit is approached; this further highlights the non trivial nature of these Lindblads and the impact they have on the system's decoherence. It was shown in the previous chapter that smaller bath cut offs can reduce the purity of the system; for this parasitic capacitive model the effect is relatively small compared to the effect of changing coupling ratio which alters the general shape of each purity curve. The well width at high cut-off also appears to remain similar, in contrast to the behaviour shown in Fig. 3.4.

The steady state purity in both Fig. 3.4 and Fig. 3.5 can be seen to fall below a half. Usually one would expect to see the purity to fall to half as the state of the isolated system is expected to become a perfect statistical mixture of localisation in each well. Further mixing suggests that the state is not only being shared by each well, but by excited states in those wells. Fig. 3.7 shows the probability density for the state at external flux values $\Phi_x = 0, 0.5\Phi_0$ with coupling ratios of $g = 0.25, 0.55$, and demonstrates an increasing population of higher energy states within each well. The master equation that has been used to model the decoherence in this thesis is similar to a weak measurement process and so the pointer state of the ensemble, of system and bath, would be expected to be in the pointer basis of the measurement apparatus, which differs from the annihilation operator used for the HO. By extracting the density matrix of the decohered system and finding its eigenvectors and eigenvalues of said matrix, the probability density functions associated to the state have been re-constructed. The initial pur-

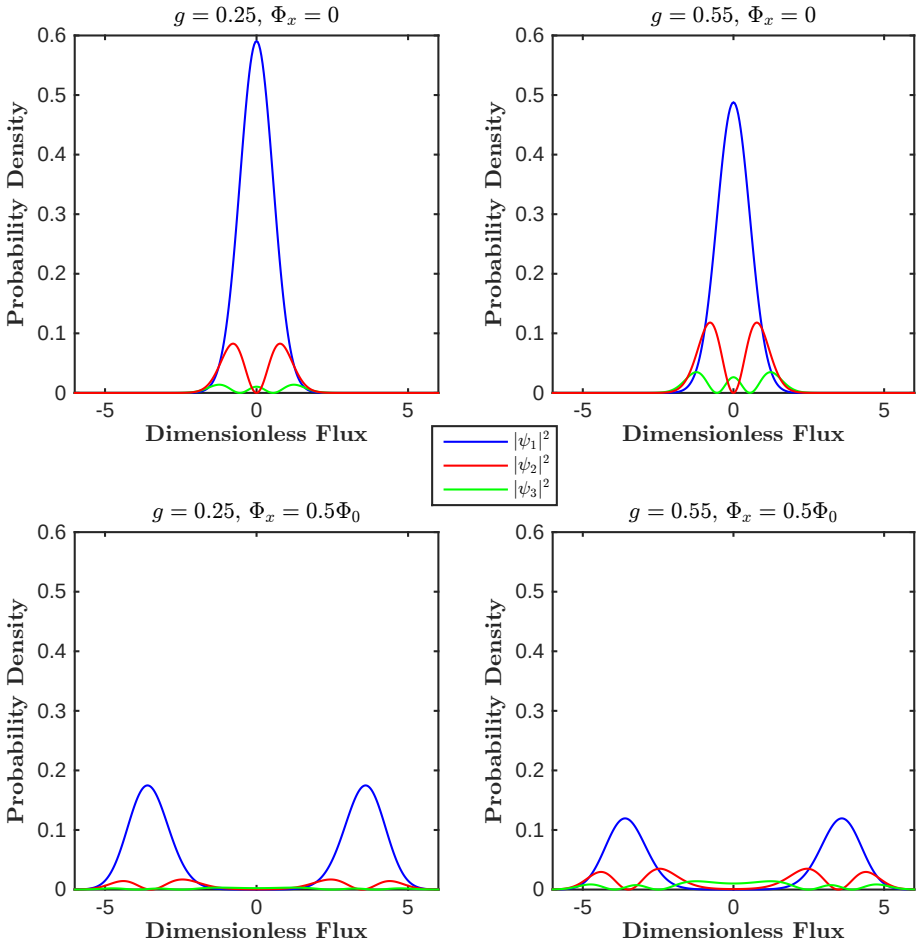

Figure 3.7: The probability density of the SQUID's ground state and first two excited states after decoherence as a function of dimensionless flux for a bath cut off frequency of $\Omega = 2\omega_0$

pose of Fig. 3.7 is to demonstrate that the system decoheres into a statistical mixture of states populating left and right wells at $\Phi_x = 0.5\Phi_0$ and this is evident in the probability distribution showing peaks in both wells, which differs from the single well population shown at $\Phi_x = 0$. Contributions also

exist from excited states, with their contributions increasing as the coupling ratio is increased (purity is decreased). Such population of higher states is characteristic of classical noise, which causes leakage to higher energy states and can inhibit the characterisation of qubits as two level systems. This behaviour is different to the spontaneous decay found in Flux qubits due to $1/f$ noise where the system would be expected to reach a purity of approximately $\mathrm{Tr}\{\rho^2\} = 0.5$ [106].

3.4 Summary

In this chapter the effect of introducing capacitive coupling to the SQUID decoherence model has been explored. In modelling a SQUID both inductively and capacitively coupled to an Ohmic bath, external flux dependent terms have arisen in the dissipation at the first order which contrasts to second order findings in the purely inductive model. This earlier order external flux dependence shows that for the inducto-capactive regime external degrees of freedom play an even larger role in this decoherence model. It was found that the $\left[\hat{Q}, \left[\hat{Q}, \rho\right]\right]$ term, added to the purely inductive model, is found naturally although an incomplete coefficient matrix is still produced.

The additional term required to produce an equation of Lindblad type was found through diagonalisation of the coefficient matrix whose eigenvectors, existing as a linear contribution of $\hat{X}$, $\hat{P}$, and $s(\hat{X}, \Phi_x)$ operators, give the Lindblad with their respective weighting given by the corresponding eigenvalue. This model appeared more 'complete' than the inductive model as the coefficient matrix possessed 8 of the 9 required elements. The additional term is therefore a 'minimum necessity' rather than 'minimally invasive' as the previous chapter discussed.

The Lindblads presented here were found to possess a non-trivial dependence on capacitive coupling strength g, and existed only in a fixed range, outside of which an analysis similar to that in the last chapter would be necessary; this was found due to the additional term becoming singular outside of the range used. It is therefore worth stressing that this model is in itself incomplete but offer good insight into the effects of capacitive coupling on the level of decoherence and energy leakage associated to inductively coupled SQUIDs.

It was shown that the SQUIDs steady state purity, and its external flux dependence varies more significantly with changing coupling strength than bath cutoff frequency, which causes a peak in purity and then settles as $\Omega \to \infty$. The purity of the SQUID was seen to fall below $\mathrm{Tr}\{\rho^2\} = 0.5$ at half integer external flux and analysis of the system's probability density functions strengthened arguments that information was being shared with excited states. The population of higher energy states demonstrated here shows a potential problem faced when creating two level qubit systems, as leakage to higher states would create a system based on more than the required levels; this was shown to increase with capacitive coupling strength, suggesting that these issues may arise in 'two level systems' where capacitive cross talk could present itself.

With its ability to produce physically realisable results and ensuring matrix positivity, the Lindblad equation acts as an important modelling tool for OQSs. A Lindblad's ability to model environmental effects leads into other appealing applications such as in Quantum State Diffusion and Quantum error correction, whilst maintaining its analytical simplicity within the

Markovian framework. This chapter however, and the chapter preceeding it (chapter 2) have highlighted numerous issues that are associated with this type of analysis, namely the addition and cancelling of terms, the logic of which is not clear. Such modifications have been argued to change the dynamics of the considered system and so it is important to better understand the impact of these terms. In the next chapter the physical significance of these terms will be explored with reference to quantum-classical correspondence along with a discussion of some experimentally verifiable effects that they may have on the system.

Chapter 4

Effective Hamiltonians in Decoherence Models

4.1 Introduction

Over the course of this thesis, Lindblad equations describing a SQUIDs decoherence channels have been derived through widely accepted techniques. As a result of producing a suitable dissipator, expressed as the non-unitary part of the Lindblad equation, terms of the form $\left[\hat{A}, \left\{\hat{B}, \rho\right\}\right]$ are split and recast so that they contribute to both the dissipator as well as the free evolution part of the system's master equation. It is then customary to absorb these free evolution terms into an effective Hamiltonian, for example see sections 3.3.1, 2.2.1.3, and 2.2.1.4. Terms like these are most commonly seen in the form of a squeezing $\mathrm{i}\mu\left[\hat{X}\hat{P} + \hat{P}\hat{X}, \rho\right]$term found when describing a damped harmonic oscillator, where μ is representative of the coupling between system and bath [45, 84, 107]. Effective Hamiltonians have already

been seen in this work as a result of a renormalisation of system parameters, such as inductance and capacitance in the case of SQUID, due to the reactive coupling between a quantum system and classical bath [82]. This is similar in nature to the Lamb shift term $C\left[\hat{X}^2,\rho\right]$ often seen in QBM and the Caldiera Leggett equation where it is argued that this term must be included to cancel unphysical frequency renormalisation [57, 66].

The existence of the squeezing term seen in the these cases has been addressed multiple times in the literature. In [51] it is argued that the presence of this term is necessary to ensure translational invariance which ensures a particle's motion is truly Brownian, satisfying Ehrenfest's theorem [8, 11, 12, 13, 108]. The presence of this term also ensures quantum to classical correspondence [61, 66, 105, 109], namely in the form of resonant frequency shifts attributed to damped systems. It has also been proposed that these terms may be renormalised by a factor of λ such that the amplitude of this squeezing becomes $(\mu-\lambda)\left[\hat{X}\hat{P}+\hat{P}\hat{X},\rho\right]$. Constraining the amplitude of this term to the range $0<\lambda\leq\mu$ is shown produce a purely dissipative model and may offer favourable conditions for exploring low temperature regimes [51, 80]. This prescription of any value other than zero does however violate Ehrenfest and quantum correspondence as previously highlighted [61, 108].

In sections 2.2.1.4 and 3.3.1, terms similar to this squeezing were found with some depending on the operator $s(\hat{X},\Phi_x)=\sin\left(\sqrt{\beta\omega_0/\nu}(\hat{X}+2\pi\Phi_x/\Phi_0)\right)$. Consequently, the decision to either include or dismiss these terms opens an argument based on their physical validity. The lack of a robust method for identifying physically significant terms poses a threat to processes such as

high precision control, which depend heavily on appropriate device characterisation [110]. Terms like these also may provide a measurable difference in a system's energy-dependent observables. Alternatively, if experiment shows no impact on the system at all, it can be concluded that these terms are negligible and bare no physical significance. Either way, it is important to address the effects of such terms and this will discussed in detail for the case of the QHO as well as the SQUID model presented in the previous chapter.

4.2 Frequency Shifts from a Classical Approach

In section 2.2.1.3 the first order Lindblad master equation for a SQUID coupled to an Ohmic bath was derived to produce an equation similar in nature to that found in QBM. As discussed in the previous section, this method produces a term which is often absorbed by the system Hamiltonian. The importance of this additional term is highlighted in much of the literature [8, 11, 12, 13, 61, 66, 105, 108, 109], giving rise to frequency shift and squeezing effects which are necessary to ensure quantum to classical correspondance. Our starting point will therefore be the damped harmonic oscillator which acts as a common classical analogue to dissipative quantum systems, and can be approached both classically and quantum mechanically. The equation of motion for the damped harmonic oscillator is given by:

$$\ddot{x} + 2\gamma\dot{x} + \omega^2 x = 0 \tag{4.1}$$

where $\ddot{x}$ and $\dot{x}$ are the system's acceleration and velocity respectively while the friction coefficent $\eta = 2m\gamma$ is given in terms of the damping rate [109] as in previous sections. A suitable ansatz for this solution is one of the form

[111]:

$$x(t) = x_0 e^{i\omega' t} \tag{4.2}$$

its corresponding time-derivatives are thus:

$$\begin{aligned} x(t) &= x_0 e^{i\omega' t} \\ \dot{x}(t) &= i\omega' x_0 e^{i\omega' t} \\ \ddot{x}(t) &= -\omega'^2 x_0 e^{i\omega' t} \end{aligned} \tag{4.3}$$

substituting this result into (4.1) gives:

$$-\omega'^2 + 2i\omega'\gamma + \omega^2 = 0 \tag{4.4}$$

This resulting expression is trivial to solve and so the frequency ω' is given by:

$$\begin{aligned} \omega' &= i\gamma \pm \omega\sqrt{1 - \frac{\gamma^2}{\omega^2}} \\ &= i\gamma \pm \tilde{\omega} \end{aligned} \tag{4.5}$$

which then gives the solution:

$$x(t) = x_+ e^{i\tilde{\omega}t} e^{-\gamma t} + x_- e^{-i\tilde{\omega}t} e^{-\gamma t} \tag{4.6}$$

The obtained solution describes oscillations at a shifted natural frequency $\tilde{\omega}$ decaying at a rate $e^{-\gamma t}$. In order to find the source of frequency shifts in the quantum case, the correspondence limit will be used once more to see if the classical system can shed light into this problem. Consider the the free

oscillator [111], the Lagrangian of which, L, is given by:

$$\begin{aligned} L &= T - V \\ &= \frac{m}{2}(\dot{x}^2 - \omega^2 x^2) \end{aligned} \tag{4.7}$$

where T and V are the kinetic and potential energies of the system respectively while $\dot{x} = \frac{dx}{dt}$ is the velocity of the system. Using the Euler-Lagrange equation, $\frac{d}{dt}\left(\frac{\partial L}{\partial \dot{x}}\right) - \frac{\partial L}{\partial x} = 0$, one can see that the equation of motion for the oscillator is given by:

$$\frac{d}{dt}\left(\frac{\partial L}{\partial \dot{x}}\right) - \frac{\partial L}{\partial x} = \frac{d}{dt}\left(\frac{m}{2} \cdot 2\dot{x}\right) + \frac{m}{2} \cdot 2\omega^2 x = m\ddot{x} + m\omega^2 x = 0 \tag{4.8}$$

This is the equation of motion for the harmonic oscillator oscillating at frequency ω.

Suppose now we add an extra term $-\gamma x \dot{x} m$ to the Lagrangian of the system where γ is a damping rate as in the previous sections. The Lagrangian becomes:

$$L = \frac{m}{2}(\dot{x}^2 - \omega^2 x^2) - \gamma x \dot{x} m \tag{4.9}$$

Using the Euler-Langrange equation once more:

$$\begin{aligned} \frac{d}{dt}\left(\frac{\partial L}{\partial \dot{x}}\right) - \frac{\partial L}{\partial x} &= \frac{d}{dt}\left(\frac{m}{2} \cdot 2\dot{x} - \gamma x m\right) - \left(-\frac{m}{2} \cdot 2\omega^2 x - \gamma \dot{x} m\right) \\ &= m\ddot{x} - \gamma \dot{x} m - m\omega^2 x + \gamma \dot{x} m = 0 \\ &\Rightarrow m\ddot{x} + m\omega^2 x = 0 \end{aligned} \tag{4.10}$$

It is evident that the addition of this term has no effect on the equation of motion of the system. Let us now consider the Hamiltonian of the new

system. The momentum, and thus the velocity, of the system is given by:

$$\begin{aligned} p &= \frac{\partial L}{\partial \dot{x}} = m\dot{x} - \gamma x m \\ \Rightarrow \dot{x} &= \frac{p + \gamma x m}{m} \end{aligned} \tag{4.11}$$

Using this result in the expression for the Hamiltonian yields [111]:

$$\begin{aligned} H &= p\dot{x} - L \\ &= p\left(\frac{p+\gamma x m}{m}\right) - \frac{m}{2}\left(\frac{(p+\gamma x m)^2}{m} - \omega^2 x^2\right) + \frac{\gamma x(p+\gamma x m)}{m} \\ &= \frac{p^2}{2m} + \frac{1}{2}m\omega^2 x^2 + \frac{1}{2}m\gamma^2 x^2 + \frac{\gamma}{2}(xp+px) \\ &= \frac{p^2}{2m} + \frac{1}{2}m\tilde{\omega}^2 x^2 + \frac{\gamma}{2}(xp+px) \end{aligned} \tag{4.12}$$

where $\tilde{\omega} = \omega\left(\sqrt{1+\frac{\gamma^2}{\omega^2}}\right)$ behaves as a shifted frequency. Since it is clear that a frequency shift cannot appear without a source it is reasonable to arrive at the conclusion that the final term in the Hamiltonian, $H_{xp} = \gamma/2\,(\hat{x}\hat{p} + \hat{p}\hat{x})$ counteracts this shift [111]. In the next section we will explore the effect of this term from a quantum mechanical approach and investigate whether or not this term does indeed create a frequency shift.

4.3 Frequency Shifts From a Quantum Mechanical Approach

A common tool used to explore quantum-classical correspondence is Ehrenfest theorem [42], which describes the behaviour of the expectation value of quantum observables. It is postulated that these expectation values should line up accordingly with classical theory for the correspondence limit to be

obeyed. Our starting point for this is therefore the evolution of the expectation value of an arbitrary operator, $\hat{A}$:

$$\frac{\mathrm{d}}{\mathrm{d}t}\left\langle \hat{A}\right\rangle = \mathrm{Tr}\left\{\frac{\mathrm{d}}{\mathrm{d}t}\left(\hat{A}\rho\right)\right\} = \mathrm{Tr}\left\{\frac{\partial\rho}{\partial t}\hat{A}\right\} + \left\langle\frac{\partial\hat{A}}{\partial t}\right\rangle \tag{4.13}$$

For a time indepedent operator, such as those used in this work, the second term on the right hand is zero and the equation reduces to:

$$\frac{\mathrm{d}}{\mathrm{d}t}\left\langle \hat{A}\right\rangle = \mathrm{Tr}\left\{\frac{\mathrm{d}}{\mathrm{d}t}\left(\hat{A}\rho\right)\right\} = \mathrm{Tr}\left\{\frac{\mathrm{d}\rho}{\mathrm{d}t}\hat{A}\right\} \tag{4.14}$$

Since the evolution of the density matrix is given by the master equation, the above can be written:

$$\frac{\mathrm{d}}{\mathrm{d}t}\left\langle \hat{A}\right\rangle = -\frac{\mathrm{i}}{\hbar}\,\mathrm{Tr}\left\{\left[\hat{H},\rho\right]\hat{A}\right\} + \mathrm{Tr}\left\{\mathcal{K}[\rho]\hat{A}\right\} \tag{4.15}$$

where the first term originates from the system's free evolution and the second is the dissipator used to describe the unitary loss. Note that the dissipator does not necessarily have to be in Lindblad form, as will be shown for the case of QBM as well as the non-Lindblad equation derived for the capacitively coupled SQUID later in this chapter. First we will however start with a Lindblad master equation. For this case the evolution of the operator $\hat{A}$ may be written:

$$\begin{aligned}\frac{\mathrm{d}}{\mathrm{d}t}\left\langle \hat{A}\right\rangle &= -\frac{\mathrm{i}}{\hbar}\left\langle\left[\hat{A},\hat{H}\right]\right\rangle + \mathrm{Tr}\left\{\left(\hat{L}\rho\hat{L}^{\dagger} - \frac{1}{2}\hat{L}^{\dagger}\hat{L}\rho - \frac{1}{2}\rho\hat{L}^{\dagger}\hat{L}\right)\hat{A}\right\} \\ &= -\frac{\mathrm{i}}{\hbar}\left\langle\left[\hat{A},\hat{H}\right]\right\rangle + \frac{1}{2}\left\{\left\langle\left[\hat{L}^{\dagger},\hat{A}\right]\hat{L}\right\rangle + \left\langle\hat{L}^{\dagger}\left[\hat{A},\hat{L}\right]\right\rangle\right\}\end{aligned} \tag{4.16}$$

where the cyclic property of trace has been used. We will now consider the case of the harmonic oscillator decohering due to a Lindblad of $\hat{L} = \sqrt{2\gamma}\hat{a}$. The evolution of the expectation value of position $\hat{x} = \sqrt{\frac{\hbar}{m\omega_0}}\hat{X} = \sqrt{\frac{\hbar}{2m\omega_0}}(\hat{a} + \hat{a}^\dagger)$ is given by:

$$\frac{\mathrm{d}}{\mathrm{d}t}\left\langle \hat{X} \right\rangle = -\mathrm{i}\omega_0 \left\langle \left[\hat{X}, \hat{n} + \frac{1}{2}\right] \right\rangle + \gamma \left(\left\langle \left[\hat{a}^\dagger, \hat{X}\right] \hat{a} \right\rangle + \left\langle \hat{a}^\dagger \left[\hat{X}, \hat{a}\right] \right\rangle \right) \tag{4.17}$$

Using the commutation relations $\left[\hat{a}, \hat{a}^\dagger\right] = \hat{\mathbb{I}}$ this reduces to:

$$\begin{aligned} \frac{\mathrm{d}}{\mathrm{d}t}\left\langle \hat{X} \right\rangle &= \omega_0 \left\langle \hat{P} \right\rangle - \frac{\gamma}{\sqrt{2}} \left(\langle \hat{a} \rangle + \langle \hat{a}^\dagger \rangle \right) \\ &= \omega_0 \left\langle \hat{P} \right\rangle - \gamma \left\langle \hat{X} \right\rangle \end{aligned} \tag{4.18}$$

In the same way as described above, as well as the commutation relation $\left[\hat{a}, \hat{P}\right] = \mathrm{i}/\sqrt{2}$, the evolution of the expectation value of momentum may also be found:

$$\frac{\mathrm{d}}{\mathrm{d}t}\left\langle \hat{P} \right\rangle = -\omega_0 \left\langle \hat{X} \right\rangle - \gamma \left\langle \hat{P} \right\rangle \tag{4.19}$$

Rearranging Eq. (4.18) in terms of $\left\langle \hat{P} \right\rangle$ and differentiating with respect to t yields:

$$\frac{\mathrm{d}}{\mathrm{d}t}\left\langle \hat{P} \right\rangle = \frac{1}{\omega_0}\left(\frac{\mathrm{d}^2}{\mathrm{d}t^2}\left\langle \hat{X} \right\rangle + \gamma \frac{\mathrm{d}}{\mathrm{d}t}\langle X \rangle \right) \tag{4.20}$$

Equating this to Eq. (4.19) then gives:

$$\begin{aligned} &\frac{1}{\omega_0}\left(\frac{\mathrm{d}^2}{\mathrm{d}t^2}\left\langle \hat{X} \right\rangle + \gamma \frac{\mathrm{d}}{\mathrm{d}t}\left\langle \hat{X} \right\rangle \right) = \omega_0 \left\langle \hat{X} \right\rangle - \gamma \left\langle \hat{P} \right\rangle \\ \Rightarrow &\frac{\mathrm{d}^2}{\mathrm{d}t^2}\left\langle \hat{X} \right\rangle + 2\gamma \frac{\mathrm{d}}{\mathrm{d}t}\langle X \rangle + \left(\omega_0^2 + \gamma^2\right)\left\langle \hat{X} \right\rangle = 0 \end{aligned} \tag{4.21}$$

Eq. (4.21) is a second order homogenous differential equation with the solution:

$$\left\langle \hat{X} \right\rangle (t) = \left\langle \hat{X}_+ \right\rangle e^{\mathrm{i}\omega_0 t} e^{-\gamma t} + \left\langle \hat{X}_- \right\rangle e^{-\mathrm{i}\omega_0 t} e^{-\gamma t} \tag{4.22}$$

Solution Eq. (4.22) describes a damped system decaying a rate of $e^{-\gamma t}$ at a natural frequency of ω_0. Although the correspondence limit is obeyed, with Eq. (4.22) being consistent with its classical counterpart Eq. (4.6), the frequency shift of the system is not accounted for as the frequency with which the solution Eq. (4.22) oscillates remains at ω_0. To address this the next natural step is to explore how things change when H_{xp} is introduced. The Hamiltonian to be considered is then given by:

$$\hat{H}_{HO} = \hbar\omega_0 \left(\hat{n} + \frac{1}{2} \right) + \frac{\hbar\gamma}{2} \left(\hat{X}\hat{P} + \hat{P}\hat{X} \right) \tag{4.23}$$

Following through the same steps to obtain Eq. (4.18) and Eq. (4.19), one now finds:

$$\frac{\mathrm{d}}{\mathrm{d}t} \left\langle \hat{X} \right\rangle = \omega_0 \left\langle \hat{P} \right\rangle \tag{4.24}$$

$$\frac{\mathrm{d}}{\mathrm{d}t} \left\langle \hat{P} \right\rangle = -\omega_0 \left\langle \hat{X} \right\rangle - 2\gamma \left\langle \hat{P} \right\rangle \tag{4.25}$$

Combining these expressions to eliminate momentum yields:

$$\begin{aligned} \frac{\mathrm{d}}{\mathrm{d}t} \left\langle \hat{P} \right\rangle =& \frac{1}{\omega_0} \frac{\mathrm{d}^2}{\mathrm{d}t^2} \left\langle \hat{X} \right\rangle = -\omega_0 \left\langle \hat{X} \right\rangle - 2\gamma \left(\frac{1}{\omega_0} \frac{\mathrm{d}}{\mathrm{d}t} \left\langle \hat{X} \right\rangle \right) \\ \Rightarrow & \frac{\mathrm{d}^2}{\mathrm{d}t^2} \left\langle \hat{X} \right\rangle + 2\gamma \frac{\mathrm{d}}{\mathrm{d}t} \left\langle \hat{X} \right\rangle + \omega_0^2 \left\langle \hat{X} \right\rangle = 0 \end{aligned} \tag{4.26}$$

Once again the solution to this second order differential equation is an exponential function of the form:

$$\begin{aligned}\left\langle \hat{X} \right\rangle (t) &= \left(\left\langle \hat{X}_+ \right\rangle e^{\mathrm{i}\omega_0 \sqrt{1-\gamma^2/\omega_0^2}\, t} + \left\langle \hat{X}_- \right\rangle e^{-\mathrm{i}\omega_0 \sqrt{1-\gamma^2/\omega_0^2}\, t} \right) e^{-\gamma t} \\ &= \left(\left\langle \hat{X}_+ \right\rangle e^{\mathrm{i}\omega' t} + \left\langle \hat{X}_- \right\rangle e^{-\mathrm{i}\omega' t} \right) e^{-\gamma t}\end{aligned} \tag{4.27}$$

where we can now see that the system oscillates at the shifted frequency $\omega' = \omega_0 \sqrt{1-\gamma^2/\omega_0^2}$, attributed to damping in the classical limit. It is clear to see what impact the additional term has on the expectation value of the position, which now describes decaying oscillations at a frequency dependent on the amount of damping on the system. Having seen that the added term changes the system's natural frequency, it is necessary to also see what impact, if any, this term has on the Hamiltonian itself. Writing the additional term in terms of annihilation and creation operators gives:

$$\begin{aligned}H_{xp} = \frac{\gamma}{2}(\hat{x}\hat{p} + \hat{p}\hat{x}) &= \frac{\hbar\gamma i}{4}\left((\hat{a} + \hat{a}^\dagger)(\hat{a}^\dagger - \hat{a}) + (\hat{a}^\dagger - \hat{a})(\hat{a} + \hat{a}^\dagger) \right) \\ &= \frac{\hbar\gamma i}{2}\left(\hat{a}^{\dagger 2} - \hat{a}^2 \right)\end{aligned} \tag{4.28}$$

And so the Hamiltonian for the harmonic oscillator becomes:

$$H' = H + H_{xp} = \hbar\omega \left(\hat{a}^\dagger \hat{a} + \frac{1}{2} \right) + \frac{\hbar\gamma i}{2}\left(\hat{a}^{\dagger 2} - \hat{a}^2 \right) \tag{4.29}$$

This expression of the Hamiltonian is not the simplest form it can take. The target now is rewrite the Hamiltonian in terms of one frequency and one product of raising and lowering operators; we do this by performing a Bogoliubov transformation [111, 112], which requires the definition of two

new operators:

$$\begin{aligned} \hat{b} &= u\hat{a} + v\hat{a}^\dagger \\ \hat{b}^\dagger &= u^*\hat{a}^\dagger + v^*\hat{a} \end{aligned} \tag{4.30}$$

where u and v are constants. Evaluation of the these constants (see Appendix E) allows the Hamiltonian to be written:

$$H' = \hbar\tilde{\omega}\hat{b}^\dagger\hat{b} \tag{4.31}$$

where $\tilde{\omega} = \omega\left(1 - \frac{\gamma^2}{\omega^2}\right)^{1/2}$ is exactly the same frequency shift that appears in the classical dynamics. This result shows that in order to model dissipation in exactly the same way as the classical dynamics, the frequency shift term H_{xp} cannot be omitted from the system Hamiltonian as it has a physical impact on the system; this result is significant when considering quantum-classical crossover as it suggests that other terms of this nature may also have a physical importance. These findings may extend into the additional terms seen in sections 2.2.1.4 and 3.3.1.

Up until this point in the chapter we have explored the dynamics of the harmonic oscillator; this produces the same $\hat{H}_{xp}$ term as that found in the first order model for the inductively coupled SQUID, seen in §2.2.1.3 and shows that this term is responsible for shifting the natural frequency of the system. We will now investigate the impact of other effective Hamiltonian terms seen in Chapters 2 and 3, using Ehrenfest theorem on the unitary

evolution of the SQUID to give some insight into their effect, for example:

$$\frac{\mathrm{d}\hat{A}}{\mathrm{d}t} = -\frac{\mathrm{i}}{\hbar}\left\langle\left[\hat{A}, \hat{H}_i\right]\right\rangle \tag{4.32}$$

where the subscript i helps to differentiate between the various effective Hamiltonians explored. We will first consider the Hamiltonian of the free SQUID:

$$\hat{H}_S = \hbar\omega_0(\hat{n} + \frac{1}{2}) - \hbar\nu\cos\left(\sqrt{\frac{\beta\omega_0}{\nu}}\hat{X} + \frac{2\pi\Phi_x}{\Phi_0}\right) \tag{4.33}$$

Applying Ehrenfest to the unitary part of the system's evolution, i.e. neglecting the dissipating effects, yields the following set of equations:

$$\begin{aligned}
&\frac{\mathrm{d}}{\mathrm{d}t}\left\langle\hat{X}\right\rangle = \omega_0\left\langle\hat{P}\right\rangle \\
&\frac{\mathrm{d}}{\mathrm{d}t}\left\langle\hat{P}\right\rangle = -\omega_0\left\langle\hat{X}\right\rangle - \sqrt{\beta\omega_0\nu}\left\langle\sin\left(\sqrt{\frac{\beta\omega_0}{\nu}}\hat{X} + \frac{2\pi\Phi_x}{\Phi_0}\right)\right\rangle
\end{aligned} \tag{4.34}$$

as expected. Combining these simultaneous equations then yields the differential equation:

$$\frac{\mathrm{d}^2}{\mathrm{d}t^2}\left\langle\hat{X}\right\rangle + \omega_0^2\left\langle\hat{X}\right\rangle = -\sqrt{\beta\omega_0\nu}\left\langle\sin\left(\sqrt{\frac{\beta\omega_0}{\nu}}\hat{X} + \frac{2\pi\Phi_x}{\Phi_0}\right)\right\rangle \tag{4.35}$$

which shows the harmonic part of the system's evolution on the left hand side and an undefined non linear contribution in the form of $\left\langle\sin\left(\sqrt{\frac{\beta\omega_0}{\nu}}\hat{X} + \frac{2\pi\Phi_x}{\Phi_0}\right)\right\rangle$ on the right. To better understand this term, we will the consider its time derivative:

$$\frac{\mathrm{d}}{\mathrm{d}t}\left\langle \sin\left(\sqrt{\frac{\beta\omega_0}{\nu}}\hat{X}+\frac{2\pi\Phi_x}{\Phi_0}\right)\right\rangle = -\mathrm{i}\omega_0\left\langle\left[\sin\left(\sqrt{\frac{\beta\omega_0}{\nu}}\hat{X}+\frac{2\pi\Phi_x}{\Phi_0}\right),\frac{\hat{P}^2}{2}\right]\right\rangle$$
$$= \frac{\omega_0}{2}\left\langle\sqrt{\frac{\beta\omega_0}{\nu}}\left\{\cos\left(\sqrt{\frac{\beta\omega_0}{\nu}}\hat{X}+\frac{2\pi\Phi_x}{\Phi_0}\right),\hat{P}\right\}\right\rangle \tag{4.36}$$

which produces another variable that is undefined. One could explore the time derivative of this term once more but it is clear to see that the commutation with the Hamiltonian will produce further expanded variables due to the continual existence of product of trigonometric function which will always commute in a similar nature to that shown in Eq. (4.36). One can therefore conclude that the expectation value of a trigonometric function is an infinite series. This is one key difference between quantum approaches and classical approaches such as the RSJ model, where it is often assumed $\left\langle f(\hat{X})\right\rangle = f\left(\left\langle\hat{X}\right\rangle\right)$. Now that the nature of these non-trivial expectation values are known, we will progress onto taking the Ehrenfest approach with the second order model for the inductively coupled SQUID, the effective Hamiltonian for which is given by:

$$\begin{aligned}\hat{H}_{2I} &= \hat{H}_S + \hat{X}_{XPI} + \hat{H}_{XSI} \\ &= \hbar\omega_0(\hat{n}+\frac{1}{2}) - \hbar\nu\cos\left(\sqrt{\frac{\beta\omega_0}{\nu}}\hat{X}+\frac{2\pi\Phi_x}{\Phi_0}\right) + \frac{\hbar\gamma}{2}\left(\hat{X}\hat{P}+\hat{P}\hat{X}\right) \\ &+ \sqrt{\frac{\beta\omega_0\nu}{\Omega^2}}\hbar\gamma\hat{X}\sin\left(\sqrt{\frac{\beta\omega_0}{\nu}}\hat{X}+\frac{2\pi\Phi_x}{\Phi_0}\right)\end{aligned} \tag{4.37}$$

where $\hat{H}_{2I}$ indicates the effective Hamiltonian terms for the second order purely inductive model. Following the same steps as before yields the com-

bined differential equation:

$$\frac{\mathrm{d}^2}{\mathrm{d}t^2}\left\langle \hat{X}\right\rangle + \left(\omega_0^2 - \gamma^2\right)\left\langle \hat{X}\right\rangle = -\sqrt{\beta\omega_0\nu}\left(1+\frac{\gamma}{\Omega}\right)\left\langle \sin\left(\sqrt{\frac{\beta\omega_0}{\nu}}\hat{X} + \frac{2\pi\Phi_x}{\Phi_0}\right)\right\rangle - \beta\omega_0\frac{\gamma}{\Omega}\left\langle \hat{X}\cos\left(\sqrt{\frac{\beta\omega_0}{\nu}}\hat{X} + \frac{2\pi\Phi_x}{\Phi_0}\right)\right\rangle \tag{4.38}$$

The left hand side of Eq. (4.38) shows the familiar frequency shift created by $\hat{H}_{xp}$, which has altered the coefficient of $\left\langle \hat{X}\right\rangle$ by a factor of $1-\gamma^2/\omega_0^2$. The right hand shows additional non-trivial terms, including a renormalising effect on the initial $\left\langle \sin\left(\sqrt{\frac{\beta\omega_0}{\nu}}\hat{X} + \frac{2\pi\Phi_x}{\Phi_0}\right)\right\rangle$ term; this is joined by the final term that is a product between position and the SQUID Josephson contribution to the potential. This further highlights that appropriate care is required when looking at non-trivial open quantum systems, such as the SQUID, and their coupling to the environment as a purely classical or semi-classical analysis may neglect the impact of these terms and coud lead to mis-characterisation of the system.

4.4 Effective Hamiltonians and the Dual coupled SQUID

For completeness we will now explore the impact of effective Hamiltonian terms on the SQUID's evolution for the SQUID both inductively and capacitively coupled to an Ohmic bath. The total Hamiltonian is therefore given by:

$$\hat{H} = \hat{H}_S + \hat{H}_{XP_Q} + \hat{H}_{XJ_Q} + \hat{H}_{PJ_Q} \tag{4.39}$$

where the effective Hamiltonians $\hat{H}_{ij_Q}$ are given by:

$$\begin{aligned}
\hat{H}_{XP_Q} &= \hbar\gamma\left(\frac{3g^2}{2} - g + \frac{1}{2}\right)(\hat{X}\hat{P} + \hat{P}\hat{X}), \\
\hat{H}_{XJ_Q} &= \frac{\hbar\gamma g}{2\Omega}\sqrt{\beta\nu\omega_0}\hat{X}\sin\left(\sqrt{\frac{\beta\omega_0}{\nu}}\hat{X} + 2\pi\frac{\Phi_x}{\Phi_0}\right), \\
\hat{H}_{PJ_Q} &= -\frac{\hbar\gamma g^2}{2}\sqrt{\frac{\beta\nu}{\omega_0}}\left(\hat{P}\sin\left(\sqrt{\frac{\beta\omega_0}{\nu}}\hat{X} + 2\pi\frac{\Phi_x}{\Phi_0}\right) + \sin\left(\sqrt{\frac{\beta\omega_0}{\nu}}\hat{X} + 2\pi\frac{\Phi_x}{\Phi_0}\right)\hat{P}\right)
\end{aligned} \tag{4.40}$$

Up until this point it has been possible to construct one single differential equation in terms of $\left\langle \hat{X} \right\rangle$ as well as some other non-trivial terms with an infinite series solution. It will be shown below that for the dual coupled SQUID, i.e. both inductively and capacitively coupled, the existence of an additional $\hat{P}$-dependent contribution in $\hat{H}_{PJ_Q}$, even in first order, adds further complexity to that seen in the second order model for purely inductive coupling. Once again going through the same steps before, one arrives at two differential equations:

$$\begin{aligned}
\frac{\mathrm{d}}{\mathrm{d}t}\left\langle \hat{X} \right\rangle = \omega_0 \left\langle \hat{P} \right\rangle &+ 2\gamma\left(\frac{3g^2}{2} - g + \frac{1}{2}\right)\left\langle \hat{X} \right\rangle \\
&- \gamma g^2\sqrt{\frac{\beta\nu}{\omega_0}}\left\langle \sin\left(\sqrt{\frac{\beta\omega_0}{\nu}}\hat{X} + 2\pi\frac{\Phi_x}{\Phi_0}\right)\right\rangle
\end{aligned} \tag{4.41}$$

$$\begin{aligned}\frac{\mathrm{d}}{\mathrm{d}t}\left\langle\hat{P}\right\rangle =& -\omega_0\left\langle\hat{X}\right\rangle - 2\gamma\left(\frac{3g^2}{2}-g+\frac{1}{2}\right)\left\langle\hat{P}\right\rangle \\ &- \sqrt{\beta\omega_0\nu}\left(1+\frac{\gamma g}{2\Omega}\right)\left\langle\sin\left(\sqrt{\frac{\beta\omega_0}{\nu}}\hat{X}+\frac{2\pi\Phi_x}{\Phi_0}\right)\right\rangle \\ &- \frac{\gamma g}{2\Omega}\beta\omega_0\left\langle\hat{X}\cos\left(\sqrt{\frac{\beta\omega_0}{\nu}}\hat{X}+\frac{2\pi\Phi_x}{\Phi_0}\right)\right\rangle \\ &+ \frac{\gamma g^2\beta}{2}\left\langle\left\{\hat{P},\cos\left(\sqrt{\frac{\beta\omega_0}{\nu}}\hat{X}+\frac{2\pi\Phi_x}{\Phi_0}\right)\right\}\right\rangle\end{aligned} \tag{4.42}$$

Eq. (4.41) and Eq. (4.42) both still show the harmonic parts to the system's evolution with terms proportional to $\left\langle\hat{P}\right\rangle$ and $\left\langle\hat{X}\right\rangle$, and a frequency shift shown to be strongly dependent on capacitive coupling strength. What is more noticeable however is how quickly the system's evolution grows in complexity as capacitive coupling is included; this suggests that only a quantum mechanical approach may be taken when analysing non-trivial models such as the above, and simple extensions to the well covered RSJ model are unlikely to suffice when characterising a device based on quantum technology.

The impact of this H_{XP} term can also be seen for the case of the SQUID. For models where an annihilator is assumed as the only Lindblad, the effect of this becomes evident when one considers the system's behaviour in phase space. One way of displaying this behaviour is by use of a Wigner function: A pseudo-probability density function that is commonly utilised to identify quantum states, areas of negativity, etc. in phase space [47]. The Wigner function is defined as:

$$W(\Phi,Q)=\frac{1}{2\pi\hbar}\int\langle\Phi+\zeta|\rho|\Phi-\zeta\rangle\exp\left(-\frac{2iQ\zeta}{\hbar}\right)d\zeta \tag{4.43}$$

where Φ and Q are the same flux and charge variables and conjugate to one another. Fig. 4.1 shows the steady state Wigner functions of a SQUID that has been left to decohere from its ground state at $\Phi_x = 0.5\Phi_0$ to its steady state. Decoherence has been implemented by use of a Lindblad $\hat{L} = \sqrt{0.2}\hat{a}$, which has been used previously in the literature [52]. The top image shows the steady state function produced when the $\hat{H}_{XP}$ is neglected. One can see that when the additional term is neglected, there is a clockwise rotation in the X-P plane about the origin. When the second image is considered, where $\hat{H}_{XP}$ is accounted for in the free Hamiltonian, this rotation is not present.

Explaining this phenomenon lies in the effect that these Hamiltonian terms have on the phase space as whole. Much like the effect of increasing anharmonic contributions of the form αx^4 on the phase space of the harmonic oscillator [113]; this Hamiltonian contribution modifies the Wigner flow, strengthening it in one direction and weakening it in the other. This leads to a squeezing effect on the Wigner function, which in [113] is seen as squeezing in X and an elongation in P. In Fig. 4.1 however this effect exists as a squeezing in both X and P, leading to a shearing effect that returns the Wigner function to its expected symmetrical form about the origin.

Another method of interpreting this squeezing makes use of Ehrenfest once more, namely Eq. (4.24) and Eq. (4.25). By including the additional term, the time derivative of the expectation values $\hat{X}$ and $\hat{P}$ also change. Eq. (4.24) shows that the position observable evolves freely in time whereas the momentum lags behind the position's evolution; this results in a slight asymmetry in the P, causing the Wigner function to elongate away from propagation and contract towards it.

It is worth noting that the damping rate used for this figure is higher than one would typically expect, one could argue that this effect would not be seen in physical models but as we saw in chapter 3, these terms become dependent on coupling strength when capacitive coupling is considered, under the right condition it may well be possible to reproduce these effects.

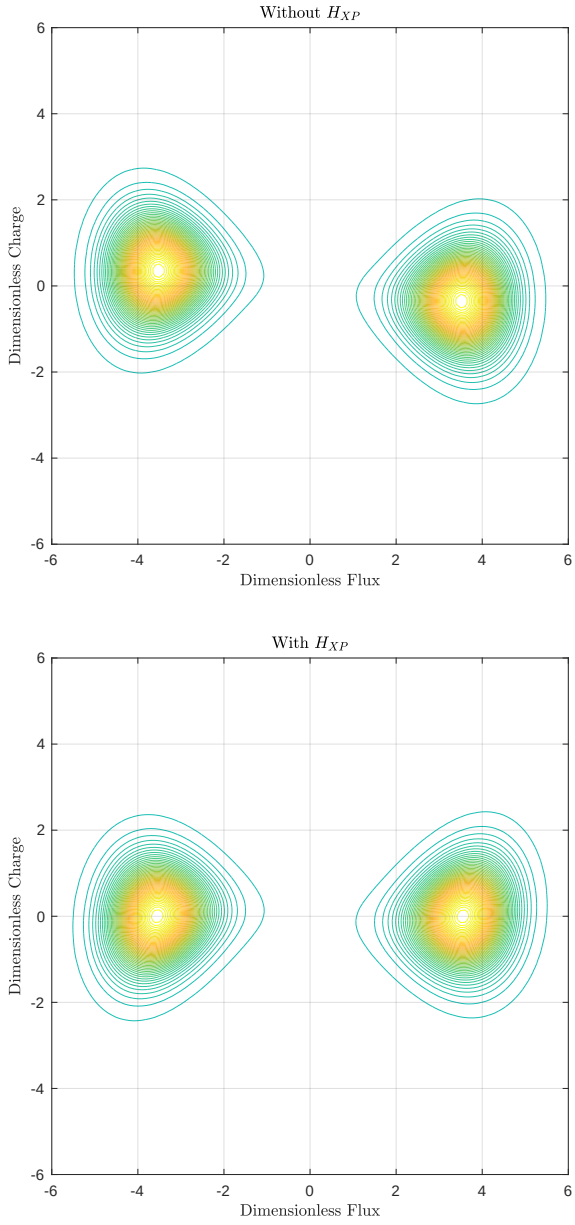

Figure 4.1: Wigner functions of the SQUID's steady state decohered through the Lindblad $\hat{L} = \sqrt{0.2}\hat{a}$ compared for cases when the Hamiltonian term $\hat{H}_{XP}$ is neglected (above) or included (below)

4.5 Impacts of Additional Terms on Energy Level Structure of a SQUID

We have already seen the impact of the standard H_{XP} term on the Hamiltonian of the harmonic oscillator, which causes a frequency shift, and we now address the additional terms which arose from the previous chapter. There has been considerable discussion in the literature as to whether these terms should be included or cancelled, let us consider them and the effective Hamiltonian:

$$\hat{\mathcal{H}}' = \hat{\mathcal{H}}_S + \hat{\mathcal{H}}_{XP} + \hat{\mathcal{H}}_{PS} + \hat{\mathcal{H}}_{XS} \tag{4.44}$$

where

$$\begin{aligned}
\hat{\mathcal{H}}_{XP} &= \frac{\gamma}{2\omega_0}\left(\frac{3g^2}{2} - g + \frac{1}{2}\right)(\hat{X}\hat{P} + \hat{P}\hat{X}), \\
\hat{\mathcal{H}}_{XS} &= -\frac{\gamma g}{2\Omega}\sqrt{\frac{\beta\nu}{\omega_0}}\hat{X}\sin\left(\sqrt{\frac{\beta\omega_0}{\nu}}\hat{X} + 2\pi\frac{\Phi_x}{\Phi_0}\right), \\
\hat{\mathcal{H}}_{PS} &= -\frac{\gamma g^2}{2\omega_0}\sqrt{\frac{\beta\nu}{\omega_0}}\left\{\hat{P}, \sin\left(\sqrt{\frac{\beta\omega_0}{\nu}}\hat{X}2\pi\frac{\Phi_x}{\Phi_0}\right)\right\} \\
&\quad - \frac{\gamma g^2\beta}{4\Omega}\cos\left(\sqrt{\frac{\beta\omega_0}{\nu}}\hat{X} + 2\pi\frac{\Phi_x}{\Phi_0}\right).
\end{aligned} \tag{4.45}$$

while $\hat{\mathcal{H}}_S$ remains the SQUID Hamiltonian with Lamb shift terms cancelled. The impact of $\hat{\mathcal{H}}_{XP}$ has already been discussed in this literature as well [45, 114] and previously noted in other contexts [61, 105, 108, 109, 110, 115, 116, 117, 118], although it has not been seen previously with a physical tunability, such could be provided by a coupling ratio, g. Terms $\hat{\mathcal{H}}_{XS}$ (in

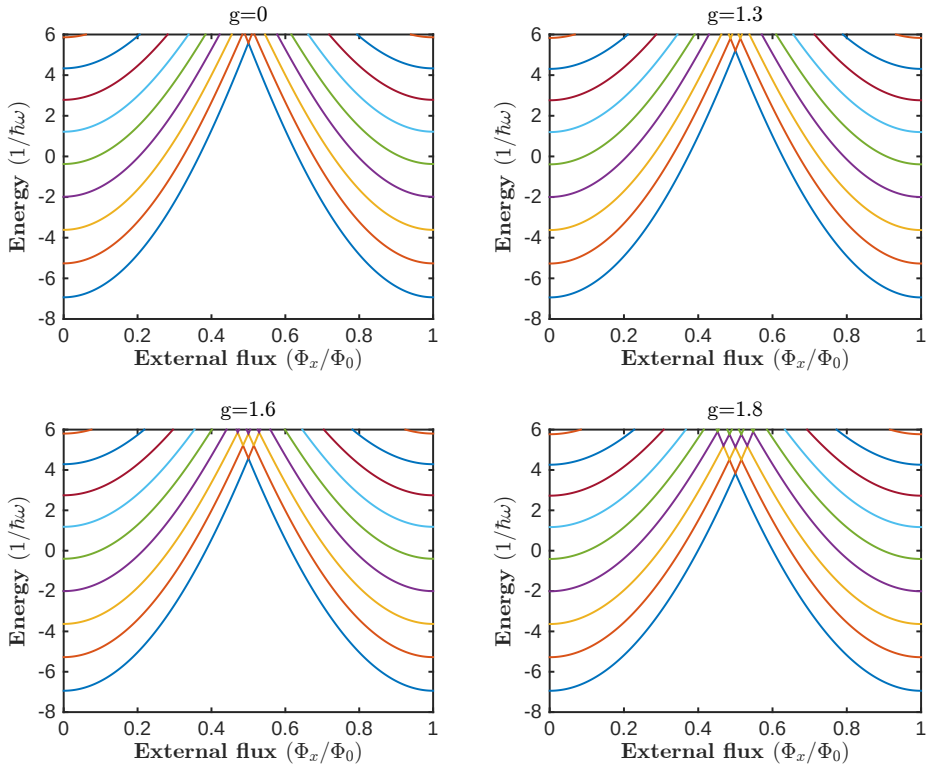

Figure 4.2: The energy eigenvalues of $\hat{\mathcal{H}}'$ as a function of external flux for varying values of capacitive coupling g. Note that the effect of the additional energy terms does not vary linearly in external flux. Values obtained with Josephson energy $\hbar\nu = 6.693 \times 10^{-22}$J, capacitance $C_0 = 5 \times 10^{-15}$F, inductance $L_0 = 3 \times 10^{-10}$H, damping rate $\gamma = 0.05\omega_0$ and bath frequency $\Omega = 10\omega_0$ [119].

ω_0/Ω) and $\hat{\mathcal{H}}_{PS}$ are new additions which arise form the extra capacitive coupling as shown, in the previous chapter. $\hat{\mathcal{H}}_{XS}$ has the form of an additional term in the purely inductive model [45] while the second term in $\hat{\mathcal{H}}_{PS}$ also includes a renormalisation of the Josephson energy.

One method of exploring the impact of these terms on the Hamiltonian is to observe the effect that they have on the energy eigenvalues. Fig. 4.2 shows this effect on the nine lowest eigenvalues of $\hat{\mathcal{H}}'$, plotted as a function of the external flux Φ_x, for varying values of g. One can see that increasing g lowers the energy values at all non-zero Φ_x value, and is most noticeable at the half integer. It is interesting that the energy eigenvalues at integer external flux remain unchanged which would suggest a dominance from external flux dependent terms and the best insensitivity to capacitive coupling.

To explore this further, it is possible to show the impact of each additional term in Eq. (4.45) as well as various linear combinations. This is displayed in Fig. 4.3 which shows the impact of cancelling certain terms, something that is often done in the literature. From this figure one can say that the effects of these terms are significant and their cancellation in order to produce a Lindblad model without these effects is likely to be unmerited [119]. With the $\hat{\mathcal{H}}_{XP}$ term already known to be of importance in quantum-classical transition, it is reasonable to suggest that these extra should also be accounted for. It is worth noting that the contribution that each individual term makes is not linear when compared to the total contribution; this is not unreasonable as $\hat{\mathcal{H}}_{PS}$ is proportional to g^2 and will naturally bring it with it such effects. The most sizeable contribution is made from $\hat{\mathcal{H}}_{XP}$ which is interesting as it does not possess any direct external flux dependence itself. To explain this one should consider the relative size of the system frequency to the Josephson frequency. By introducing the additional $\hat{\mathcal{H}}_{XP}$ term the natural frequency is reduced, as shown earlier in this chapter for the case of the HO; this makes the Josephson frequency relatively larger and essentially gives this term an

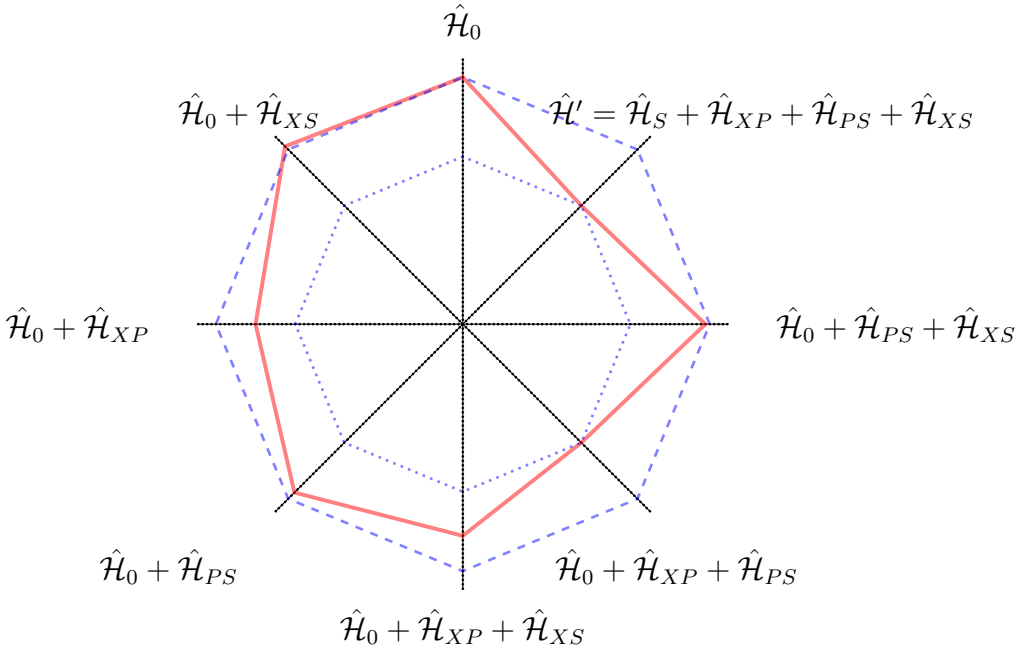

Figure 4.3: Spiderweb Diagram where: the solid line shoes the lowest eigenvalues each combination of the SQUID Hamiltonian plus combinations of additional terms as labeled; the dashed and dotted lines show, for comparison, the lowest eigenvalues of $\hat{\mathcal{H}}_0$ and $\hat{\mathcal{H}}'$ respectively. The origin refers to $E = 0$ and the outer radius corresponds to $E = 6.0$. All values taken at $\Phi_x = 0.5\Phi_0$ and with a coupling ratio of $g = 1.8$ [119].

indirect dependence on external flux.

Fig. 4.2 also shows a change in gradient as g is varied, this result corresponds directly to a experimentally verifiable effect through the system's magnetic susceptibility, which in its ground state is given by:

$$\chi_0(\Phi_x; g) = -L\frac{\partial^2 E_0(\Phi_x; g)}{\partial \Phi_x^2}, \tag{4.46}$$

This therefore provides a pathway through which the ground energy eigenstate dependence on external parameters, g and Φ_x can be measured [120];

this is shown in Fig. 4.4 where the ground state magnetic susceptibility (in the form $\chi_0(\Phi_x; g)/L$) is plotted for a range of g values. It is evident that the susceptibility has a significant nonlinear variation with Φ_x and g. The sharp drop at the half integer is characteristic of the SQUID as this is when the ground state is a Schrödinger Cat causing a negative magnetic susceptibility - a measure of its quantum nature. This result is of importance as a suitable selection of capacitive coupling and external flux should provide an experimental arrangement through which the validity of including or neglecting these additional terms. It should therefore be possible to decide (perhaps once and for all) whether these terms have an experimentally reproducible significance, thus cementing their consideration when characterising devices.

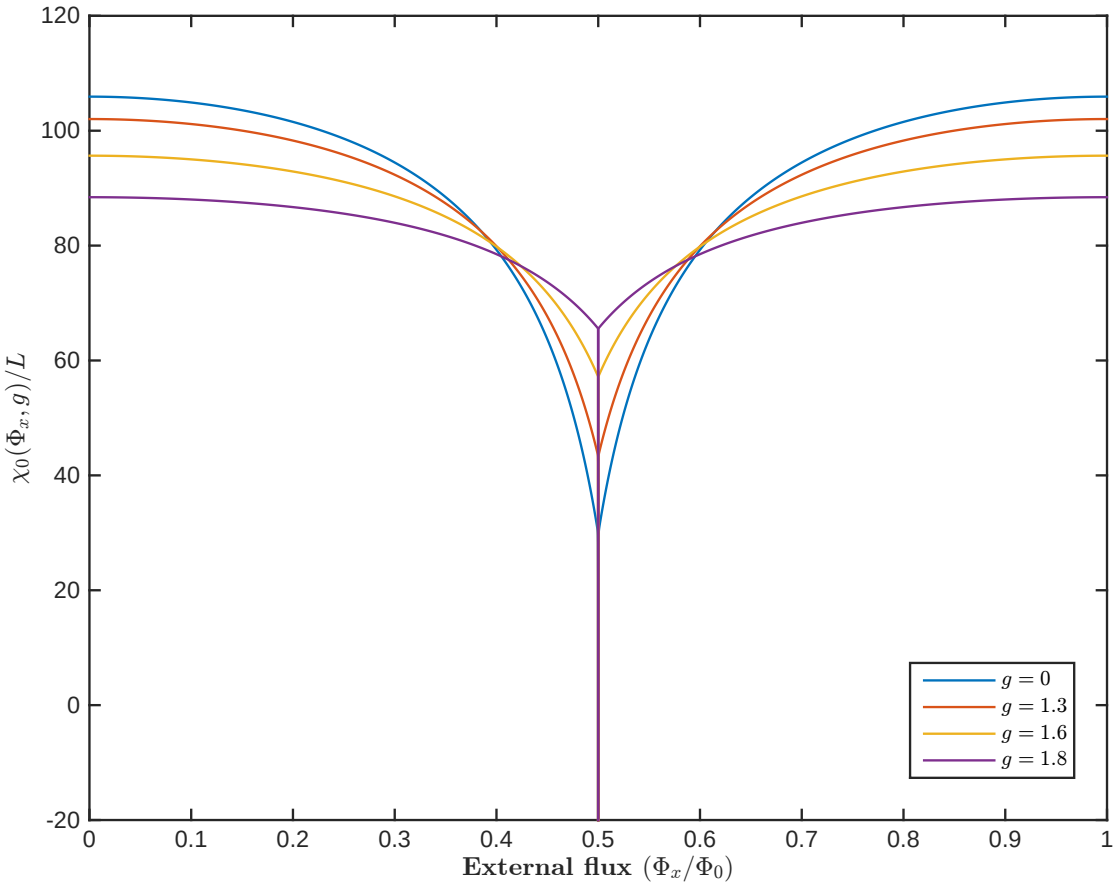

Figure 4.4: Ground state magnetic susceptibility as a function of the external flux Φ_x with varying values of capacitive coupling strength g [119].

4.6 Summary

In this chapter we have shown the nature of additional Hamiltonian terms which are produced naturally as a result of the Born-Markov master equation approach when putting it into Lindblad form. The most primitive and yet most significant term, $\hat{H}_{XP}$ was found to be responsible for the shift in natural frequency of a damped system; this was displayed by use of a classical approach combined with Ehrenfest's theorem. The argument of the necessity of this term in to order preserve quantum-classical correspondence was further strengthened. It was shown that these terms impact on the ensemble average operators, such as position and momentum, where momentum is seen to lag behind the freely evolving position; this, alongside discussion of decay rates, was used to explain rotation and squeezing effects in phase space, shown by use of Wigner functions. The impact of more exotic terms, found as a result of the capacitively coupled SQUID, were shown through the transformation of the energy eigenvalues and more crucially, through the system's magnetic susceptibility, a measurable quantity that could be used to validate the inclusion or neglect of these terms. With scalability of quantum technologies being of great importance, the need to reliably model and simulate has never been so far at the forefront. In order to achieve this it is necessary to characterise a device accurately, which raises difficult questions when terms such as those discussed above are seen to be neglected or renormalised. The model discussed at the end of this chapter contained two control parameters Φ_x and g which provide a pathway through which the energy level structure can be tested by use of the very much measurable magnetic susceptibility. With experimental set ups reaching the sophistica-

tion necessary to test these qualities, it should be possible to verify whether these terms impact on the system's energy in way described by the above analysis.

Chapter 5

Conclusions

In this thesis we have discussed the multiple issues raised in characterising quantum technologies through simulation, and as a consequence how one chooses to model a quantum system under influence from the environment. The Lindblad was introduced as the most widely used tool for describing environmental effects, due to its numerous applications and analytical simplicity within the Markovian framework.

As part of the Introduction to this thesis, the general Markovian master equation was derived and then applied to a SQUID coupled to an Ohmic bath in chapters 2 and 3, with chapter 2 providing both first and second order truncations of the BCH series for the inductively coupled SQUID, and chapter 3 only providing a first order analysis of the dual coupled system. The microscopic approach applied to the ensemble provided master equations that were not found to be of Lindblad form; raising questions as to their validity.

One solution to this problem is simply taking a phenomenological ap-

proach, where a Lindblad is often assumed for a system and the dynamics modelled. Such an approach is evident in the literature where an annihilator is assumed for systems other than the HO; this often comes with the neglect of effective Hamiltonian terms which arise naturally in the microscopic analysis and are unique to the system considered; the effect of such terms and their significance was discussed in chapter 4.

Another solution to this "non-Lindblad" problem, is to provide additional terms in the master equation to ensure positivity. It was discussed in both chapters 2 and 3 that the addition of any term to the master equation changes the physics of the ensemble as a whole, with both chapters suggesting that adding a charge dependent term into the master equation for an inductively coupled SQUID essentially brings an element of parasitic capacitance. Each chapter provided a different way in which the master equation may be brought into Lindblad form, with chapter 2 using comparison of coefficients, and chapter 3 implementing the more rigorous diagonalisation of the coefficient matrix. The difference in approach arose from the necessity to provide a 'minimally invasive' change to the system, which is far simpler to justify for the high temperature case found in QBM, where a term inversely proportional to temperature is introduced. In the zero temperature limit with a 'minimum necessity' protocol, the additional terms have a fixed weighting and their addition therefore becomes harder to justify.

Both the phenomenological approach and the addition of terms are testable via QBM and more specifically Ehrenfest to ensure quantum-to-classical transition, where the importance of frequency shift terms become most evident. In transforming a master equation into Lindblad form, many terms are swept

into the unitary evolution to provide an effective Hamiltonian. The impact of these terms are shown in chapter 4 and analysis using Ehrenfest shows how a quantum mechanical approach differs from the semi-classical RSJ model; due to the non-trivial nature of the expectation values of the Josephson terms for the case of the SQUID, which is greatly simplified in a semi-classical analysis. The effects of these terms further raises questions as to why these terms are neglected in some models whilst renormalised or included in others.

Throughout this thesis, a QBM approach has been taken for the case for a SQUID coupled to an Ohmic bath. In both second order inductive, and first order dual coupled models the corresponding Lindblads were found to depend on the control parameter Φ_x. Regardless of any possible failings of a microscopic analysis of this system, it is perfectly reasonable to suggest that environmental decoherence may be tuneable using environmental degrees of freedom and the findings here further support that claim. The appearance of a Φ_x-dependence in the Lindblad therefore highlights the oversight of many phenomenological approaches where control is not taken into consideration.

The impacts of frequency shifts, renormalisations and 'minimally invasive' additions have been covered well in chapters 2,3 and 4 and it is discussed which contributions should be considered, and which should be neglected. The renormalisation terms, originating from Lamb shift effects were found throughout the analysis and were cancelled through the impact of creating *effective* system variables on coupling with the environment. In chapter 4 a term similar in form to that of the Josephson term in the SQUID Hamiltonian is created alongside the effective Hamiltonian, suggesting these shifts impact on both harmonic and anharmonic parts of the SQUID potential.

The effective Hamiltonians produced from analysis in chapters 2 and 3 were shown to be responsible for frequency shifts and squeezing. The significance of these terms was discussed in chapter 4, specifically their role in the correspondence limit as well as their impact on the system's energy level structure, and consequently magnetic susceptibility; suggesting that their effect may be experimentally verifiable and may finally settle the argument on whether inclusion or neglect of effective Hamiltonian terms are physically justifiable.

From 'minimally invasive' additions to effective Hamiltonians, undertaking a microscopic analysis of any system brings with it many complications. Such examples have been presented in this thesis which highlight just a few issues for modelling systems, such as the physical validity of many seemingly *ad hoc* processes. With such an array of terms and effects which vary in their significance, it is safe to say that care must be taken in order to correctly characterise a quantum mechanical device and overlooking or discrediting some of the effects observed here may lead to unexpected mis-characterisations.

The Lindblad equation is very attractive theoretically. It is the basis of the commonly used Quantum jumps and Quantum State Diffusion and the developments of Quantum Error Correcting code to counter the effect of a particular type of Lindblad. The work here suggests there are many subtleties which must be addressed for their widespread use.

Bibliography

[1] Matthias Steffen, Frederico Brito, David DiVincenzo, Shwetank Kumar, and Mark Ketchen. Decoherence of floating qubits due to capacitive coupling. *New Journal of Physics*, 11(3):033030, 2009.

[2] T. H. Morshed et al. *BSIM4v4.7 MOSFET mode-users manual*, 2011.

[3] Enrico Arrigoni, Michael Knap, and Wolfgang von der Linden. Nonequilibrium dynamical mean-field theory: An auxiliary quantum master equation approach. *Phys. Rev. Lett.*, 110:086403, Feb 2013.

[4] Jeppe C. Dyre. Master-equation appoach to the glass transition. *Phys. Rev. Lett.*, 58:792–795, Feb 1987.

[5] V. Giovannetti and G. M. Palma. Master equations for correlated quantum channels. *Phys. Rev. Lett.*, 108:040401, Jan 2012.

[6] Wojciech Hubert Zurek. Decoherence, einselection, and the quantum origins of the classical. *Rev. Mod. Phys.*, 75:715–775, May 2003.

[7] Lian-Ao Wu, Gershon Kurizki, and Paul Brumer. Master equation and control of an open quantum system with leakage. *Phys. Rev. Lett.*, 102:080405, Feb 2009.

[8] L. Ferialdi. Exact closed master equation for gaussian non-markovian dynamics. *Phys. Rev. Lett.*, 116:120402, Mar 2016.

[9] Michael J. W. Hall, James D. Cresser, Li Li, and Erika Andersson. Canonical form of master equations and characterization of non-markovianity. *Phys. Rev. A*, 89:042120, Apr 2014.

[10] Daniel Maldonado-Mundo, Patrik Öhberg, Brendon W. Lovett, and Erika Andersson. Investigating the generality of time-local master equations. *Phys. Rev. A*, 86:042107, Oct 2012.

[11] Chaitanya Joshi, Patrik Öhberg, James D. Cresser, and Erika Andersson. Markovian evolution of strongly coupled harmonic oscillators. *Phys. Rev. A*, 90:063815, Dec 2014.

[12] Bassano Vacchini. Generalized master equations leading to completely positive dynamics. *Phys. Rev. Lett.*, 117:230401, Nov 2016.

[13] L. Diósi and L. Ferialdi. General non-markovian structure of gaussian master and stochastic Schrödinger equations. *Phys. Rev. Lett.*, 113:200403, Nov 2014.

[14] Alex I. Braginski and John Clarke. *The SQUID Handbook*, volume 1. Wiley-VCH Verlag GmbH & Co. KGaA, Weinheim, 2005.

[15] H. K. Onnes. *Comm. Phys. Lab. Univ. Leiden*, 119,120,122, 1911.

[16] D. van Delft and P. Kes. The discovery of superconductivity. *Physics Today*, September 2010.

[17] W. Meissner and R. Ochsenfeld. *Naturwiss*, 21:787, 1933.

[18] J. Bardeen, L. N. Cooper, and J. R. Schrieffer. Theory of superconductivity. *Phys. Rev.*, 108:1175–1204, Dec 1957.

[19] F. London and H. London. The electromagnetic equations of the supraconductor. *Proceedings of the Royal Society of London A: Mathematical, Physical and Engineering Sciences*, 149(866):71–88, 1935.

[20] L. Landau and L.G. Ginzburg. *Zh.Eksp.Teor.Fiz*, 20:1064, 1960.

[21] A. A. Abrikosov. On the magnetic properties of superconductors of the second group. 32(6):1442, 1957.

[22] Leon N. Cooper. Bound electron pairs in a degenerate fermi gas. *Phys. Rev.*, 104:1189–1190, Nov 1956.

[23] A. B. Pippard. An experimental and theoretical study of the relation between magnetic field and current in a superconductor. *Proceedings of the Royal Society of London A: Mathematical, Physical and Engineering Sciences*, 216(1127):547–568, 1953.

[24] Elbio Dagotto. Correlated electrons in high-temperature superconductors. *Rev. Mod. Phys.*, 66:763–840, Jul 1994.

[25] M. K. Wu, J. R. Ashburn, C. J. Torng, P. H. Hor, R. L. Meng, L. Gao, Z. J. Huang, Y. Q. Wang, and C. W. Chu. Superconductivity at 93 k in a new mixed-phase Y-Ba-Cu-O compound system at ambient pressure. *Phys. Rev. Lett.*, 58:908–910, Mar 1987.

[26] A. P. Drozdov, M. I. Eremets, A. Tryoan, V. Ksenofontov, and S. I. Shylin. Conventional superconductivity at 203 kelvin at high pressures in the sulfur hydride system. *Nature*, 525:73–76, 2015.

[27] B.D. Josephson. Possible new effects in superconductive tunnelling. *Physics Letters*, 1(7):251 – 253, 1962.

[28] A. H. Silver and J. E. Zimmerman. Quantum states and transitions in weakly connected superconducting rings. *Phys. Rev.*, 157:317–341, May 1967.

[29] V. V. Danilov, K. K. Likharev, and O. V. Snigirev. *Signal and noise parameters of SQUIDs*. de Gruyter, Berlin, 1980.

[30] K. K. Likharev. *Dynamics of Josephson Junctions and Circuits*. CRC press, Amsterdam, 1986.

[31] R. P. Feynman, R. B. Leighton, and M. L. Sands. *The Feynman Lectures on Physics, Volume 3: Quantum Mechanics*. Basic Books, 2010.

[32] J. E. Zimmerman, Paul Thiene, and J. T. Harding. Design and operation of stable rfbiased superconducting pointcontact quantum devices, and a note on the properties of perfectly clean metal contacts. *Journal of Applied Physics*, 41(4):1572–1580, 1970.

[33] Eyal Buks and M. P. Blencowe. Decoherence and recoherence in a vibrating rf squid. *Phys. Rev. B*, 74:174504, Nov 2006.

[34] G. Wendin and V. S. Shumeiko. Superconducting Quantum Circuits, Qubits and Computing. *arXiv preprint condmat/0508729*, (c):59, 2005.

[35] M. J. Everitt. On the correspondence principle: Implications from a study of the nonlinear dynamics of a macroscopic quantum device. *New Journal of Physics*, 11, 2009.

[36] T. P. Spiller, D. A. Poulton, T. D. Clark, R. J. Prance, and H. Prance. The dyanmics of a quantum circuit connected to a classical lossy oscillator. *International Journal of Modern Physics B*, 5:1437–1455, 1991.

[37] *Superconductivity: Volume 1: Conventional and Unconventional Superconductors*. Springer Science & Business Media, Leipzig, 2008.

[38] M. J Everitt, T. D Clark, P. Stiffell, H. Prance, R. J Prance, a. Vourdas, and J. Ralph. Quantum Statistics and Entanglement of Two Electromagnetic Field Modes Coupled via a Mesoscopic SQUID Ring. *Phys. Rev. B*, 64(14):184517, 2001.

[39] P. A. M. Dirac. *Principles of Quantum Mechanics*. Oxford University Press, New York, 1982.

[40] Allan Widom. Quantum electrodynamic circuits at ultralow temperature. *Journal of Low Temperature Physics*, 37(3):449–460, Nov 1979.

[41] M. J. Everitt, T. D. Clark, P. B. Stiffell, J. F. Ralph, and C. J. Harland. Energy downconversion between classical electromagnetic fields via a quantum mechanical squid ring. *Phys. Rev. B*, 72:094509, Sep 2005.

[42] C Cohen-Tannoudji, B Diu, and F Laloe. *Quantum Mechanics*. Wiley-VCH, 2005.

[43] J. Diggins, R. Whiteman, T.D. Clark, R.J. Prance, H. Prance, J.F. Ralph, A. Widom, and Y.N. Srivastava. Solutions of the time dependent Schrödinger equation for a squid ring. *Physica B: Condensed Matter*, 233(1):8 – 16, 1997.

[44] T.D. Clark, J. Diggins, J.F. Ralph, M. Everitt, R.J. Prance, H. Prance, R. Whiteman, A. Widom, and Y.N. Srivastava. Coherent evolution and quantum transitions in a two level model of a squid ring. *Annals of Physics*, 268(1):1 – 30, 1998.

[45] S. N. A. Duffus, K. N. Bjergstrom, V. M. Dwyer, J. H. Samson, T. P. Spiller, A. M. Zagoskin, W. J. Munro, Kae Nemoto, and M. J. Everitt. Some implications of superconducting quantum interference to the application of master equations in engineering quantum technologies. *Phys. Rev. B*, 94:064518, Aug 2016.

[46] Alex I. Braginski and John Clarke. *The SQUID Handbook*, volume 2. Wiley-VCH Verlag GmbH & Co. KGaA, Weinheim, 2005.

[47] M. J. Everitt, T. D. Clark, P. B. Stiffell, A. Vourdas, J. F. Ralph, R. J. Prance, and H. Prance. Superconducting analogs of quantum optical phenomena: Macroscopic quantum superpositions and squeezing in a superconducting quantum-interference device ring. *Physical Review A - Atomic, Molecular, and Optical Physics*, 69(4):043804–1, 2004.

[48] M.A. Schlosshauer. *Decoherence: And the Quantum-To-Classical Transition*. Springer, 2007.

[49] H. M. Wiseman and G. J. Milburn. *Quantum Measurement and Control*. Cambridge University Press, 2010.

[50] Xiaobo Zhu, Shiro Saito, Alexander Kemp, Kosuke Kakuyanagi, Shinichi Karimoto, Hayato Nakano, William J. Munro, Yasuhiro Tokura, Mark S. Everitt, Kae Nemoto, Makoto Kasu, Norikazu Mizuochi, and Kouichi Semba. Coherent coupling of a superconducting flux qubit to an electron spin ensemble in diamond. *Nature*, 478(7368):221–224, 2011.

[51] Pietro Massignan, Aniello Lampo, Jan Wehr, and Maciej Lewenstein. Quantum Brownian Motion with inhomogeneous damping and diffusion. *Phys. Rev. A*, 91:033627, Mar 2015.

[52] Mark J. Everitt, Timothy P. Spiller, Gerard J. Milburn, Richard D. Wilson, and Alexandre M. Zagoskin. Engineering dissipative channels for realizing Schrödinger cats in SQUIDs. *Frontiers in ICT*, 1:1, 2014.

[53] Eli Y. Wilner, Haobin Wang, Michael Thoss, and Eran Rabani. Subohmic to super-ohmic crossover behavior in nonequilibrium quantum systems with electron-phonon interactions. *Phys. Rev. B*, 92:195143, Nov 2015.

[54] Katarzyna Roszak, Radim Filip, and Tomáš Novotný. Decoherence control by quantum decoherence itself. *Scientific reports*, 5:9796, 2015.

[55] M. J. Everitt, W. J. Munro, and T. P. Spiller. Overcoming decoherence in the collapse and revival of spin schrödinger-cat states. *Phys. Rev. A*, 85:022113, Feb 2012.

[56] C. W. Gardiner and M. J. Collett. Input and output in damped quantum systems: Quantum stochastic differential equations and the master equation. *Phys. Rev. A*, 31:3761–3774, Jun 1985.

[57] H.P. Breuer and F. Petruccione. *The Theory of Open Quantum Systems*. Oxford University Press, New York, 2002.

[58] Stanislaw Kryszewski and Justyna Czechowska-Kryszk. Master equation - tutorial approach, 2008. arXiv:0801.1757v1.

[59] U. Weiss. *Quantum Dissipative Systems*. World Scientific Publishing, 2 edition, 1999.

[60] W. Munro and C. Gardiner. Non-rotating-wave master equation. *Physical Review A*, 53(4):2633–2640, 1996.

[61] G. Lindblad. On the generators of quantum dynamical semigroups. *Communications in Mathematical Physics*, 48(2):119–130, 1976.

[62] B. M. Garraway. Nonperturbative decay of an atomic system in a cavity. *Physical Review A*, 55(3):2290–2303, 1997.

[63] Carole Addis, Bogna Bylicka, Dariusz Chruściński, and Sabrina Maniscalco. Comparative study of non-markovianity measures in exactly solvable one- and two-qubit models. *Phys. Rev. A*, 90:052103, Nov 2014.

[64] Inés de Vega and Daniel Alonso. Dynamics of non-markovian open quantum systems. *Rev. Mod. Phys.*, 89:015001, Jan 2017.

[65] R.P Feynman and F.L Vernon. The theory of a general quantum system interacting with a linear dissipative system. *Annals of Physics*, 24:118 – 173, 1963.

[66] A.O Caldeira and A.J Leggett. Quantum tunnelling in a dissipative system. *Annals of Physics*, 149(2):374 – 456, 1983.

[67] J. Diggins, J. F. Ralph, T. P. Spiller, T. D. Clark, H. Prance, and R. J. Prance. Chaotic dynamics in the rf superconducting quantum-interference-device magnetometer: A coupled quantum-classical system. *Phys. Rev. E*, 49:1854–1859, Mar 1994.

[68] J. F. Ralph, T. D. Clark, M. J. Everitt, and P. Stiffell. Nonlinear backreaction in a quantum mechanical SQUID. *Physical Review B*, 64(18):9, 2001.

[69] V. S. Varadarajan. *Lie groups, Lie algebras, and their representations.* Springer-Verlag New York, 1984.

[70] Maximilian Schlosshauer, A. P. Hines, and G. J. Milburn. Decoherence and dissipation of a quantum harmonic oscillator coupled to two-level systems. *Phys. Rev. A*, 77:022111, Feb 2008.

[71] R. J. Prance, T. P. Spiller, H. Prance, T. D. Clark, J. Ralph, A. Clippingdale, Y. Srivastava, and A. Widom. The response of a superconducting weak-link ring to external adiabatic noise. *Il Nuovo Cimento B Series 11*, 106(4):431–450, 1991.

[72] C. H. Fleming, Albert Roura, and B. L. Hu. Exact analytical solutions to the master equation of quantum Brownian motion for a general environment. *Annals of Physics*, 326(5):1207–1258, 2011.

[73] Pietro Massignan, Aniello Lampo, Jan Wehr, and Maciej Lewenstein. Quantum Brownian motion with inhomogeneous damping and diffusion. *Physical Review A - Atomic, Molecular, and Optical Physics*, 91(3):033627, 2015.

[74] Guido Burkard. Circuit theory for decoherence in superconducting charge qubits. *Physical Review B - Condensed Matter and Materials Physics*, 71(14):1–8, 2005.

[75] Yongbao Sun, Patrick Wen, Yoseob Yoon, Gangqiang Liu, Mark Steger, Loren N. Pfeiffer, Ken West, David W. Snoke, and Keith A. Nelson. Bose-einstein condensation of long-lifetime polaritons in thermal equilibrium. *Phys. Rev. Lett.*, 118:016602, Jan 2017.

[76] K. F. Riley, M. P. Hobson, and S. J. Bence. *Mathematical Methods for Physics and Engineering*. Cambridge University Press, Cambridge, 3rd edition, 2006.

[77] J.G. Proakis. *Advanced Digital Signal Processing*. Macmillan, London, 1992.

[78] Diósi. L. Ohmic vs Markovian heat - two page tutorial. *Wigner Research Centre for Physics, Budapest*, 2012.

[79] G. Ritschel and A. Eisfeld. Analytic representations of bath correlation functions for ohmic and superohmic spectral densities using simple poles. *arXiv:1405.2440v2*, 2014.

[80] Shiwu Gao. Dissipative Quantum Dynamics with a Lindblad Functional. *Physical Review Letters*, 79(17):3101–3104, 1997.

[81] M. Abramowitz and I. E. Stegan. *Handbook of Mathematical Functions*. Dover Publications, New York, 1970.

[82] Prance R J Diggins J, Ralph J F, Spiller T P, Clark T D, Prance H. Chaotic dynamics in the rf superconducting quantum-interference-device magnetometer: A coupled quantum-classical system. *Physical Review E*, 49(3):1854, 1994.

[83] H. M. Wiseman and W. J. Munro. Comment on "dissipative quantum dynamics with a Lindblad functional". *Phys. Rev. Lett.*, 80:5702–5702, Jun 1998.

[84] M. J. Everitt, W. J. Munro, and T. P. Spiller. Quantum-classical crossover of a field mode. *Physical Review A - Atomic, Molecular, and Optical Physics*, 79(3):21–23, 2009.

[85] Arie Kapulkin and Arjendu K. Pattanayak. Nonmonotonicity in the quantum-classical transition: Chaos induced by quantum effects. *Physical Review Letters*, 101(7):6–9, 2008.

[86] Haifeng Li, Jiushu Shao, and Shikuan Wang. Derivation of exact master equation with stochastic description: Dissipative harmonic oscillator.

Physical Review E - Statistical, Nonlinear, and Soft Matter Physics, 84(5), 2011.

[87] John Clarke and I. Braginski, Alex, editors. *The SQUID Handbook*, volume 1. Wiley-VCH, Weinheim, 2004.

[88] Lorenza Viola, Roberto Onofrio, and Tommaso Calarco. Macroscopic quantum damping in SQUID rings. *Measurement*, 9601(April):7, 1997.

[89] M. A. Nielsen and I. L. Chuang. *Quantum Computation and Quantum Information*. Cambridge University Press, Cambridge, 2000.

[90] Jerzy Dajka and Jerzy Łuczka. Magnetic flux in a mesoscopic SQUID controlled by nonclassical electromagnetic fields. *Physical Review B - Condensed Matter and Materials Physics*, 80(17):174529, 2009.

[91] H Nakano, H Tanaka, S Saito, K Semba, H Takayanagi, and M Ueda. A theoretical analysis of flux-qubit measurements with a dc-SQUID. *Science And Technology*, page 15, 2004.

[92] M. Everitt, P. Stiffell, T. Clark, a. Vourdas, J. Ralph, H. Prance, and R. Prance. Fully quantum-mechanical model of a SQUID ring coupled to an electromagnetic field. *Physical Review B*, 63(14):144530, 2001.

[93] Y. X Liu, L. F. Wei, and Franco Nori. Measuring the quality factor of a microwave cavity using superconducting qubit devices. *Physical Review A*, 72(3):033818, 2005.

[94] J. D. Whittaker, F. C S Da Silva, M. S. Allman, F. Lecocq, K. Cicak, A. J. Sirois, J. D. Teufel, J. Aumentado, and R. W. Simmonds.

Tunable-cavity QED with phase qubits. *Physical Review B - Condensed Matter and Materials Physics*, 90(2):1–15, 2014.

[95] Yuriy Makhlin, Gerd Schön, and Alexander Shnirman. Dissipative effects in Josephson qubits. *Chemical Physics*, 296(2-3):315–324, 2004.

[96] Alexander Shnirman, Yuriy Makhlin, Yuriy Makhlin, and Gerd Schön. Noise and Decoherence in Quantum Two-Level Systems. *Physica Scripta*, T102(1):147, 2002.

[97] Patrick Rooney, Anthony M. Bloch, and C. Rangan. Flag-based control of orbit dynamics in quantum Lindblad systems. *arXiv:1602.06353v1*, 2016.

[98] D. DAlessandro, E. Jonckheere, and R. Romano. Control of open quantum systems in a bosonic bath. *Proceedings of 54th IEEE Conference on Decision and Control (CDC), 15-18 Dec., Osaka, Japan*, 2015.

[99] Shwetank Kumar and David P. DiVincenzo. Exploiting Kerr cross nonlinearity in circuit quantum electrodynamics for nondemolition measurements. *Phys. Rev. B*, 82:014512, Jul 2010.

[100] M. J. Everitt, T. D. Clark, P. B. Stiffell, J. F. Ralph, and C. J. Harland. Energy downconversion between classical electromagnetic fields via a quantum mechanical SQUID ring. *Physical Review B - Condensed Matter and Materials Physics*, 72(9):094509, 2005.

[101] Informal communications with Kieran Bjergstrom, 2017.

[102] G. Ithier, E. Collin, P. Joyez, P. J. Meeson, D. Vion, D. Esteve, F. Chiarello, A. Shnirman, Y. Makhlin, J. Schriefl, and G. Schön. Decoherence in a superconducting quantum bit circuit. *Phys. Rev. B*, 72:134519, Oct 2005.

[103] Matthias Steffen, Frederico Brito, David DiVincenzo, Matthew Farinelli, George Keefe, Mark Ketchen, Shwetank Kumar, Frank Milliken, Mary Beth Rothwell, Jim Rozen, and Roger H Koch. Quantum information storage using tunable flux qubits. *Journal of Physics: Condensed Matter*, 22(5):053201, 2010.

[104] Ji Ying-Hua and Xu Lin. Controlled decoherence of floating flux qubits. *Chinese Physics B*, 19(11):110305, 2010.

[105] A Sandulescu and H Scutaru. Open quantum systems and the damping of collective modes in deep inelastic collisions. *Annals of Physics*, 173(2):277 – 317, 1987.

[106] F. Yoshihara, K. Harrabi, A. O. Niskanen, Y. Nakamura, and J. S. Tsai. Decoherence of flux qubits due to 1/f flux noise. *Phys. Rev. Lett.*, 97:167001, Oct 2006.

[107] A. Isar and W. Scheid. Uncertainty functions of the open quantum harmonic oscillator in the Lindblad theory. *Phys. Rev. A*, 66:042117, Oct 2002.

[108] H. M. Wiseman and W. J. Munro. Comment on "dissipative quantum dynamics with a Lindblad functional". *Phys. Rev. Lett.*, 80:5702–5702, Jun 1998.

[109] Shiwu Gao. Dissipative quantum dynamics with a Lindblad functional. *Phys. Rev. Lett.*, 79:3101–3104, Oct 1997.

[110] R Schack, T A Brun, and I C Percival. Quantum state diffusion, localization and computation. *Journal of Physics A: Mathematical and General*, 28(18):5401, 1995.

[111] Spiller. T. Informal communications with Tim Spiller, 2015.

[112] N Bogoliubov. On The Theory of Superfluidity. *Journal of Physics*, 9(1):23–32, 1947.

[113] H. Bauke and N. R. Itzhak. Visualizing quantum mechanics in phase space. *arXiv:1101.2683v1*, 2011.

[114] Simon J Devitt, William J Munro, and Kae Nemoto. Quantum error correction for beginners. *Reports on Progress in Physics*, 76(7):076001, 2013.

[115] Aniello Lampo, Soon Hoe Lim, Jan Wehr, Pietro Massignan, and Maciej Lewenstein. Lindblad model of quantum Brownian motion. *Phys. Rev. A*, 94:042123, Oct 2016.

[116] M J Everitt. On the correspondence principle: implications from a study of the nonlinear dynamics of a macroscopic quantum device. *New Journal of Physics*, 11(1):013014, 2009.

[117] M.J. Everitt, W.J. Munro, and T.P. Spiller. Quantum measurement with chaotic apparatus. *Physics Letters A*, 374(28):2809 – 2815, 2010.

[118] M J Everitt, W J Munro, and T P Spiller. Quantum measurement and the quantum to classical transition in a non-linear quantum oscillator. *Journal of Physics: Conference Series*, 306(1):012045, 2011.

[119] S. N. A. Duffus, V. M. Dwyer, and M. J. Everitt. On open quantum systems, effective hamiltonians and device characterization. *arXiv:1707.00593v1[quant-ph]*, 2017.

[120] R. J. Prance, J. E. Mutton, E. P. Shephard, T. D. Clark, H. Prance, and T. P. Spiller. *SQUID '85 Superconducting Quantum Interference Devices and their Applications*. June 1985.

[121] Rüdiger Achilles and Andrea Bonfiglioli. The early proofs of the theorem of Campbell, Baker, Hausdorff, and Dynkin. *Archive for History of Exact Sciences*, 66(3):295–358, May 2012.

Appendices

Appendix A

Translation into External Flux Basis

It was shown in Chapter 1 that the Hamiltonian may be transformed into the what is known as the external flux basis, which aids numerical calculations as the Hamiltonian can be written in the HO basis with a JJ extension. To add clarity to this representation we will briefly discuss the application of translation operators. The majority of the material covered here is described in [43, 44, 42] and the following analysis acts as an introduction.

A.1 Unitary Transformations

It is possible to define an operator $S(\lambda)$ which depends on the real parameter λ such that:

$$S(\lambda) = e^{-\frac{i\lambda\hat{Q}}{\hbar}}$$

where $\hat{Q}$ is the charge operator analogous to momentum in the $\{|q\rangle\}$ (position) representation. The operator is unitary since:

$$S^{\dagger}(\lambda) = S^{-1}(\lambda) = S(-\lambda) = e^{\frac{i\lambda\hat{Q}}{\hbar}}$$

and so:

$$SS^{-1} = SS^{\dagger} = \mathbb{1}$$

By calculating the commutator $[\hat{\Phi}, S(\lambda)]$ the effect of $\hat{\Phi}$ on $S(\lambda)$ can be shown:

$$\begin{aligned} [\hat{\Phi}, S(\lambda)] &= \left(-\frac{i\lambda}{\hbar}\right) e^{-\frac{i\lambda\hat{Q}}{\hbar}} [\hat{\Phi}, \hat{Q}] = \left(-\frac{i\lambda}{\hbar}\right) e^{-\frac{i\lambda\hat{Q}}{\hbar}} (i\hbar) = \lambda S(\lambda) \\ \Rightarrow \hat{\Phi}S(\lambda) &= S(\lambda)\hat{\Phi} + \lambda S(\lambda) \\ &= S(\lambda)(\hat{\Phi} + \lambda) \end{aligned} \tag{A.1}$$

It is also worth noting that $S(\lambda)S(\mu) = S(\lambda + \mu)$. We now turn our focus towards the eigenvectors and eigenvalues of $\hat{\Phi}$. Assuming that $\hat{\Phi}$ has a non-zero eigenvector $|\phi\rangle$ with eigenvalue ϕ, that is to say:

$$\hat{\Phi}\,|\phi\rangle = \phi\,|\phi\rangle$$

Applying relation (A.1) yields:

$$\begin{aligned} \hat{\Phi}S(\lambda)\,|\phi\rangle &= S(\lambda)(\hat{\Phi} + \lambda)\,|\phi\rangle \\ &= S(\lambda)(\phi + \lambda)\,|\phi\rangle \\ &= (\phi + \lambda)S(\lambda)\,|\phi\rangle \end{aligned}$$

This equation shows that $S(\lambda)\,|\phi\rangle$ is also a non-zero eigenvector of $\hat{\Phi}$ with an eigenvalue of $(\phi + \lambda)$. As a result, any eigenvector of $\hat{\Phi}$ can be transformed into another eigenvector of the same operator, with any real eigenvalue since λ can take on any value. It is possible to fix the relative phases of the different eigenvectors of $\hat{\Phi}$ with respect to the eigenvector $|0\rangle$ eigenvalue 0, by setting:

$$|\phi\rangle = S(\phi)\,|0\rangle$$

Applying the unitary transformation $S(\lambda)$ to both sides gives:

$$S(\lambda)\,|\phi\rangle = S(\lambda)S(\phi)\,|0\rangle = S(\lambda+\phi)\,|0\rangle = |\phi+\lambda\rangle$$

The adjoint expression is written:

$$\langle\phi|\,S^{\dagger}(\lambda) = \langle\phi+\lambda|$$

While using the property $S^{\dagger}(\lambda) = S(-\lambda)$ gives,

$$\langle\phi|\,S(\lambda) = \langle\phi|\,S^{\dagger}(-\lambda) = \langle\phi-\lambda|$$

A.2 Actions in the $\{|\phi\rangle\}$ Representation

The following notes will outline the effect of $S(\lambda)$ and operators $\hat{\Phi}$ and $\hat{Q}$ in the $\{|\phi\rangle\}$ representation. Since $\hat{\Phi}$ is an observable, the set of eigenvectors $\{|\phi\rangle\}$ constitutes a basis in the Hilbert space. It is therefore possible to

describe each ket by a wave function in the $\{|\phi\rangle\}$ representation:

$$\psi(\phi) = \langle\phi|\psi\rangle$$

With this representation, the action of $\hat{\Phi}$ is given by:

$$\hat{\Phi}\psi(\phi) = \langle\phi|\hat{\Phi}|\psi\rangle = \phi\,\langle\phi|\psi\rangle = \phi\psi(\phi)$$

since $\hat{\Phi}$ is Hermitian. The effect of $S(\lambda)$ in the $\{|\phi\rangle\}$ representation is just as trivial and is given by:

$$\begin{aligned} S(\lambda)\psi(\phi) = \langle\phi|S(\lambda)|\psi\rangle &= \langle\phi|S^{\dagger}(-\lambda)|\psi\rangle \\ &= \langle\phi-\lambda|\psi\rangle \\ &= \psi(\phi-\lambda) \end{aligned}$$

The action of unitary operator $S(\lambda)$ is thus a translation of the wave function over the 'distance' λ parallel to the ϕ axis. Thus $S(\lambda)$ is called the translation operator. The effect of $\hat{Q}$ in the $\{|\phi\rangle\}$ representation is somewhat more complex but nonetheless is easy to find. for an infinitesimal quantity, ε, we have:

$$S(-\varepsilon) = e^{\frac{i\varepsilon\hat{Q}}{\hbar}} = \mathbb{1} + \frac{i\varepsilon\hat{Q}}{\hbar} + O(\varepsilon^2)$$

As a result:

$$\langle\phi|S(-\varepsilon)|\psi\rangle = \psi(\phi+\varepsilon) = \langle\phi|\mathbb{1}|\psi\rangle + \frac{i\varepsilon}{\hbar}\,\langle\phi|\hat{Q}|\psi\rangle$$

And so:

$$\begin{aligned}\hat{Q}\psi(\phi) = \langle\phi|\hat{Q}|\psi\rangle &= \frac{\hbar}{i}\lim_{\varepsilon\to 0}\frac{\psi(\phi+\varepsilon)-\psi(\phi)}{\varepsilon} \\ &= -i\hbar\frac{d}{d\phi}\psi(\phi)\end{aligned}$$

which shows that in this representation the effect of $\hat{Q}$ remains unchanged regardless of translation.

A.3 Transformation of the Hamiltonian

We will now explore the effect of a unitary transformation on the Hamiltonian of a system. Let us consider the TDSE:

$$i\hbar\frac{\partial\,|\psi\rangle}{\partial t} = H\,|\psi\rangle$$

We will now see the effect of the same equation in a rotated frame:

$$i\hbar\frac{\partial\,|\psi'\rangle}{\partial t} = i\hbar\frac{\partial\hat{U}^\dagger\,|\psi\rangle}{\partial t} = i\hbar\frac{\partial\hat{U}^\dagger}{\partial t}\,|\psi\rangle + i\hbar\hat{U}^\dagger\frac{\partial\,|\psi\rangle}{\partial t}$$

Where $\hat{U}^\dagger = e^{\frac{i\hat{A}t}{\hbar}}$ a unitary transformation and $\hat{A}$ is an arbitrary operator. Thus:

$$\begin{aligned}i\hbar\frac{\partial\,|\psi'\rangle}{\partial t} &= \hat{U}^\dagger H\,|\psi\rangle - \hat{A}\hat{U}^\dagger\,|\psi\rangle \\ &= (\hat{U}^\dagger H\hat{U} - \hat{A})\hat{U}^\dagger\,|\psi\rangle \\ \Rightarrow i\hbar\frac{\partial\,|\psi'\rangle}{\partial t} &= (H' - \hat{A})\,|\psi'\rangle\end{aligned}$$

where $H' = \hat{U}^\dagger H \hat{U}$ is the Hamiltonian in the rotated frame. Now that the translation operator and the effect of unitary transformations on the Hamiltonian have been discussed, the effect of the translation:

$$\hat{T} = e^{-\frac{i\Phi_x \hat{Q}}{\hbar}}$$

On the SQUID Hamiltonian:

$$H_S = \frac{\hat{Q}^2}{2C} + \frac{(\hat{\Phi} - \Phi_x)^2}{2L} - \hbar\nu \cos\left(\frac{2\pi\hat{\Phi}}{\hat{\Phi}_0}\right)$$

can be shown. The Hamiltonian acting in the $\{|\phi\rangle\}$ representation is given by:

$$H_S\psi(\phi) = \langle\phi|H_S|\psi\rangle = \left[-\frac{\hbar^2}{2C}\frac{d^2}{d\phi^2} + \frac{(\phi - \Phi_x)^2}{2L} - \hbar\nu\cos\left(\frac{2\pi\phi}{\hat{\Phi}_0}\right)\right]\psi(\phi)$$

In the external flux basis, where the space is translated by Φ_x, this becomes:

$$H'_S\psi'(\phi) = \langle\phi|H'_S|\psi'\rangle = \langle\phi|\hat{T}^\dagger H_S \hat{T}|\psi'\rangle$$

When Φ_x is time independent, the above can be written as:

$$H'_S\psi'(\phi) = \langle\phi|\hat{T}^\dagger H_S \hat{T}|\psi'\rangle = \langle\phi + \Phi_x|H_S\hat{T}|\psi\rangle$$

Since H'_S is Hermitian, this yields:

$$\begin{aligned} H'_S\psi'(\phi) &= \left[-\frac{\hbar^2}{2C}\frac{d^2}{d(\phi+\Phi_x)^2} + \frac{(\phi+\Phi_x-\Phi_x)^2}{2L} - \hbar\nu\cos\left(\frac{2\pi(\phi+\Phi_x)}{\hat{\Phi}_0}\right)\right]\langle\phi+\Phi_x|\hat{T}|\psi'\rangle \\ &= \left[-\frac{\hbar^2}{2C}\frac{d^2}{d\phi^2} + \frac{\phi^2}{2L} - \hbar\nu\cos\left(\frac{2\pi(\phi+\Phi_x)}{\hat{\Phi}_0}\right)\right]\langle\phi+\Phi_x|\hat{T}|\psi'\rangle \\ &= \left[-\frac{\hbar^2}{2C}\frac{d^2}{d\phi^2} + \frac{\phi^2}{2L} - \hbar\nu\cos\left(\frac{2\pi(\phi+\Phi_x)}{\hat{\Phi}_0}\right)\right]\psi'(\phi) \end{aligned}$$

and so the Hamiltonian of a SQUID in the Φ_x- translated basis is given by:

$$H'_S = \frac{\hat{Q}^2}{2C} + \frac{\hat{\Phi}^2}{2L} - \hbar\nu\cos\left(\frac{2\pi(\hat{\Phi}+\Phi_x)}{\Phi_0}\right) \tag{A.2}$$

with the Hamiltonian becoming that of the SHO with an additional non-linear Φ_x-dependent potential term. In terms of representation, the minimum of the SQUID potential is now centred about the origin instead of at point Φ_x.

Appendix B

The Baker-Campbell-Hausdorff Formula

We will now discuss the Baker Campbell Hausdorff formula and the origin of one of its lemmas. The Baker-Campbell-Hausdorff formula offers an expansion to an expression of the form [121]:

$$Z = \log\left(e^X e^Y\right) \tag{B.1}$$

in terms of commutators and commutators of commutators, and so on. It is of great importance here as it allows observables in the interaction picture to be written as a power series of their argument. To demonstrate this, consider an operator of the form:

$$f(s)\hat{Y} = e^{s\hat{X}}\hat{Y}e^{-s\hat{X}} \tag{B.2}$$

By taking a series expansion of $f(s)$ and evaluating it at $s = 1$ it is possible to produce an expression for an operator of the form $\hat{Y}(\hat{X}) = e^{\hat{X}}\hat{Y}e^{-\hat{X}}$. The series expansion of $\hat{Y}(\hat{X})$ is therefore given by:

$$\begin{aligned}\hat{Y}(\hat{X}) = e^{\hat{X}}\hat{Y}e^{-\hat{X}} &= f(s)\hat{Y}|_{s=1} \\ &= f(0)|_{s=1}\hat{Y} + f'(0)s|_{s=1}\hat{Y} + f''(0)\frac{s^2}{2!}\bigg|_{s=1}\hat{Y} + \cdots\end{aligned} \tag{B.3}$$

Applying the above expression to Eq. (B.2) gives the expansion:

$$\begin{aligned}\hat{Y}(\hat{X}) = e^{(s=0)\hat{X}}\hat{Y}e^{-(s=0)\hat{X}} &\\ + \left(\hat{X}e^{(s=0)\hat{X}}\hat{Y}e^{-(s=0)\hat{X}} - e^{(s=0)\hat{X}}\hat{Y}e^{-(s=0)\hat{X}}\hat{X}\right) &\\ + \frac{1}{2!}\Bigg(\hat{X}^2e^{(s=0)\hat{X}}\hat{Y}e^{-(s=0)\hat{X}} &\\ - 2\hat{X}e^{(s=0)\hat{X}}\hat{Y}e^{-(s=0)\hat{X}}\hat{X} + e^{(s=0)\hat{X}}\hat{Y}e^{-(s=0)\hat{X}}\hat{X}^2\Bigg) &\\ + \cdots & \\ \Rightarrow \hat{Y}(\hat{X}) = \hat{Y} + \hat{X}\hat{Y} - \hat{Y}\hat{X} + \frac{1}{2!}\left(\hat{X}^2\hat{Y} - 2\hat{X}\hat{Y}\hat{X} + \hat{Y}\hat{X}^2\right) + \cdots &\end{aligned} \tag{B.4}$$

which simplifies to give the final expression:

$$\boxed{e^{\hat{X}}\hat{Y}e^{-\hat{X}} = \hat{Y} + [\hat{X},\hat{Y}] + \frac{1}{2!}[\hat{X},[\hat{X},\hat{Y}]] + \frac{1}{3!}[\hat{X},[\hat{X},[\hat{X},\hat{Y}]]] + ...}$$

The power of this formula can be seen throughout the analysis supporting this work: from the definition of bath operators and the order of approximation for the master equations, to an alternative method to show the transformation of the SQUID Hamiltonian into the external flux basis.

Appendix C

Kernel Evaluation

C.1 Inductively coupled SQUID

The following calculations will show the how the explicit forms of dissipation and noise kernels for the inductively coupled SQUID may be found using residue theory [76]. Let us begin with the dissipation kernel, using the expression for the spectral density Eq. (2.19) for large Ω and substituting it into the integral definition of the kernel Eq. (2.17) yields:

$$D(-\tau) = 2\hbar \int_0^\infty \mathrm{d}\omega \frac{2C\gamma}{\pi} \omega \frac{\Omega^2}{\Omega^2 + \omega^2} \sin(\omega\tau)$$

By acknowledging the even nature of the above kernel one can see that the integral is simply half of that taken over the whole real line. Using this quality, as well as expressing the oscillatory term as the imaginary contribution

in Euler's formula [76], allows the integral to be written:

$$\begin{aligned} D(-\tau) &= \frac{2C\gamma\hbar\Omega^2}{\pi}\int_{-\infty}^{\infty}\mathrm{d}\omega\frac{\omega}{\Omega^2+\omega^2}\sin(\omega\tau) \\ &= \frac{2C\gamma\hbar\Omega^2}{\pi}\mathrm{Im}\left[\int_{-\infty}^{\infty}\mathrm{d}\omega\frac{\omega}{\Omega^2+\omega^2}e^{\mathrm{i}\omega\tau}\right] \end{aligned}$$

which may be evaluated by considering the contour integral of the function, closing the contour by the semi-circle at infinity in the positive imaginary half space, $f(z) = \frac{z}{(z^2+\Omega^2)}e^{\mathrm{i}z\tau}$ in the complex plane enclosing a singularity at the point $z = \mathrm{i}\Omega$:

$$\oint_C f(z)dz = \oint_C \frac{z}{(z+\mathrm{i}\Omega)(z-\mathrm{i}\Omega)}e^{\mathrm{i}z\tau}dz$$

which may be evaluated by use of residue theory [76]:

$$\oint f(z)dz = 2\pi\mathrm{i}\sum_k \mathrm{Res}(z,k) = 2\pi\mathrm{i}\lim_{z\to z_0}(z-z_0)f(z)$$

and so:

$$\begin{aligned} \oint_C f(z)dz &= 2\pi\mathrm{i}\lim_{z\to i\Omega}\frac{z}{z+\imath\Omega}e^{\mathrm{i}z\tau} \\ &= \pi\mathrm{i}e^{-\Omega\tau} \end{aligned}$$

Since this term is purely imaginary, this allows us to write the dissipation kernel as:

$$D(-\tau) = \frac{2C\gamma\hbar\Omega^2}{\pi}\mathrm{Im}\left[\int_{-\infty}^{\infty}\mathrm{d}\omega\frac{\omega}{\Omega^2+\omega^2}e^{\mathrm{i}\omega\tau}\right]$$
$$= 2C\gamma\hbar\Omega^2 e^{-\Omega\tau}$$

which, when taking $\tau > 0$ gives the dissipation kernel in its familiar form [48, 57]. For $\tau < 0$ we simply observe that $\sin(-\omega\tau) = -\mathrm{Im}\left[e^{-\mathrm{i}\omega|\tau|}\right]$ which allows the kernel to be written:

$$D(-\tau) = 2C\gamma\hbar\Omega^2 e^{-\Omega|\tau|}\,\mathrm{sgn}\,\tau$$

where $\mathrm{sgn}(\pm|\tau|) = \pm 1$ is the signum function. With the dissipation kernel defined we now consider the noise kernel which, due to the zero temperature limit being implemented, will use an approximation used in [80] which differs from some of the literature [48, 57] in its consideration of the smoothness of integral terms to yield analytical solutions. For more information on the justification of this approximation, please see the next section. We begin with the integral form of the noise kernel:

$$D_1(-\tau) = 2\hbar\int_0^{\infty}\mathrm{d}\omega J(\omega)\cos(\omega\tau)$$
$$= \frac{4C\hbar\gamma\Omega^2}{\pi}\int_0^{\infty}\mathrm{d}\omega\frac{\omega}{\Omega^2+\omega^2}\cos(\omega\tau)$$

The observation that $\cos(\omega\tau)$ in the integral which is fast oscillating when compared to ω [80] allows us to approximate ω to take a constant value ω_c:

$$D_1(-\tau) = \frac{4C\hbar\gamma\Omega^2\omega_c}{\pi}\int_0^{\infty}\mathrm{d}\omega\frac{1}{\Omega^2+\omega^2}\cos(\omega\tau)$$

where ω_c acts as the centre of the spectral density band [80]. The integral can therefore be solved using residue theory once more. Observing the even nature of the integrand and expressing $\cos(\omega\tau)$ by use of Euler's formula the yields:

$$D_1(-\tau) = \frac{2C\hbar\gamma\Omega^2\omega_c}{\pi}\mathrm{Re}\left[\int_{-\infty}^{\infty}\mathrm{d}\omega\frac{1}{(\omega^2+\Omega^2)}e^{\mathrm{i}\omega\tau}\right]$$

Following the same method as for the dissipation kernel, we find that:

$$D_1(-\tau) = \frac{2C\hbar\gamma\Omega^2\omega_c}{\pi}\frac{\pi}{\Omega}e^{-\Omega|\tau|}$$

By making the approximation that $\omega_c = \frac{\omega_0}{2}$ [80] where $\omega_0 = 1/\sqrt{L_0C_0}$ defines the characteristic frequency of the system, the explicit form for the noise kernel is given by:

$$D_1(-\tau) = C\hbar\gamma\Omega\omega_0 e^{-\Omega|\tau|}$$

C.2 Noise Kernel Approximation

In this section the approximation used to produce the explicit expression of the noise kernel given above, as in [80], will be explained in greater detail. To start, we must first recall the dissipator for a SQUID inductively coupled to an Ohmic bath:

$$\mathcal{K} = \frac{1}{\hbar^2}\int_0^{\infty}\mathrm{d}\tau\Big(\frac{\mathrm{i}}{2}D(-\tau)[\hat{\Phi},\{\hat{\Phi}(-\tau),\rho_S(t)\}] - \frac{1}{2}D_1(-\tau)[\hat{\Phi},[\hat{\Phi}(-\tau),\rho_S(t)]]\Big) \tag{C.1}$$

Justification of the Born-Markov approximation, which extends the upper limit in time to infinity, requires both the dissipation and noise kernels $D(-\tau)$

and $D_1(-\tau)$ to decay sufficiently quickly. The dissipation kernel $D(-\tau)$ has already been found to satisfy this, showing exponential decay in its time evolution. In order to justify the behaviour of the noise kernel one must consider its form in the $\tau \to 0$ limit. In this limit, $D_1(0)$ may be written:

$$\begin{aligned} D_1(0) = 2\hbar \int_0^\infty J(\omega)\mathrm{d}\omega &= \frac{4C\hbar\gamma\Omega^2}{\pi} \int_0^\infty \frac{\omega}{\omega^2+\Omega^2}\mathrm{d}\omega \\ &= \frac{2C\hbar\Omega^2}{\pi}[\mathrm{Ln}(\omega^2+\Omega^2)]_0^\infty \end{aligned} \tag{C.2}$$

Consequently $D_1(-\tau)$ has a logarithmic singularity at $\tau = 0$ which is not the case for other cut-off functions. Evaluating at finite τ it is clear that the D_1 function obtained does not die off sufficiently rapidly to warrant the Born-Markov ($\int_0^{t\to\infty} \mathrm{d}\tau$) approximation which implies that the Lorentz-Drude on its own is inadequate as a result; this is evident in the consideration a hard cut off enforced within the integral itself, which gives the convergent result

$$\begin{aligned} D_{1\Omega}(0) = 2\hbar \int_0^\Omega J(\omega)\mathrm{d}\omega &= \frac{4\hbar C\gamma}{\pi} \int_0^\Omega \omega\mathrm{d}\omega \\ &= \frac{2\hbar C\gamma\Omega^2}{\pi} \end{aligned} \tag{C.3}$$

at $\tau \to 0$, where $D_{1\Omega}$ denotes the kernel evaluated by the finite integral up to the bath cut off frequency. To ensure convergence for finite τ within the Born-Markov regime, a convergent factor $e^{-\theta\tau}$ can be introduced, doing so yields:

$$D_{1\Omega}(-\tau) = \frac{2\hbar C\gamma}{\pi} e^{-\theta\tau} \tag{C.4}$$

Since $D_1(-\tau)$ is closely related to the bath correlation function $\langle BB(\tau)\rangle_B$ it is natural to define θ as the inverse of the bath correlation time τ_B, the maximum value of which is equal to the bath cut off frequency within the Born-Markov regime [48, 57], so that $\theta = 1/\tau_B = \Omega$. The noise kernel $D_{1\Omega}(-\tau)$ can therefore be written:

$$D_{1\Omega}(-\tau) = \frac{2\hbar C\gamma\Omega^2}{\pi} e^{-\Omega\tau} \tag{C.5}$$

which decays sufficiently with $D(-\tau)$ in Eq. (C.1). The approach taken to derive the explicit value for the noise kernel with a Lorentz-Drude cut off, as shown in the previous section, observes the smoothness of functions to produce a kernel with the same decaying behaviour as the kernel given in Eq. (C.5), but differs by a factor proportional to ω_0/Ω; this suggests that the effects attributed to $D_1(-\tau)$ are likely to be underestimated. Nonetheless, this approach shows the desired decaying behaviour and therefore still provides good insight into environmental effects.

Appendix D

Calculation of Kernels for Capacitively Coupled SQUID

D.1 Purely Capacitive Terms

We will start by considering the bath correlation functions $\left\langle \hat{B}_Q \hat{B}_Q(-\tau) \right\rangle_B$ and $\left\langle \hat{B}_Q(-\tau) \hat{B}_Q \right\rangle_B$ which may be written in terms of bosonic annihilation and creation operators $\hat{b}$ and $\hat{b}^\dagger$ respectively:

$$\begin{aligned} \left\langle \hat{B}_Q \hat{B}_Q(-\tau) \right\rangle_B = &- \sum_n \frac{\eta_n^2 C_n \omega_n \hbar}{2} \times \\ &\left\langle \left(\hat{b}_n - \hat{b}_n^\dagger \right) \left(e^{-\frac{\mathrm{i}\hat{H}_B \tau}{\hbar}} \hat{b}_n e^{\frac{\mathrm{i}\hat{H}_B \tau}{\hbar}} - e^{-\frac{\mathrm{i}\hat{H}_B \tau}{\hbar}} \hat{b}_n^\dagger e^{\frac{\mathrm{i}\hat{H}_B \tau}{\hbar}} \right) \right\rangle_B \end{aligned} \tag{D.1}$$

Using the Baker-Campbell-Hausdorff expansion, this may be written as:

$$\begin{aligned}\left\langle \hat{B}_Q\hat{B}_Q(-\tau)\right\rangle_B &= -\sum_n \frac{\eta_n^2 C_n\omega_n\hbar}{2}\left\langle\left(\hat{b}_n-\hat{b}_n^\dagger\right)\left(\hat{b}_n e^{\mathrm{i}\omega_n\tau}-\hat{b}_n^\dagger e^{-\mathrm{i}\omega_n\tau}\right)\right\rangle_B \\ &= -\sum_n \frac{\eta_n^2 C_n\omega_n\hbar}{2}\Big\langle \hat{b}_n^{\dagger 2}e^{-\mathrm{i}\omega_n\tau}-\hat{b}_n^\dagger\hat{b}_n e^{\mathrm{i}\omega_n\tau} \\ &\qquad -\hat{b}_n\hat{b}_n^\dagger e^{-\mathrm{i}\omega_n\tau}+\hat{b}_n^2 e^{\mathrm{i}\omega_n\tau}\Big\rangle_B\end{aligned} \tag{D.2}$$

keeping only energy preserving terms, as in §2.2.1, reduces the above to:

$$\left\langle \hat{B}_Q\hat{B}_Q(-\tau)\right\rangle_B = \sum_n \frac{\eta_n^2 C_n\omega_n\hbar}{2}\left\langle \hat{b}_n^\dagger\hat{b}_n e^{\mathrm{i}\omega_n\tau}+\hat{b}_n\hat{b}_n^\dagger e^{-\mathrm{i}\omega_n\tau}\right\rangle_B \tag{D.3}$$

Note that this approximation has been made for the capacitive case to comply with the master equation framework, a more detailed approach may be taken and the impact of the linear combinations of the non-conserving terms may be found; this is however beyond the scope of this work and we will proceed without this consideration. Using the thermal state of the bath in the same fashion as the analysis presented from Eq. (2.9) to Eq. (2.13) this correlation function may be written:

$$\left\langle \hat{B}_Q\hat{B}_Q(-\tau)\right\rangle_B = \sum_n \frac{\eta_n^2 C_n\omega_n\hbar}{2}\left(\coth\left(\frac{\hbar\omega_n}{2k_BT}\right)\cos\left(\omega_n\tau\right)-\mathrm{i}\sin\left(\omega_n\tau\right)\right) \tag{D.4}$$

Whilst its conjugate may be written:

$$\left\langle \hat{B}_Q(-\tau)\hat{B}_Q \right\rangle_B = \sum_n \frac{\eta_n^2 C_n \omega_n \hbar}{2} \left(\coth\left(\frac{\hbar\omega_n}{2k_B T}\right)\cos(\omega_n\tau) + \mathrm{i}\sin(\omega_n\tau) \right) \tag{D.5}$$

The purely capacitive commutator terms in Eq. (3.5) may therefore be written:

$$\begin{aligned} \left\langle \left[\hat{B}_Q, \hat{B}_Q(-\tau) \right] \right\rangle_B &= -2\mathrm{i}\hbar \sum_n \frac{\eta_n^2 C_n \omega_n}{2} \sin(\omega_n\tau) = \mathrm{i}D_Q(\tau) \\ \left\langle \left\{ \hat{B}_Q, \hat{B}_Q(-\tau) \right\} \right\rangle_B &= 2\hbar \sum_n \frac{\eta_n^2 C_n \omega_n}{2} \coth\left(\frac{\hbar\omega_n}{2k_B T}\right)\cos(\omega_n\tau) = D_{Q1}(\tau) \end{aligned} \tag{D.6}$$

where $D_Q(\tau)$ and $D_{Q1}(\tau)$ are the purely capacitive dissipation and noise kernels respectively and may be written in terms of the spectral density $J_Q(\omega)$, which again can be found through the Fourier transform of the bath correlation function, thus :

$$\begin{aligned} D_Q(-\tau) &= 2\hbar \int_0^\infty \mathrm{d}\omega J(\omega)\sin(\omega\tau) \\ D_{Q1}(-\tau) &= 2\hbar \int_0^\infty \mathrm{d}\omega J(\omega)\cos(\omega\tau)\coth\left(\frac{\hbar\omega}{2k_B T}\right) \end{aligned} \tag{D.7}$$

here:

$$J_Q(\omega) = \sum_n \frac{\eta_n^2 C_n \omega_n}{2}\delta(\omega - \omega_n) \tag{D.8}$$

For Ohmic dissipation this finds a similar form to the spectral density in

the inductive coupling regime:

$$J_Q(\omega) = \frac{2L\omega\gamma_Q}{\pi}\frac{\Omega^2}{\Omega^2+\omega^2} \tag{D.9}$$

where γ_Q and Ω denote the capacitive damping rate and bath cut off frequency respectively. Here we use the same cut-off Ω for J_Q and J_Φ but different coupling strengths γ_Q, γ_Φ equivalent to $\frac{\kappa_n^2}{C_n\omega_n} = g^2\frac{\eta_n^2}{L_n\omega_n}$

In the zero temperature limit, kernels $D_Q(\tau)$ and $D_Q1(\tau)$ may be evaluated using residue theory, yielding the expressions:

$$\begin{aligned} D_Q(\tau) &= 2L\gamma_Q\hbar\Omega^2 e^{-\Omega\tau}\,\mathrm{sgn}\,\tau \\ D_{Q1}(\tau) &= L\hbar\gamma_Q\Omega\omega_0 e^{-\Omega\tau} \end{aligned} \tag{D.10}$$

D.2 Flux-Charge Terms

The bath correlation functions $\left\langle \hat{B}_\Phi\hat{B}_Q(-\tau)\right\rangle_B$ and $\left\langle \hat{B}_Q(-\tau)\hat{B}_\Phi\right\rangle_B$ may be written in terms of bosonic annihilation and creation operators $\hat{b}$ and $\hat{b}^\dagger$ respectively:

$$\begin{aligned} \left\langle \hat{B}_\Phi\hat{B}_Q(-\tau)\right\rangle_B = \sum_n \frac{\eta_n\kappa_n\hbar}{2\mathrm{i}}\Bigg\langle \left(\hat{b}_n+\hat{b}_n^\dagger\right)\Bigg(&(e^{-\frac{\mathrm{i}\hat{H}_B\tau}{\hbar}}\hat{b}_n e^{\frac{\mathrm{i}\hat{H}_B\tau}{\hbar}} \\ &- e^{-\frac{\mathrm{i}\hat{H}_B\tau}{\hbar}}\hat{b}_n^\dagger e^{\frac{\mathrm{i}\hat{H}_B\tau}{\hbar}}\Bigg\rangle_B \end{aligned} \tag{D.11}$$

which differs to the purely inductive and capacitive functions found in Eq. (2.9) and Eq. (D.1) through the presence of both coupling constants as well as the change of sign. Using the Baker-Campbell-Hausdorff expansion once expansion, this may be written as:

$$\begin{aligned}\left\langle \hat{B}_\Phi \hat{B}_Q(-\tau)\right\rangle_B &= \sum_n \frac{\eta_n\kappa_n\hbar}{2\mathrm{i}}\left\langle \left(\hat{b}_n+\hat{b}_n^\dagger\right)\left(\hat{b}_n e^{\mathrm{i}\omega_n\tau}-\hat{b}_n^\dagger e^{-\mathrm{i}\omega_n\tau}\right)\right\rangle_B \\ &= \sum_n \frac{\eta_n\kappa_n\hbar}{2\mathrm{i}}\left\langle \hat{b}_n^2 e^{\mathrm{i}\omega_n\tau}+\hat{b}_n^\dagger\hat{b}_n e^{\mathrm{i}\omega_n\tau}-\hat{b}_n\hat{b}_n^\dagger e^{-\mathrm{i}\omega_n\tau}-\hat{b}_n^{\dagger 2}e^{-\mathrm{i}\omega_n\tau}\right\rangle_B\end{aligned} \tag{D.12}$$

and, keeping only energy preserving terms once more reduces the above to:

$$\left\langle \hat{B}_\Phi \hat{B}_Q(-\tau)\right\rangle_B = \sum_n \frac{\eta_n\kappa_n\hbar}{2\mathrm{i}}\left\langle \hat{b}_n^\dagger\hat{b}_n e^{\mathrm{i}\omega_n\tau}-\hat{b}_n\hat{b}_n^\dagger e^{-\mathrm{i}\omega_n\tau}\right\rangle_B \tag{D.13}$$

Using the thermal state of the bath again allows this correlation function to be written:

$$\left\langle \hat{B}_\Phi \hat{B}_Q(-\tau)\right\rangle_B = \sum_n \frac{\eta_n\kappa_n\hbar}{2}\left(\coth\left(\frac{\hbar\omega_n}{2k_BT}\right)\sin(\omega_n\tau)+\mathrm{i}\cos(\omega_n\tau)\right) \tag{D.14}$$

together with its conjugate:

$$\left\langle \hat{B}_Q(-\tau)\hat{B}_\Phi\right\rangle_B = \sum_n \frac{\eta_n\kappa_n\hbar}{2}\left(\coth\left(\frac{\hbar\omega_n}{2k_BT}\right)\sin(\omega_n\tau)-\mathrm{i}\cos(\omega_n\tau)\right) \tag{D.15}$$

The cross-correlation commutator terms in Eq. (3.5) finally become:

$$\begin{aligned}\left\langle\left[\hat{B}_\Phi,\hat{B}_Q(-\tau)\right]\right\rangle_B &= 2\mathrm{i}\hbar\sum_n\frac{\eta_n\kappa_n}{2}\cos(\omega_n\tau)=\mathrm{i}D_{\Phi Q}(\tau) \\ \left\langle\left\{\hat{B}_\Phi,\hat{B}_Q(-\tau)\right\}\right\rangle_B &= 2\hbar\sum_n\frac{\eta_n\kappa_n}{2}\coth\left(\frac{\hbar\omega_n}{2k_BT}\right)\sin(\omega_n\tau)=D_{\Phi Q1}(\tau)\end{aligned} \tag{D.16}$$

where $D_{\Phi Q}(\tau)$ and $D_{\Phi Q1}(\tau)$ are the cross dissipation and noise kernels respecitvely, named to follow convention in §2.2.1, and may be written in terms of the spectral density, $J_{\Phi Q}(\omega)$:

$$\begin{aligned} D_{\Phi Q}(-\tau) &= 2\hbar \int_0^\infty \mathrm{d}\omega J_{\Phi Q}(\omega) \cos(\omega\tau) \\ D_{\Phi Q1}(-\tau) &= 2\hbar \int_0^\infty \mathrm{d}\omega J_{\Phi Q}(\omega) \sin(\omega\tau) \coth\left(\frac{\hbar\omega}{2k_B T}\right) \end{aligned} \tag{D.17}$$

The spectral density may be defined in terms of the density of states ω_n and the associated coupling constants $\eta_n\kappa_n/2$ as:

$$J_{\Phi Q}(\omega) = \sum_n \frac{\eta_n\kappa_n}{2}\delta(\omega - \omega_n) \tag{D.18}$$

For Ohmic dissipation this finds a similar form to the spectral density in the inductive coupling regime:

$$J_{\Phi Q}(\omega) = \frac{2\gamma_{\Phi Q}}{\pi}\frac{\omega}{\omega_0}\frac{\Omega^2}{\Omega^2 + \omega^2} \tag{D.19}$$

where $\gamma_{\Phi Q}$ and Ω denote the cross-effect damping rate and bath cut off frequency respectively. Employing a previous method used by Gao [80] which analyses the smoothness of the functions, allows the following approximation to be made:

$$\begin{aligned} D_{\Phi Q}(-\tau) &\approx \frac{4\hbar\Omega^2\gamma_{\Phi Q}}{\pi}\frac{\omega_c}{\omega_0}\int_0^\infty \frac{\cos(\omega\tau)}{\Omega^2 + \omega^2}\mathrm{d}\omega \\ &= \hbar\Omega\gamma_{\Phi Q} e^{-\Omega\tau} \end{aligned} \tag{D.20}$$

where the residue theorem has once again been applied. The method used in [80] allows for an analytical solution to be found in the zero temperature

limit.

Finding an explicit expression for the noise kernel is a simpler process. In the zero temperature limit $D_{\Phi Q1}$ may be written:

$$\begin{aligned} D_{\Phi Q1}(-\tau) &= 2\hbar \int_0^\infty \mathrm{d}\omega J(\omega) \sin(\omega\tau) \\ &= \frac{4\hbar\gamma_{\Phi Q}\Omega^2}{\pi\omega_0} \int_0^\infty \mathrm{d}\omega \frac{\omega \sin(\omega\tau)}{\Omega^2+\omega^2} \\ &= \frac{2\hbar\gamma_{\Phi Q}\Omega^2}{\omega_0} e^{-\Omega\tau} \end{aligned} \tag{D.21}$$

D.3 Charge-Flux Terms

The correlation functions $\left\langle \hat{B}_Q \hat{B}_\Phi(-\tau) \right\rangle_B$ and $\left\langle \hat{B}_\Phi(-\tau) \hat{B}_Q \right\rangle_B$ may be written in terms bosonic creation and annihilation operators:

$$\begin{aligned} \left\langle \hat{B}_Q \hat{B}_\Phi(-\tau) \right\rangle_B = \sum_n \frac{\eta_n \kappa_n \hbar}{2\mathrm{i}} \Big\langle \left(\hat{b}_n - \hat{b}_n^\dagger\right) \Big(& e^{-\frac{\mathrm{i}\hat{H}_B\tau}{\hbar}} \hat{b}_n e^{\frac{\mathrm{i}\hat{H}_B\tau}{\hbar}} \\ & + e^{-\frac{\mathrm{i}\hat{H}_B\tau}{\hbar}} \hat{b}_n^\dagger e^{\frac{\mathrm{i}\hat{H}_B\tau}{\hbar}} \Big) \Big\rangle_B \end{aligned} \tag{D.22}$$

Using the Baker-Campbell-Hausdorff expansion, this may be written as:

$$\begin{aligned} \left\langle \hat{B}_Q \hat{B}_\Phi(-\tau) \right\rangle_B &= \sum_n \frac{\eta_n \kappa_n \hbar}{2\mathrm{i}} \left\langle \left(\hat{b}_n - \hat{b}_n^\dagger\right) \left(\hat{b}_n e^{\mathrm{i}\omega_n\tau} + \hat{b}_n^\dagger e^{-\mathrm{i}\omega_n\tau}\right) \right\rangle_B \\ &= \sum_n \frac{\eta_n \kappa_n \hbar}{2\mathrm{i}} \left\langle \hat{b}_n^2 e^{\mathrm{i}\omega_n\tau} - \hat{b}_n^\dagger \hat{b}_n e^{\mathrm{i}\omega_n\tau} + \hat{b}_n \hat{b}_n^\dagger e^{-\mathrm{i}\omega_n\tau} - \hat{b}_n^{\dagger 2} e^{-\mathrm{i}\omega_n\tau} \right\rangle_B \end{aligned} \tag{D.23}$$

Keeping only energy preserving terms again reduces the above to:

$$\left\langle \hat{B}_Q \hat{B}_\Phi(-\tau) \right\rangle_B = -\sum_n \frac{\eta_n \kappa_n \hbar}{2\mathrm{i}} \left\langle \hat{b}_n^\dagger \hat{b}_n e^{\mathrm{i}\omega_n\tau} - \hat{b}_n \hat{b}_n^\dagger e^{-\mathrm{i}\omega_n\tau} \right\rangle_B \tag{D.24}$$

Using the thermal state of the bath in the same fashion as previous works this correlation function may be written as:

$$\left\langle \hat{B}_Q \hat{B}_\Phi(-\tau) \right\rangle_B = -\sum_n \frac{\eta_n \kappa_n \hbar}{2} \left(\coth\left(\frac{\hbar\omega_n}{2k_B T}\right) \sin(\omega_n \tau) + \mathrm{i}\cos(\omega_n \tau) \right) \tag{D.25}$$

with its conjugate:

$$\left\langle \hat{B}_\Phi(-\tau) \hat{B}_Q \right\rangle_B = -\sum_n \frac{\eta_n \kappa_n \hbar}{2} \left(\coth\left(\frac{\hbar\omega_n}{2k_B T}\right) \sin(\omega_n \tau) - \mathrm{i}\cos(\omega_n \tau) \right) \tag{D.26}$$

Appendix E

Details of Bogoliubov transformations to find the physical significance of H_{xp}

The conditions for the constants u and v can be found using the commutation relation:

$$[\hat{b}, \hat{b}^\dagger] = [u\hat{a} + v\hat{a}^\dagger, u^*\hat{a}^\dagger + v^*\hat{a}] = \left(|u|^2 - |v|^2\right)[\hat{a}, \hat{a}^\dagger] \tag{E.1}$$

As $\gamma \to 0$, it is a requirement that $\hat{b} \to \hat{a}$ and $u \to 1$[111, 45]. Since $[\hat{a}, \hat{a}^\dagger] = \mathbb{1}$, $\hat{b}$ and $\hat{b}^\dagger$ can only be canonical ladder operators if they satisfy the same condition, thus u and v must satisfy the condition:

$$|u|^2 - |v|^2 = 1 \tag{E.2}$$

Inverting expressions (4.30) yields expressions for $\hat{a}$ and $\hat{a}^\dagger$ in terms of the new operators:

$$\begin{aligned} \hat{a} &= u^*\hat{b} - v\hat{b}^\dagger \\ \hat{a}^\dagger &= u\hat{b}^\dagger - v^*\hat{b} \end{aligned} \tag{E.3}$$

Substituting this expression into the Hamiltonian (4.29) gives the result:

$$H' = \hbar\omega\left[\left(u\hat{b}^\dagger - v^*\hat{b}\right)\left(u^*\hat{b} - v\hat{b}^\dagger\right) + \frac{1}{2} + \frac{i\zeta}{2}\left(\left(u\hat{b}^\dagger - v^*\hat{b}\right)^2 - \left(u^*\hat{b} - v\hat{b}^\dagger\right)^2\right)\right] \tag{E.4}$$

where we have introduced the term $\zeta = \frac{\gamma}{\omega}$ [111, 45]. Simplifying then yields:

$$\begin{aligned} H' = \Bigg[&|u|^2\hat{b}^\dagger\hat{b} + |v|^2(\hat{b}^\dagger\hat{b} + 1) - v^*u^*\hat{b}^2 - uv\hat{b}^{\dagger 2} + \frac{1}{2} \\ &+ \frac{i\zeta}{2}\left((u^2 - v^2)\hat{b}^{\dagger 2} + (v^{*2} - u^{*2})\hat{b}^2 - uv^*(2\hat{b}^\dagger\hat{b} + 1) + u^*v(2\hat{b}^\dagger\hat{b}) + 1)\right)\Bigg] \end{aligned} \tag{E.5}$$

Imposing the condition that the coefficients of $\hat{b}^2$ and $\hat{b}^{\dagger 2}$ vanish gives two equivalent expressions [111, 45]:

$$\begin{aligned} -v^*u^* + \frac{i\zeta}{2}(v^{*2} - u^{*2}) &= 0 \\ -uv + \frac{i\zeta}{2}(u^2 - v^2) &= 0 \end{aligned} \tag{E.6}$$

Guessing solutions $u = \sec\theta$ and $v = i\tan\theta$ such that $\theta \to 0$ as $\gamma \to 0$ and $|u|^2 - |v|^2 = \sec^2\theta - \tan^2\theta = 1$ gives:

$$i\sec\theta\tan\theta + \frac{i\zeta}{2}\left(\sec^2\theta - 0\tan^2\theta\right) = 0 \tag{E.7}$$

Defining $S = \sec^2\theta$ allows the above expression to be simplified:

$$S(S-1) = \frac{\zeta^2}{4}(2S-1)^2 \tag{E.8}$$

The parameter S can therefore be solved in terms of ζ. Expanding and then factorising yields:

$$\begin{aligned} S^2 - S &= \frac{\zeta^2}{4}(4S^2 - 4S + 1) \\ \Rightarrow S = \sec^2\theta &= \frac{1}{2}\left(1 + \sqrt{1-\zeta^2}\right) \end{aligned} \tag{E.9}$$

where the positive root has been taken so that $S \to 1$ as $\gamma \to 0$ which is necessary to match the behaviour of the oscillator. Inserting this result into the expression (E.5) allows the coefficient of $\hat{b}^\dagger\hat{b}$ to be found [111, 45]. The Hamiltonian now reads:

$$\begin{aligned} H' &= \hbar\omega\left[2S - 1 + \frac{i\zeta}{2}\left(-2S^{\frac{1}{2}}\cdot -i(S-1^{\frac{1}{2}} + 2S^{\frac{1}{2}}i(S-1)^{\frac{1}{2}})\right)\right]\hat{b}^\dagger\hat{b} \\ &= \hbar\omega\left(2S - 1 - 2\zeta S^{\frac{1}{2}}(S-1)^{\frac{1}{2}}\right)\hat{b}^\dagger\hat{b} \\ &= \hbar\omega\left((1-\zeta^2)^{-\frac{1}{2}} - 2\zeta\cdot\frac{\zeta}{2}(1-\zeta^2)^{-\frac{1}{2}}\right)\hat{b}^\dagger\hat{b} \\ &= \hbar\omega(1-\zeta^2)^{\frac{1}{2}} = \hbar\tilde{\omega}\hat{b}^\dagger\hat{b} \end{aligned} \tag{E.10}$$

where $\tilde{\omega} = \omega\left(1 - \frac{\gamma^2}{\omega^2}\right)^{1/2}$ is exactly the same frequency shift that appears in the classical dynamics. This result shows that in order to model dissipation in exactly the same way as the classical dynamics, the frequency shift term H_{xp} cannot be omitted from the system Hamiltonian as it has a physical impact on the system; this result is significant when considering quantum-

classical crossover as it suggests that other terms of this nature may also have a physical importance. These findings may extend into the additional terms seen in sections 2.2.1.4 and 3.3.1.

With the Hamiltonian written in terms of the new operators $\hat{b}, \hat{b}^\dagger$ and the dissipator still written in terms of the original ladder operators, one must check that the equations are equivalent in both representations and the method used to find Eq. (4.27) produces the same result for this case. To prove this one must consider the commutation relation of the original ladder operators:

$$\left[\hat{a}, \hat{a}^\dagger\right] = \hat{\mathbb{I}} \tag{E.11}$$

Rewriting this expression in terms of the new transformed operators yields:

$$\begin{aligned}
\left[\hat{a}, \hat{a}^\dagger\right] &= \left[\sec\theta\hat{b} - \mathrm{i}\tan\theta\hat{b}^\dagger, \sec\theta\hat{b}^\dagger + \mathrm{i}\tan\theta\hat{b}\right] \\
&= \left[\sec\theta\hat{b}, \sec\theta\hat{b}^\dagger\right] - \left[\mathrm{i}\tan\theta\hat{b}^\dagger, \mathrm{i}\tan\theta\hat{b}\right] \\
&= \left(\sec^2\theta - \tan^2\theta\right)\left[\hat{b}, \hat{b}^\dagger\right] \\
\Rightarrow \left[\hat{a}, \hat{a}^\dagger\right] &= \left[\hat{b}, \hat{b}^\dagger\right] = \hat{\mathbb{I}}
\end{aligned} \tag{E.12}$$

It therefore follows that the commutation relations of the position and momentum operators with the original and transformed number operators, $\hat{a}^\dagger\hat{a}$ and $\hat{b}^\dagger\hat{b}$ respectively, are the same:

$$\begin{aligned}
\left[\hat{X}, \hat{a}^\dagger\hat{a}\right] &= \left[\hat{X}, \hat{b}^\dagger\hat{b}\right] = \mathrm{i}\hat{P} \\
\left[\hat{P}, \hat{a}^\dagger\hat{a}\right] &= \left[\hat{P}, \hat{b}^\dagger\hat{b}\right] = -\mathrm{i}\hat{X}
\end{aligned} \tag{E.13}$$

It is therefore permissible to write the Lindblad equation in terms of either

operator or even both and still produce the same result. It is advantageous to to write the free evolution in terms of the new operators and the dissipator in terms of the original ones as this takes the most compact form; clearly showing the impact on the Hamiltonian whilst keeping the dissipator trivial. It is important however to write other operators, such as $\hat{X}$ and $\hat{P}$, in their respective form. That is to say:

$$\begin{aligned}\hat{X} &= \frac{\hat{a}+\hat{a}^\dagger}{\sqrt{2}} = \frac{\sec\theta\left(\hat{b}+\hat{b}^\dagger\right)}{\sqrt{2}} + \frac{\mathrm{i}\tan\theta\left(\hat{b}-\hat{b}^\dagger\right)}{\sqrt{2}} \\ \hat{P} &= \frac{\hat{a}-\hat{a}^\dagger}{\sqrt{2}\mathrm{i}} = \frac{\sec\theta\left(\hat{b}-\hat{b}^\dagger\right)}{\sqrt{2}\mathrm{i}} - \frac{\tan\theta\left(\hat{b}+\hat{b}^\dagger\right)}{\sqrt{2}}\end{aligned} \tag{E.14}$$

where it is clear to see that these operators offer as a combination of canonical ladder operators.

Appendix F

Steady State Calculation

F.1 Introduction

This appendix contains an example of the code used to calculate the steady state density matrix elements of the SQUID, seen in chapters 2, and specifically here, 3.

F.2 Code

```
%top programme
close all
clear all
qxs=[0 0.05 0.1 0.15 0.2 0.25 0.3 0.35 0.4 0.425 0.45 0.475 0.48 0.485
 0.49 0.495 0.4975 0.4995 0.49995 0.5 0.50005 0.5005 0.5025 0.505
  0.51 0.515 0.52 0.525 0.55 0.575 0.6 0.6 0.65 0.7 0.75 0.8 0.85 0.9
   0.95 1];
n=40;
X=zeros(n);A=X;AP=X;SQ=X;H=X;H0=X;
```

```
%constants
hv=0.67*9.99*10^-22;h=1.0547*10^-34;v=hv/h;
C=5*10^-15;L=3*10^-10;w=1/sqrt(L*C);hw=h*w;
phi0=2.067*10^-15;
a=hv/hw;
kQ=2*pi*sqrt(hw*L)/phi0;
g=0.55;
W=25*w;
beta= 4*pi^2*hv*L/(phi0^2);
goverw=0.005;%qx is really qx/phi0


% annihilation operator
for j=1:n-1,
    A(j,j+1)=sqrt(j);
end
%other operators
AP=A';
X=(AP+A)/sqrt(2);
P=(A-AP)/(sqrt(2)*1i)
ID=eye(n);
H0=AP*A+1/2*ID;

A1=0.9348;
x1=0.4464;
p1=-0.07082-0.8887i;
j1=0.07002-0.03285i;

A2=4.79;
x2=0.6321;
```

```
p2=0.005154+0.371i;
j2=0.6802-0.009269i;
load expvals120 e;
e=e(1:40,1:40);
vals=[];
for k=1:length(qxs),
    k
    qx=qxs(k)
    e1=e*exp(1i*2*pi*qx);CosQ=real(e1); SinQ=imag(e1);
    HXP=goverw*(3*g^2/2-g+1/2)*(X*P+P*X);
    HXJ=goverw*w/(2*W)*sqrt(beta*v/w)*X*SinQ;
    HPJ= goverw*g^2/2*(sqrt(beta*v/w)*(P*SinQ+SinQ*P)+beta*w/(2*W)*CosQ);
    %HPJ=0;
    H=H0+HXP-HXJ-HPJ-a*CosQ;
    %Lindblad
    L1=sqrt(A1*goverw)* (x1*X +p1*P+ j1*SinQ);
    LP1=L1';
    L2=sqrt(A2*goverw)*(x2*X+ p2*P +j2*SinQ);
    LP2=L2';
    %L = sqrt(goverw)*A;
    %LP=L';
    %Solve AMp + pBM+ CMpDM=0
    %0=-i[H,p]+LpLP-0.5LPLp-0.5pLLP
    AM=-1i*H-LP1*L1/2-LP2*L2/2;
    BM=+1i*H-LP1*L1/2-LP2*L2/2;
    CM=L1;
    DM=LP1;
    EM=L2;
    FM=LP2;
```

```
    G=kron(ID,AM)+kron(transpose(BM),ID)...
    +kron(transpose(DM),CM)+kron(transpose(FM),EM);
    Solve G*vec[rho]=0
    rhonull=null(G);
    rankG=rank(G)%should be n^2-1
    M=G(1:n^2-1,1:n^2-1);
    rankM=rank(M)%should still be n^2-1
    v1=zeros(1,n^2-1);
    v1(1:n+1:n^2-1)=1;
    v2(1:n^2-1)=G(1:n^2-1,n^2);
    clear G
    M1=transpose(v2)*v1;
    M2=M-M1;clear M M1 rho
    rho=-M2\transpose(v2);rho=[rho;0];%extend rho to n^2 terms
    clear M2
    rho=reshape(rho,n,n);%turn square
    rho(n,n)=1-trace(rho);
    [UU,DD]=eig(rho);
    evals=diag(DD);
    evals(1:6)
    purity(k)=trace(rho*rho)
    vals=[vals,[purity(k);qxs(k)]]
    Z=AM*rho + rho*BM+ CM*rho*DM +EM*rho*FM;%check that everything works out
    ck(k)=max(max(abs(Z)));
    ks=num2str(k);
    str=['rho_g055_W25w_n40_',ks];
    save(str, 'rho', 'Z')%, 'rhonull')
end

purityg055W25wn40 = purity;
```

```
 save('purityg055W25wn40', 'purityg055W25wn40')

figure
plot(qxs,purity,'kd-');
axis([0 1 0 1])
xlabel('external flux, $$\Phi_x/\Phi_0$$','interpreter', 'latex');
ylabel('steady state purity, Tr$$(\rho^2)$$','interpreter', 'latex')
title('g=0.55, $$\Omega=25\omega_0$$','interpreter', 'latex')
```

Appendix G

Lindblad calculation

G.1 Introduction

This appendix contains the code used for the calculation of the Lindblads in Chapter 3 for the dual coupled SQUID.

G.2 Code

```
close all
clear all

hv=0.67*9.99*10^-22;h=1.0547*10^-34;v=hv/h;
C=5*10^-15;L=3*10^-10;w=1/sqrt(L*C);hw=h*w;
phi0=2.067*10^-15;
a=hv/hw;
kQ=2*pi*sqrt(hw*L)/phi0;
W=2*w;
beta= 4*pi^2*hv*L/(phi0^2);
```

```
zeta= w/(2*W);
%zeta=0
Gmin = 0.225;
Gmax = 0.55;
G=Gmin:0.0001:Gmax;
A=zeros(3);ep=0.0;
posneg = 1;
for k=1:length(G),
   g=G(k);
   A(1,1) = 2*g+1;
   A(1,2) = -1i*(1+g^2-g)-zeta*(1-g^2);
   A(1,3) = g*sqrt(beta*a)*(1+1i*zeta);
   A(2,1)= 1i*(1+g^2-g)-zeta*(1-g^2);
   A(2,2) = 2*g +g^2;
   A(2,3)= g^2*sqrt(beta*a)*(zeta+1i);
   A(3,1) = g*sqrt(beta*a)*(1-1i*zeta);
   A(3,2)=g^2*sqrt(beta*a)*(zeta-1i);
   A(3,3)= (beta*a)*(4*g^4+8*zeta^2*g^3)/(-g^4*(1+zeta^2)
   +4*g^3+2*g^2*(1+zeta^2)+4*g-(1+zeta^2));
   B(1,1)=A(3,3);B(1,2)=A(3,2);B(1,3)=A(3,1);
   B(2,1)=A(2,3);B(2,2)=A(2,2);B(2,3)=A(2,1);
   B(3,1)=A(1,3);B(3,2)=A(1,2);B(3,3)=A(1,1);
   A=B;
   D=det(A);
   [U,V]=eig(A);
   e=diag(V);
   evals(k,1:3)=e;
   U1(k,1:3)=U(1:3,1).';
   U2(k,1:3)=U(1:3,2).';
   U3(k,1:3)=U(1:3,3).';
```

```
    a33(k)=B(1,1);

    %{
    if k==1
        U2old(k) = U2(k,2)
    elseif abs((U2(k,2)-U2(k-1,2))/(G(k)-G(k-1)))>100
        posneg = -posneg;
        U2old(k)= posneg*U2(k,2);
    else
        posneg = posneg;
        U2old(k)= posneg*U2(k,2);
    end
    %}
%     if k==1
%         U3old(k) = U2(k,3)
%     elseif abs((U2(k,3)-U2(k-1,3))/(G(k)-G(k-1)))>100
%         posneg = -posneg;
%         U3old(k)= posneg*U2(k,3);
%     else
%         posneg = posneg;
%         U3old(k)= posneg*U2(k,3);
%     end
%

    if k==1
        U3old(k,1) = U2(:,3);
    else
        if U2(k,3)*U2(k-1,3)<0
            U3old(k,1) = -U2(k,3);
        else
```

```
        U3old(k,1) = U2(k,3);
    end

    if U2(k,3)' * U3old(k) < 0
        U2(k,3) = -U2(k,3);
    end
    U3old(k,1) = U2(k,3);
end




  if k==1
    U2old(k,1) = U2(:,2);
else
    if real(U2(k,2))*real(U2(k-1,2))<0
        U2old(k,1) = -U2(k,2);
    else
        U2old(k,1) = U2(k,2);
    end

    if real(U2(k,2))' * real(U2old(k)) < 0
        U2(k,2) = -U2(k,2);
    end
    U2old(k,1) = U2(k,2);
  end
```

```
        if k==1
        U1old(k,1) = U2(:,1);
    else
        if real(U2(k,1))*real(U2(k-1,1))<0
            U1old(k,1) = -U2(k,1);
        else
            U1old(k,1) = U2(k,1);
        end

        if real(U2(k,1))' * real(U1old(k)) < 0
            U2(k,1) = -U2(k,1);
        end
        U1old(k,1) = U2(k,1);
        end




 end


figure
plot(G,evals(:,1),'r-',G,evals(:,2),'g--',G,evals(:,3),'b:')
axis ([Gmin Gmax -10 10])
title('Eigenvalues of the coefficent matrix', 'interpreter', 'latex')
xlabel('Coupling Ratio, $g$', 'interpreter','latex')
ylabel('Magnitude', 'interpreter', 'latex')
BOB=legend('$\lambda_1$','$\lambda_2$','$\lambda_3$','Location', 'northeast');
set(BOB, 'interpreter','latex')
```

```
figure
subplot(211)
plot(G,-real(U1old),'r:',G,-real(U2old),'g--',G,real(U3old),'b-')
axis([Gmin Gmax -1 1])
xlabel('Coupling strength, $g$','interpreter','latex')
ylabel('Magnitude', 'interpreter', 'latex')
title('Re($\underline{u}_2$)', 'interpreter', 'latex')
Legend=legend('$\hat{S}$', '$\hat{P}$', '$\hat{X}$', 'Location', 'east');
set(Legend,'interpreter', 'latex')

subplot(212)
plot(G,-imag(U1old),'r:',G,-imag(U2old),'g--',G,imag(U3old),'b-')
axis([Gmin Gmax -0.2 1])
xlabel('Coupling strength, $g$','interpreter','latex')
ylabel('Magnitude', 'interpreter', 'latex')
title('Im($\underline{u}_2$)', 'interpreter', 'latex')
Legend=legend('$\hat{S}$', '$\hat{P}$', '$\hat{X}$', 'Location', 'east');
set(Legend,'interpreter', 'latex')
axis ([Gmin Gmax -1 1])
hold off


figure
subplot(211)
plot(G,real(U3(:,1)),'r:',G,real(U3(:,2)),'g--',G,real(U3(:,3)),'b-')
axis([Gmin Gmax -0.2 1])
xlabel('Coupling strength, $g$','interpreter','latex')
ylabel('Magnitude', 'interpreter', 'latex')
title('Re($\underline{u}_3$)', 'interpreter', 'latex')
Legend=legend('$\hat{S}$', '$\hat{P}$', '$\hat{X}$', 'Location', 'east');
```

```
set(Legend,'interpreter', 'latex')
subplot(212)
plot(G,imag(U3(:,1)),'r:',G,abs(imag(U3(:,2))),...
'g--',G,abs(imag(U3(:,3))),'b-')
axis([Gmin Gmax -0.3 0.5])
xlabel('Coupling strength, $g$','interpreter','latex')
ylabel('Magnitude', 'interpreter', 'latex')
title('Im($\underline{u}_3$)', 'interpreter', 'latex')
Legend=legend('$\hat{S}$', '$\hat{P}$', '$\hat{X}$', 'Location', 'east');
set(Legend,'interpreter', 'latex')
```

Appendix H

Energy Eigenvalue Calculation

H.1 Introduction

This appendix contains an example of the code used to calculate and display the energy level strucutre of the dual coupled SQUID, seen in chapter 4.

H.2 Code

```
close all
clear all
%hv=0.45*9.99*10^-22;h=1.0547*10^-34;
hv=0.67*9.99*10^-22;h=1.0547*10^-34;
v=hv/h;
C=5*10^-15;L=3*10^-10;w=1/sqrt(L*C);hw=h*w;
phi0=2.067*10^-15;
a=hv/hw;
kQ=2*pi*sqrt(hw*L)/phi0;
```

```
gs=[ 0 1.3 1.6 1.8];

W=10*w;
beta= 4*pi^2*hv*L/(phi0^2);
goverw=0.05;%qx is really qx/phi0

qxs=0:0.1:0.5
%qxs=0:0.001:1;
n=40;
X=zeros(n);A=X;AP=X;SQ=X;H=X;H0=X;

for j=1:n-1,
    A(j,j+1)=sqrt(j);
end
%other operators
AP=A';
X=(AP+A)/sqrt(2);
P=(A-AP)/(sqrt(2)*1i)
ID=eye(n);
H0=AP*A+1/2*ID;

load expvals120 e;
e=e(1:n,1:n);


for z=1:length(gs),
  z;
  g=gs(z);

for k=1:length(qxs),
```

```
k;
qx=qxs(k);
e1=e*exp(1i*2*pi*qx);CosQ=real(e1); SinQ=imag(e1);
%HXP=goverw*(3*g^2/2-g+1/2)*(X*P+P*X);
HXP=0
HXJ=goverw*g*w/(4*W)*sqrt(beta*v/w)*(X*SinQ+SinQ*X);
%HXJ=0;
HPJ= goverw*g^2/2*(sqrt(beta*v/w)*(P*SinQ+SinQ*P)+beta*w/(2*W)*CosQ);
%HPJ=0;
H=H0+HXP-HXJ-HPJ-a*CosQ;
%H=H0+HXP-a*CosQ;
%H=H0-a*CosQ;
%H=H0+HXP;
E=eig(H);
n=length(E);
for j=1:1:n-1;
for i=1:1:n-1;
    if E(i)>E(i+1);
        temp=E(i);
        E(i)=E(i+1);
        E(i+1)=temp;
    end
end
end
E40(k)=E(40);


E1(k)=E(1);
E2(k)=E(2);
E3(k)=E(3);
```

```
   E4(k)=E(4);
   E5(k)=E(5);
   E6(k)=E(6);
   E7(k)=E(7);
   E8(k)=E(8);
   E9(k)=E(9);
   E10(k)=E(10);
   E11(k)=E(11);

end


%subplot(2,2,z)

plot (qxs, E1, '-')




hold on
plot(qxs, E2, '-')
plot(qxs, E3, '-')
plot(qxs,E4,'-')
plot(qxs, E5, '-')
plot(qxs, E6, '-')
plot(qxs, E7, '-')
plot(qxs, E8, '-')
plot(qxs, E9, '-')
```

```
plot(qxs, E10, '-')
plot(qxs, E11, '-')
hold off
axis([0 0.5 -8 8])

title('$$\gamma=0.1\omega$$','interpreter', 'latex')
string={'g=0', 'g=1.3', 'g=1.6','g=1.8'}

title(string{z},'interpreter','latex');
ylabel('\textbf{Energy $$(1/ \hbar \omega)$$}','interpreter', 'latex')
xlabel('\textbf{External flux $$(\Phi_x/\Phi_0)$$}','interpreter', 'latex')%}



end
```